

Air Force Institute of Technology

**AFIT Scholar**

---

[Theses and Dissertations](#)

[Student Graduate Works](#)

---

3-1-2002

## Alternative Pulse Detonation Engine Ignition System Investigation through Detonation Splitting

August J. Rolling

Follow this and additional works at: <https://scholar.afit.edu/etd>



Part of the [Propulsion and Power Commons](#)

---

### Recommended Citation

Rolling, August J., "Alternative Pulse Detonation Engine Ignition System Investigation through Detonation Splitting" (2002). *Theses and Dissertations*. 4371.

<https://scholar.afit.edu/etd/4371>

This Thesis is brought to you for free and open access by the Student Graduate Works at AFIT Scholar. It has been accepted for inclusion in Theses and Dissertations by an authorized administrator of AFIT Scholar. For more information, please contact [richard.mansfield@afit.edu](mailto:richard.mansfield@afit.edu).



**ALTERNATIVE PULSE DETONATION ENGINE IGNITION  
SYSTEM INVESTIGATION THROUGH DETONATION SPLITTING**

THESIS

August J. Rolling, Captain, USAF  
AFIT/GAE/ENY/02-10

**DEPARTMENT OF THE AIR FORCE  
AIR UNIVERSITY**

***AIR FORCE INSTITUTE OF TECHNOLOGY***

---

Wright-Patterson Air Force Base, Ohio

APPROVED FOR PUBLIC RELEASE; DISTRIBUTION UNLIMITED

## Report Documentation Page

<b>Report Date</b> 26 Mar 2002	<b>Report Type</b> Final	<b>Dates Covered (from... to)</b> -
<b>Title and Subtitle</b> Alternative Pulse Detonation Engine Ignition System Investigation through Detonation Splitting	<b>Contract Number</b>	
	<b>Grant Number</b>	
	<b>Program Element Number</b>	
<b>Author(s)</b> Capt August J. Rolling, USAF	<b>Project Number</b>	
	<b>Task Number</b>	
	<b>Work Unit Number</b>	
<b>Performing Organization Name(s) and Address(es)</b> Air Force Institute Technology Graduate School of Engineering and Mangement (AFIT/EN) 2950 P Street, Bldg 640 WPAFB OH 4543-7765	<b>Performing Organization Report Number</b> AFIT/GAE/ENY/02-10	
<b>Sponsoring/Monitoring Agency Name(s) and Address(es)</b> Attn: Mr. Fred Schauer AFRL/PRTS WPAFB, OH 45433	<b>Sponsor/Monitor's Acronym(s)</b>	
	<b>Sponsor/Monitor's Report Number(s)</b>	
<b>Distribution/Availability Statement</b> Approved for public release, distribution unlimited		
<b>Supplementary Notes</b> The original document contains color images.		

**Abstract**

: A Pulse Detonation Engine (PDE) combusts fuel air mixtures through a form of combustion: detonation. Recent PDE research has focused on designing working subsystems. This investigation continued this trend by examining ignition system alternatives. Existing designs required spark plugs in each separate thrust tube to ignite premixed reactants. A single thrust tube could require the spark plug to fire hundreds of times per second for long durations. The goal was to minimize hardware and increase reliability by limiting the number of ignition sources. This research used a continuously propagating detonation wave as both a thrust mechanism and an ignition system and required only one initial ignition source. This investigation was a proof of concept for such an ignition system. First a systematic look at various geometric effects on detonations was made. These results were used to further examine configurations for splitting detonations, physically dividing one detonation wave into two separate detonation waves. With this knowledge a dual thrust tube system was built and tested proving that a single spark could be used to initiate detonation in separate thrust tubes. Finally, a new tripping device for better deflagration to detonation transition (DDT) was examined. Existing devices induced DDT axially. The new device attempted to reflect an incoming detonation to initiate direct DDT in a cross flow.

**Subject Terms**

Pulse Detonation Engines, Single Spark Ignition System, Detonation Splitting

**Report Classification**

unclassified

**Classification of this page**

unclassified

**Classification of Abstract**

unclassified

**Limitation of Abstract**

UU

**Number of Pages**

115

AFIT/GAE/ENY/02-10

The views expressed in this thesis are those of the author and do not reflect the official policy or position of the United States Air Force, Department of Defense, or the U. S. Government.

AFIT/GAE/ENY/02-10

ALTERNATIVE PULSE DETONATION ENGINE IGNITION SYSTEM  
INVESTIGATION THROUGH DETONATION SPLITTING

THESIS

Presented to the Faculty

Department of Aeronautical and Astronautical Engineering

Graduate School of Engineering and Management

Air Force Institute of Technology

Air University

Air Education and Training Command

In Partial Fulfillment of the Requirements for the  
Degree of Master of Science in Aeronautical Engineering

August J. Rolling, B.S.

Captain, USAF

March 2002

APPROVED FOR PUBLIC RELEASE; DISTRIBUTION UNLIMITED.

AFIT/GAE/ENY/02-10

ALTERNATIVE PULSE DETONATION ENGINE IGNITION SYSTEM  
INVESTIGATION THROUGH DETONATION SPLITTING

August J. Rolling, BS  
Captain, USAF

Approved:

\_\_\_\_\_  
Paul I. King (Chairman)

\_\_\_\_\_  
date

\_\_\_\_\_  
Ralph A. Anthenien (Member)

\_\_\_\_\_  
date

\_\_\_\_\_  
William C. Elrod (Member)

\_\_\_\_\_  
date

\_\_\_\_\_  
Milton E. Franke (Member)

\_\_\_\_\_  
date

## Acknowledgments

First, I would like to thank Dr. Paul King. His unmatched dedication and enthusiasm really motivated me on this project. He took a risk delving into PDE's with a new student, and I appreciate his confidence. My thanks to Dr. Fred Schauer, who I first knew as 'Animal' on the soccer field and later discovered is a brilliant and dedicated scientist and engineer. He's been an inspiration and role model, who sees challenges and creatively defies them. His cohort includes Dr. John Hoke, who as another mad-scientist has helped me see new ways to make things happen, especially if it involved using junkyard car parts or toilet paper! Royce Bradley would not let me run an experiment without helping me set up and spending long hours running the engine. Jeff Stutrud, Dr. Vish Kutta, Dwight Fox, Curt Rice, and Jason Parker round out the crew of pulse detonation engine gurus who get things done and made my job fun. I also thank Dr. Dillip Ballal whose course work on combustion gave me a great foundation for understanding detonations. I thank my AFIT friends who have made the past 18 months something I will never forget, and yes that is a good thing. I thank my wife for surviving the storm and giving me unbelievable support. And finally, thank you daughter for understanding when Dad read to you about compressible flow instead of Green Eggs and Ham.

AJ Rolling



# Table of Contents

	Page
Acknowledgments.....	i
Table of Contents .....	v
List of Figures .....	vii
List of Tables.....	ix
List of Symbols .....	x
Abstract .....	xi
1 Introduction.....	1-1
1.1 General .....	1-1
1.2 Background .....	1-1
1.3 Problem statement.....	1-4
1.4 Objectives.....	1-5
2 Theory .....	2-1
2.1 Introduction.....	2-1
2.2 1-Dimensional detonation wave model.....	2-1
2.3 Zeldovich, von Neumann, Döring (ZND) wave model .....	2-7
2.4 3-Dimensional detonation wave structure.....	2-10
2.4.1 Detonation to deflagration transition (DDT) mechanism .....	2-12
2.4.2 Modes of DDT .....	2-12
3 Materials and Method.....	3-1
3.1 Detonation initiation.....	3-1
3.2 Engine cycle .....	3-1

	Page
3.3 Integrated propulsion system .....	3-2
3.4 Research facility .....	3-2
3.5 Data acquisition.....	3-3
3.6 Experimental configurations .....	3-4
3.6.1 Single tube configurations.....	3-5
3.6.2 Split tube configurations .....	3-8
3.6.3 Dual thrust tube - single ignition source .....	3-11
3.6.4 DDT trip device.....	3-14
4 Results and Analysis .....	4-1
4.1 Data post processing.....	4-1
4.2 Single tube results .....	4-3
4.3 Split tube results .....	4-7
4.4 Dual thrust tube – single ignition source results .....	4-10
4.5 DDT trip device results .....	4-17
5 Conclusions and Recommendations.....	5-1
5.1 Conclusions .....	5-1
5.2 Recommendations .....	5-1
Appendix A Rayleigh and Rankine-Hugonit Development	A-1
Appendix B ZND Detonation Analysis H <sub>2</sub> and Air	B-1
Appendix C Tables of Test Results	C-1
References	REF-1

## List of Figures

Figure	Page
Fig. 1.1 Building 71 Test Pulse Detonation Engine.....	1-2
Fig. 1.2 Concept art for integrated PDE ignition system.....	1-4
Fig. 2.1 1-D detonation wave control volume analysis.....	2-2
Fig. 2.2 Raleigh Line Eqn. 4.....	2-4
Fig. 2.3 Rankine-Hugoniot curve.....	2-5
Fig. 2.4 Gas properties through ZND structure.....	2-8
Fig. 2.5 Von Neumann spike.....	2-9
Fig. 2.6 Mach stem (cell triple point).....	2-11
Fig. 2.7 Cell structure (Katta 1999).....	2-11
Fig. 2.8 Deflagration to detonation transition (adapted from Kuo 1986 268:269).....	2-13
Fig. 3.1 PDE engine cycle.....	3-2
Fig. 3.2 Schematic of research facility.....	3-3
Fig. 3.3 Baseline test configuration.....	3-5
Fig. 3.4 Test matrix 1A: axially converging geometries.....	3-6
Fig. 3.5 Test matrix 1B: axial diverging.....	3-7
Fig. 3.6 Test matrix 1C: 90-degree turns.....	3-8
Fig. 3.7 Test matrix 2A: tee geometries.....	3-9
Fig. 3.8 Test matrix 2B: wye geometries.....	3-10
Fig. 3.9 Test matrix 2C: capped geometries.....	3-11
Fig. 3.10 Dual thrust tube design.....	3-12

Figure	Page
Fig. 3.11 Cycle diagrams and firing window .....	3-13
Fig. 4.1 Results: test matrix 1A: axial converging.....	4-4
Fig. 4.2 Results: test matrix 1B: axial diverging.....	4-5
Fig. 4.3 Results test matrix 1C: 90-degree turns.....	4-6
Fig. 4.4 Results test matrix 2A: tees.....	4-7
Fig. 4.5 Results test matrix 2B: wyes.....	4-8
Fig. 4.6 Results test matrix 2C: caps.....	4-9
Fig. 4.7 Fill fraction effects.....	4-10
Fig. 4.8 Single spark – dual detonation configuration .....	4-11
Fig. 4.9 Dual detonation configuration results.....	4-12
Fig. 4.10 Dual tube transducer 3 pressure trace .....	4-15
Fig. 4.11 Dual tube transducer 4 pressure trace .....	4-16
Figure 4.12 Dual tube transducer 5 pressure trace.....	4-16
Figure 4.13 Dual thrust tube time line (ms) .....	4-17
Fig. 4.14 Reflector.....	4-18
Fig. 4.15 Reflector results .....	4-18
Fig. 5.1 Recommended machined testing configurations .....	5-2

## List of Tables

Table	Page
Table 2.1 Properties of Hugoniot curve (Williams 1965:35).....	2-5
Table 2.2 Comparison of normal shock, detonation, and deflagration properties .....	2-6
Table 2.3 ZND Properties for H <sub>2</sub> and air .....	2-10
Table 3.1 Ignition delay time vs. frequency.....	3-13
Table 4.1 Example data table: results test matrix 1B configuration a.....	4-2
Table 4.2 Classification by %CJ .....	4-3
Table 4.3 Successful double detonation - run 1 data.....	4-14
Table 4.4 Successful double detonation – run 2 data.....	4-14

## List of Symbols

Symbol	Definition	Dimension
<u>Regular Symbols</u>		
$c_p$	Specific heat (constant pressure)	J/kgK
$h$	Specific enthalpy	J/kg
$\dot{m}''$	1-D mass flow	kg/s m <sup>2</sup>
$M$	Mach number	--
$P$	Pressure	N/m <sup>2</sup>
$q$	Heat per unit mass	J/kg
$T$	Temperature	K
$u$	Velocity in x-direction	m/s
<u>Greek Symbols</u>		
$\gamma$	Ratio of specific heats	--
$\rho$	Density	kg/m <sup>3</sup>
<u>Subscripts</u>		
1	Condition of reactants	
2	Condition of products	

## Abstract

A Pulse Detonation Engine (PDE) combusts fuel air mixtures through a form of combustion: detonation. The resulting change in momentum produces thrust. Recent PDE research has focused on designing working subsystems. This investigation continued this trend by examining ignition system alternatives. Existing designs required spark plugs in each separate thrust tube to ignite premixed reactants. A single thrust tube could require the spark plug to fire hundreds of times per second for long durations. The goal was to minimize complexity and increase reliability by limiting the number of ignition sources. This research examined using a continuously propagating detonation wave as both a thrust mechanism and an ignition system requiring only one initial ignition source.

This investigation was a proof of concept for such an ignition system. First a systematic look at single tube geometric effects on detonations was made. These results were used to further examine configurations for splitting detonations, physically dividing one detonation wave into two separate detonation waves. With this knowledge a dual thrust tube system was built and tested proving that a single spark could be used to initiate detonation in separate thrust tubes. Finally, a new *tripping* device for better deflagration to detonation transition (DDT) was examined. Existing devices induced DDT axially. The new device attempted to reflect an incoming detonation to initiate direct DDT in a cross flow.

# **ALTERNATIVE PULSE DETONATION ENGINE IGNITION SYSTEM INVESTIGATION THROUGH DETONATION SPLITTING**

## **1 Introduction**

### ***1.1 General***

This project investigated the ability to split and utilize a propagating detonation wave as both an ignition source and a thrust producer. The resulting hardware could be directly employed in ignition system design. The research is aimed toward practical application, and therefore investigates using commercially available components rather than design optimization. Though system level effects were addressed in this work, the focus was on successful proof of concept.

The Air Force Research Laboratory Propulsion Directorate, Turbine Engine Division, Combustion Sciences Branch at Wright-Patterson AFB, Ohio, sponsored this research. All testing was conducted in the D-Bay test cell of Building 71 at Wright-Patterson AFB.

### ***1.2 Background***

A Pulse Detonation Engine, PDE, is a tube, filled with a combustible mixture, closed at one end, and ignited. The high pressure behind the detonation wave against the closed end of the tube and the rapid expulsion of products out the open end produces



thrust. Fig. 1.1 shows the test PDE located in Building 71 at Wright-Patterson AFB. Although the photographed configuration has four thrust tubes, testing for this project used one or two thrust tubes. The expelled flames visible in Fig. 1.1 are a result of detonation combustion.

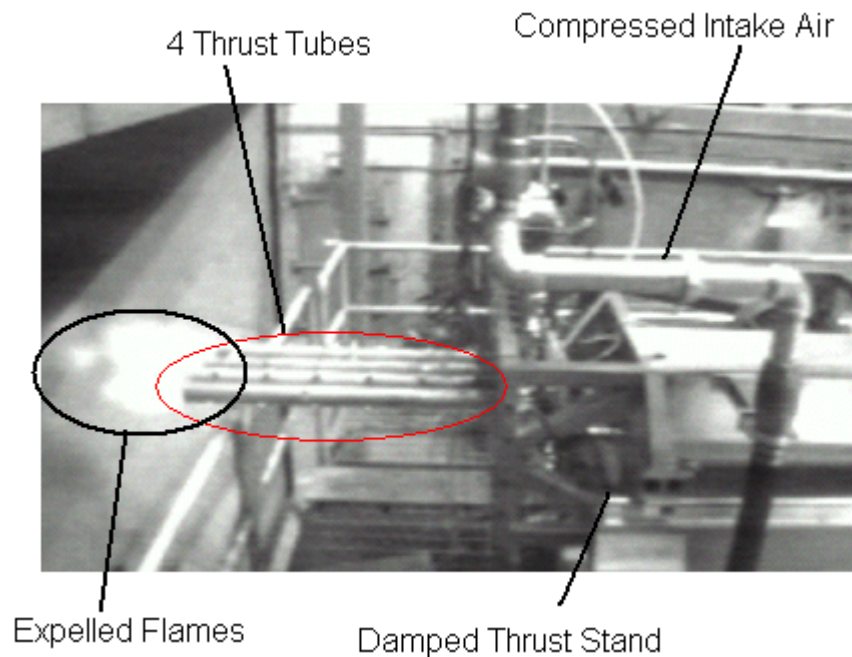


**Fig. 1.1 Building 71 Test Pulse Detonation Engine**

Detonation combustion differs from deflagration combustion. Typically, when a fuel air mixture is ignited, deflagration ensues (Kuo 1986:234). The observed flame speeds are on the order of one meter per second. Although there is a temperature rise from the chemical reactions, the pressure remains nearly constant, with only a slight decrease. Relative to deflagration, detonation has high wave speed and pressure rise. Detonations involve dynamic thermo-chemistry, multiple shock interaction, and three-

dimensional effects. Before leaping into the physics and corresponding theoretical development, historical perspective is needed.

The first indication of achieving detonation occurred during the late nineteenth century (Morrison, 1955: 1). Through experiments with combustible mixtures, the French physicists Vielle, Berthelot, Mallard, and Le Chatelier must have been astounded when they saw flame speeds, which for deflagration typically fix around one meter per second, on the order of one thousand meters per second. About 1900 Chapman and Jouguet independently proposed that this detonation wave was a shock wave followed by combustion. Furthermore, they suggested that the high temperatures produced through the shock rather than the typical diffusion process initiated the combustion. The special properties resulting from the detonation combustion process demanded a search for application.

Perhaps the first attempt to utilize detonations to produce thrust on a large scale came during WWII (Oppenheim, 1949). The German V-1 buzz bomb was a failed attempt to build a PDE. Rather than detonating, the V-1 only achieved deflagration and was relegated to a pulse jet. Since that time, the PDE was shelved in favor of the gas turbine. With the need for a cheap, reliable, and even disposable engine, the PDE has recently gained a resurgence of interest. The PDE may not require rotating machinery to operate. Ram air compression could provide aspiration and all of the thrust could be obtained through the change of momentum of the expelled gases. The only moving parts would be valving for introducing fuel and air into individual thrust tubes. The relative simplicity greatly reduces overall system cost while increasing reliability.

### 1.3 Problem statement

Due to the high temperatures and harsh vibrations, the integration of components and systems into a PDE has posed new challenges. One example is the ignition system. Using spark plugs for ignition was convenient for small scale testing at low frequencies. Larger scale testing and practical systems could require frequencies on the order of 100 Hertz for long durations. These requirements and the relative complexity of a multi-tube engine required a sophisticated ignition system that could endure this punishing environment.

The approach replaced the spark plug ignition with the hot exhaust gases trailing a detonation wave diverted from the main thruster tube. Fig. 1.2 shows how combusting reactants in thrust tube 1 could divert into a split tube. Part of the detonation would continue through the thrust tube to produce thrust. The second part would enter a split tube to ignite the reactant mixture in thrust tube 2. Combusting reactants from this thrust tube then split off and ignite a reactant mixture in a third tube, and so on. By the time the ignition source reaches the original thrust tube, fresh reactants would be available for detonation. The entire sequence would repeat as long as reactants were available.

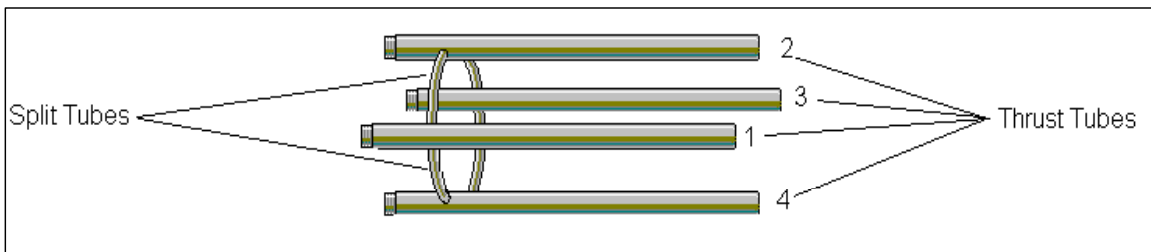


**Fig. 1.2 Concept art for integrated PDE ignition system**

#### ***1.4 Objectives***

The ability to split a propagating detonation wave and use the first component for thrust and the second component for ignition needs to be shown viable. To do this four phases of research were conducted prior to full-scale design:

1. Determination of single tube geometric effect on detonations.
2. Examination of split tube effects on detonations.
3. Construction of a dual thrust tube system with a single ignition source.
4. Examination of a new deflagration to detonation (DDT) tripping device.

## 2 Theory

### 2.1 Introduction

Pulse Detonation Engines (PDE's) employ detonation combustion rather than typical combustion, deflagration. This chapter establishes the detonation criteria for a stoichiometric H<sub>2</sub> and air mixture. A 1-Dimensional analytical solution is compared to semi-empirical results. Criteria for the expected wave speed, pressure, and pressure trace shape are established.

Stephan R. Turns defines detonation as “a shock wave sustained by the energy released by combustion (Turns, 2000:598).” Additionally, the high-temperatures from shock-wave compression initiate combustion. Thus, the detonation is the coupling of a hydrodynamic process, the shock wave, and a thermo-chemical process, combustion. Modeling of detonation waves has progressed considerably over the past century; however, a return to early approximation methods provides tremendous physical insight. A chronological investigation of different analysis methods includes:

- 1-D
- ZND Structure
- 3-D Detonation Mechanism - CFD

### 2.2 1-Dimensional detonation wave model

When Chapman attempted to explain detonations in 1899, he used a 1-D approach similar to a control volume analysis for determining downstream properties across a normal shock wave (Chapman, 1899:90-103). Figure 2.1 represents a detonation wave traveling from left to right in a constant area duct where the reference frame moves with

the detonation wave. Although the fully dimensioned detonation mechanism is quite complicated, this 1-D model is extremely useful and accurate for making certain predictions.

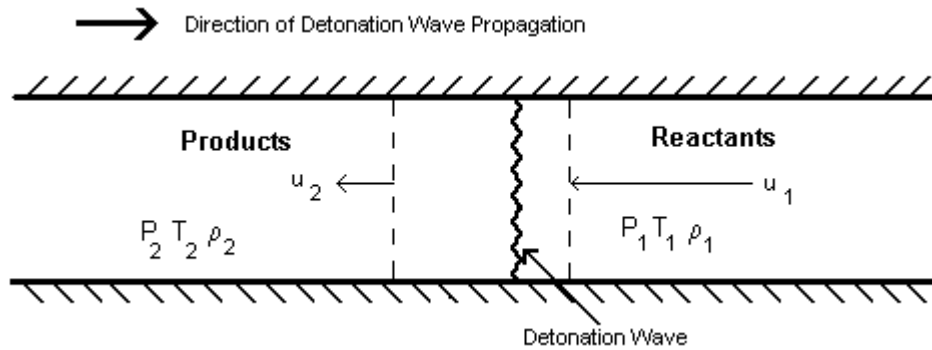


**Fig. 2.1 1-D detonation wave control volume analysis**

Starting with the control volume in Fig. 2.1 and the following assumptions, the conservation laws are reduced to the forms shown in Eqn.'s 1, 2, and 3. Additionally, by combining these equations and using the assumptions above, the Rayleigh and Rankine-Hugoniot relations, Eqn.'s 4 and 5, were developed. In Eqn. 3, the values for  $c_p$  and  $q$  depend on the type of fuel/oxidizer mixture and the equivalence ratio. (Appendix A contains a full development of these relations.)

#### ASSUMPTIONS

1-D	Calorically Perfect Gas
Steady	Negligible body forces
Constant Area	

#### CONSERVATION LAWS

##### Continuity

$$\dot{m}'' = \rho_1 \cdot u_1 = \rho_2 \cdot u_2 \quad [1]$$

**X-Momentum**

$$P_1 + \rho_1 \cdot u_1^2 = P_2 + \rho_2 \cdot u_2^2 \quad [2]$$

**Energy**

$$c_p \cdot T_1 + \frac{u_1^2}{2} + q = c_p \cdot T_2 + \frac{u_2^2}{2} \quad [3]$$

**Rayleigh Line Relation**

$$-\dot{m}'' = \frac{P_2 - P_1}{\frac{1}{\rho_2} - \frac{1}{\rho_1}} \quad [4]$$

**Rankine-Hugoniot Relation**

$$\frac{\gamma}{\gamma-1} \cdot \left( \frac{P_2}{\rho_2} - \frac{P_1}{\rho_1} \right) - \frac{1}{2} \cdot (P_2 - P_1) \cdot \left( \frac{1}{\rho_1} + \frac{1}{\rho_2} \right) - q = 0 \quad [5]$$

By fixing  $P_1$  and  $1/\rho_1$  to sea level standard conditions, the Rayleigh line relationship is examined. Equation 4 is solved for  $P_2$ . The downstream density is the independent variable in Equation 4. The  $\rho_2$  range is set to  $[0.5 \text{ kg/m}^3, 2.0 \text{ kg/m}^3]$  in order to determine the effect on the dependant variable, the downstream pressure,  $P_2$ , in the Rayleigh equation. Fig. 2.2 shows the effect of changing the mass flow rate. Clearly the mass flow cannot be smaller than  $0.0 \text{ kg/sm}^2$  or greater than infinity. Therefore, the bottom left and top right quadrants in Fig. 2.2 are unattainable. The  $1.72 \text{ kg/sm}^2$  represents the 1-D approximate mass flow rate for a stoichiometric  $\text{H}_2$  and air mixture.

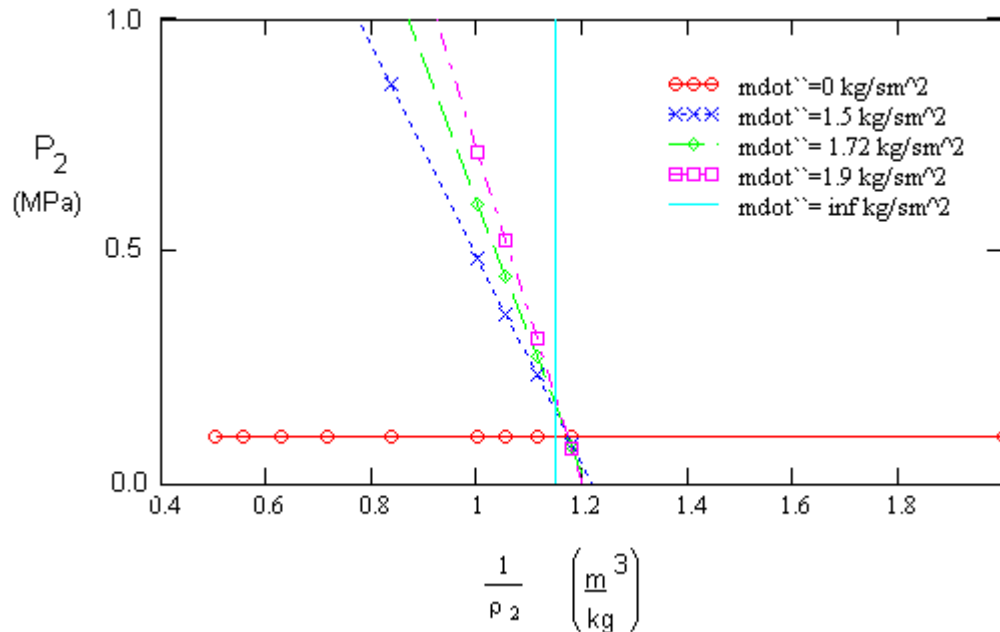


**Fig. 2.2 Raleigh Line Eqn. 4**

The Rankine-Hugoniot curve is developed by solving Eqn. 5 for  $P_2$ . Sea level standard conditions set the values for  $T_1$ ,  $P_1$ , and  $\rho_1$ . The other parameters set are  $\gamma = 1.4$  and  $q = 3.421 \text{ MJ/kg}$ . A 1-D analysis of a first order  $\text{H}_2$  and air reaction mechanism provided the value for heat release,  $q$ . The curve in Fig. 2.3 results from allowing  $\rho_2$  to range from  $0.5 \text{ kg/m}^3$  to  $2 \text{ kg/m}^3$  and solving for  $P_2$ . The scales have been removed to allow for trends to be discussed. Here, the curve is divided into 5 sections. These are solutions to the combustion equation. The first region represents strong detonations. Region II represents weak detonations. Between these two is the upper Chapman Jouguet point. This point denotes the properties of a stable detonation (Williams 1965:35). Its counterpart, the lower Chapman Jouguet, is the stable deflagration solution, which provides the properties seen with typical combustion.



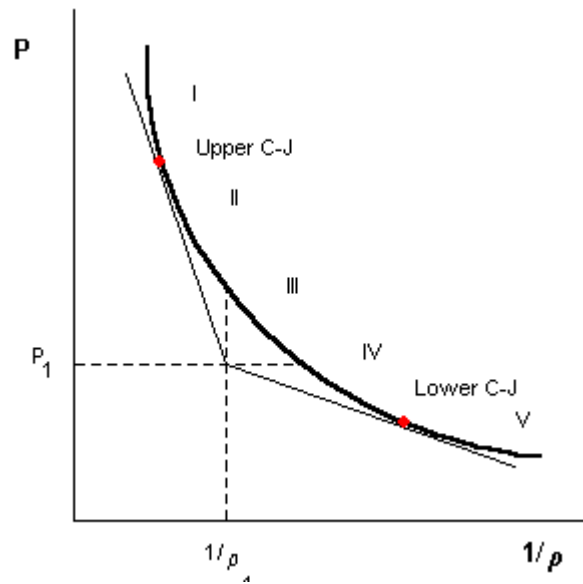


Fig. 2.3 Rankine-Hugoniot curve

Table 2.1 explains what each of the different segments on the curve represents.

Table 2.1 Properties of Hugoniot curve (Williams 1965:35)

Region	Combustion	M2	
<b>Upper Branch</b>			
<b>Segment I</b>	Strong Detonation	<1	Needs special experimental conditions
<b>Upper C-J Point</b>	C-J Detonation	1	Waves propagating in tubes
<b>Segment II</b>	Weak Detonation	>1	Requires special gas mixtures
<b>Segment III</b>	Unrealizable		
<b>Lower Branch</b>			
<b>Segment IV</b>	Weak Deflagration	<1	Common
<b>Lower C-J Point</b>	CJ Deflagration	1	Not observed
<b>Segment V</b>	Strong Deflagration	>1	Not observed (wave structure limited)

Given the upstream properties, the Raleigh and Rankine-Hugoniot relations were solved for  $P_2$ ,  $\rho_2$ , and  $T_2$ . Each mechanism upstream and downstream of the reaction was considered to get a quantitative feel for the difference between normal shocks, detonations, and deflagrations. Table 2.2 shows properties for a pre-mixed stoichiometric reaction of  $H_2$  and Air at 25 deg C and 1 atm. Normal shock and detonation values were

calculated using the previously described 1-D analysis and assuming  $P_2 \gg P_1$  and neglecting dissociation. Laminar flame speeds were taken from Glassman (Glassman, 1996:578). The other deflagration properties were from Friedman using several different fuel-air mixtures (Friedman, 1953: 349-354).

**Table 2.2 Comparison of normal shock, detonation, and deflagration properties**

<b>Property</b>	<b>Normal Shock</b>	<b>Detonation</b>	<b>Deflagration</b>
M1	4.9	4.9	0.0001-0.03
M2	0.42	1	4-6
$P_2/P_1$	28.3	15.3	~0.98
$T_2/T_1$	5.7	9.9	4-16
$\rho_2/\rho_1$	5	1.8	0.06-0.25
$u_1$ (m/s)	2012	2012	1.7
$u_2$ (m/s)	405	1112	
$u_2/u_1$	0.20	0.55	

Immediately certain trends became apparent. The normal shock and detonation shared many qualities. In fact, the principal difference between downstream properties was that downstream of a normal shock the velocity was subsonic, but for an upper CJ detonation, the velocity is the speed of sound (Turns, 2000:599). Clearly the deflagration only shared the increased temperature at state 2. In contrast to deflagrations or detonations, explosions have an extremely fast heat generation rate, but without requiring the passage of a combustion wave through the exploding medium (Kuo, 1986:233).

An approximation method was used in this 1-D analysis to determine  $u_1$ , the detonation wave velocity. This was a first order approximation based on Turns's assumption that  $P_2 \gg P_1$  (Turns, 2000:609). Kuo provides 2 methods, a trial-and-error method, and a Newton-Raphson iteration method for determining the wave speed without making the assumption that  $P_2 \gg P_1$ . As shown in the next section, the first order

approximation was accurate within 2% of semi-empirical data for this mixture and equivalence ratio.

Perhaps one of the most important pieces of information from this Rankine-Hugoniot investigation was the effect on thrust. The upper CJ point corresponds to the point along the solution curve of minimum mass flow rate, the tangent Raleigh line intersection. Though Turns and Kuo do not investigate the design effect, the simplified rocket equation,  $\text{Thrust} = \dot{m} u_e$  provides a baseline. The rocket equation is for a continuous process, but it still captures the important parameters in the unsteady detonation at high frequency. In order to increase thrust, the mass flow rate and the exit velocity have to increase. Going toward a strong or weak detonation would increase the mass flow rate. Only the strong detonation would have products that travel at subsonic velocities away from the detonation wave. The exit velocity would be closer to the detonation wave velocity behind a strong detonation. Therefore, strong detonation combustion would provide more thrust than a CJ detonation. Unfortunately, a strong detonation is only transient (Glassman 1996).

### ***2.3 Zeldovich, von Neumann, Döring (ZND) wave model***

The 1-D control volume analysis only incorporated part of the physical structure of a detonation wave. In the 1940's Zeldovich, von Neumann, and Döring independently proposed modeling a detonation wave as a shock wave followed by combustion (Turns 2000:613). This simple structure was named the ZND detonation wave after these three individuals. Though this simplified the actual structure, it closely modeled the observed pressure trace produced as a detonation wave passed a pressure transducer. Since the

shock wave region was thin, the chemical reactions occurred in a thicker region behind the shock wave. The combustion zone was further separated to reveal an induction zone, slow chemistry, and a reaction zone, fast chemistry with large changes in properties (Kuo 1986:261). The properties of this model are shown Fig. 2.4.

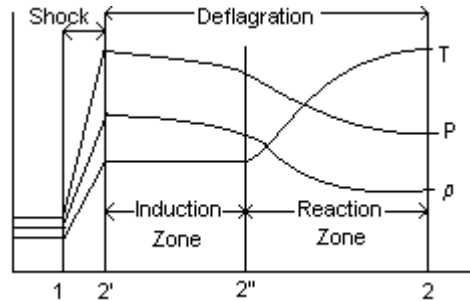


**Fig. 2.4 Gas properties through ZND structure**

As well as showing the flow properties in this small region, the ZND analysis reveals the path the reactants take to reach the upper CJ point (Kuo 1986:262). Fig. 2.5 shows several potential paths to achieve this condition on the Rankine-Hugoniot curve. Path *a* lacks the compression necessary to get the temperature rise required for chemical reactions. Path *b* requires fast chemical kinetics. Path *c* requires slow chemical kinetics. Path *d* is the most likely. It represents adiabatic compression where the peak is called the von Neumann spike. The CJ point has a pressure between 70-90% of the peak. The actual maximum pressure observed during experiment was less than the predicted max of the von-Neumann spike.

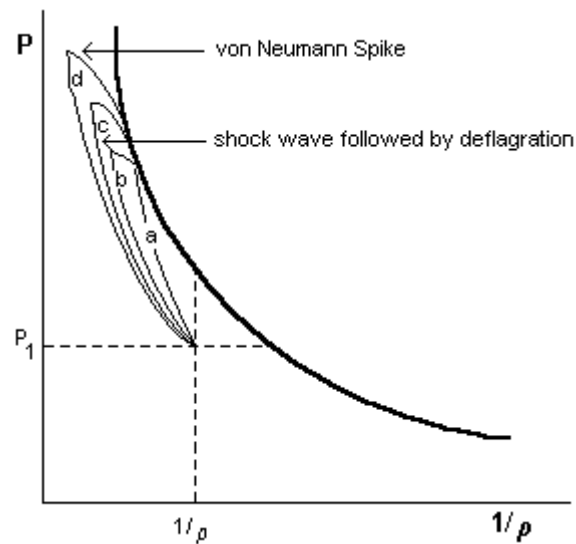


**Fig. 2.5 Von Neumann spike**

A classic utility of this simple model is the determination of the detonation velocity. As an example, consider  $H_2$  for fuel and compressed air as the oxidizer. By treating the detonation as a ZND structure, the detonation velocity was predicted by analyzing a balanced thermo-chemical equation and then applying normal shock relations. The closed form solution is located in Appendix B. From this analysis, the combustion released 3 MJ/kg. The calculated velocity is 2012 m/s. This value is extremely close to the semi-empirical value of 1968 m/s published by Soloukhin (Soloukhin, 1966:136). The predicted value improves by accounting for dissociation, which lowers the heat release and decreases the wave speed. Table 2.3 compares values predicted using this 1D model and Soloukhin's data. Here the state 2' properties follow directly after the von Neumann spike. The state 2 properties follow after the combustion zone.

Table 2.3 ZND Properties for H<sub>2</sub> and air

Property	State 1	State 2`	State 2	Property	Soloukhin	% Difference
M	4.9	0.42	1	M1	4.83	-1.4%
T(K)	298	2954	1696	T2(K)	2951	-0.1%
$\rho/\rho_1$	1	5	1.8	$\rho_1/\rho_2$	1.805	0.3%
P/P1	1	28.3	15.3	P2/P1	15.62	2.0%
$\gamma$	1.401	1.401	1.236	$\gamma_2$	1.245	0.7%

This analysis provided the key for determining detonation quality for this thesis. Since the analysis verified the reasonability of Soloukhin's data, his published values were used as criteria for testing. Wave speeds and pressures were measured at several points along any test configuration. For wave speed, 1968 m/s is used. Using 15.62 as the pressure ratio across the detonation wave and 14.7 psi, 101.3 kPa, as a baseline pressure, the P<sub>2</sub> pressure should have be at least 229.6 psi (1.583 Mpa) following the passage of a detonation wave.

#### 2.4 3-Dimensional detonation wave structure

As noted throughout this discussion, the actual detonation mechanism and structure is quite complicated. A realistic understanding of results can only be discussed after considering detonation development and fully dimensioned structure. The actual structure involved a fully dimensioned process that included thermo-chemistry and multiple shock interaction. "According to Strehlow, the first evidence of multidimensional wave structure was obtained in 1926 by Campbell and Woodhead" (Kuo, 1986:263). They noted the non-steady and 3-dimensional nature of detonations. Denisov and Troshin in 1959 were the first to capture the visible cell pattern that defined detonation passage. They coated the interior wall with soot that collected the record of

the passing detonation. Example photos of smoked-foil records are available in Kuo (Kuo 1986:264-265) The physics of this pattern is the intersection of Mach-stem, reflected, and incident shock waves. At this intersection, called the triple point, the heightened energy level prompts ignition. This detonation structure depends on the geometry of the enclosure (Turns, 2000:617) Fig. 2.6 shows the structure of the Mach stem through a confining ramp. Fig. 2.7 shows a CFD model of the cell structure, which acts as time trace of the motion of the cell triple point.

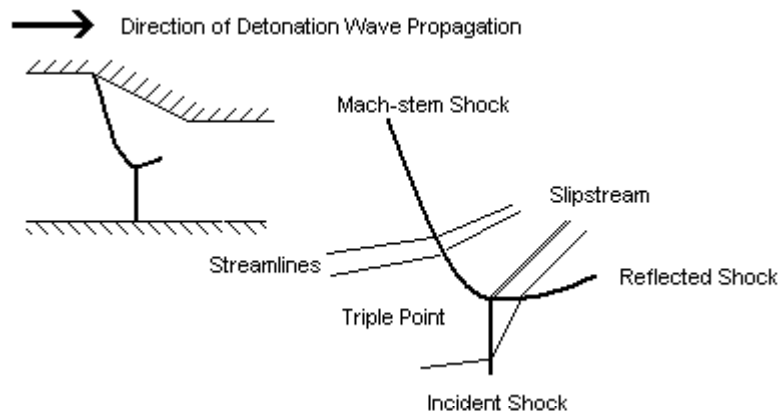


**Fig. 2.6 Mach stem (cell triple point)**

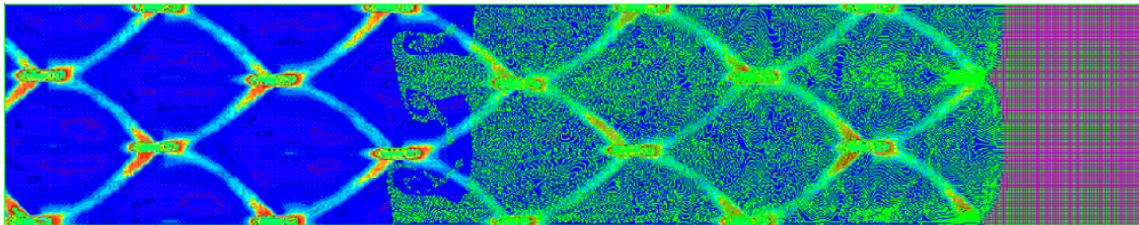


**Fig. 2.7 Cell structure (Katta 1999)**

This *steady* detonation structure only represents an established detonation. With the continual advancement in experimental instrumentation, the deflagration to detonation transition (DDT) mechanism has been recorded using laser schlieren

photography. Kuo has many examples of these studies (Kuo 1986:267-273).

Additionally, he summarized this DDT mechanism in a seven-step process outlined below (Kuo, 1986:267-273). Fig. 2.8 shows some of the key physical features of this DDT mechanism.

#### **2.4.1 Detonation to deflagration transition (DDT) mechanism**

- 1) Compression waves form ahead of an accelerating laminar flame.
- 2) Waves coalesce into a shock. (Fig. 2.8a)
- 3) Shock moved gases tripping a turbulent flame brush.
- 4) Inside turbulent reaction an “explosion in an explosion” formed transverse waves: superdetonation (downstream) and retonation (upstream).
- 5) Spherical shock developed. (Fig. 2.8b)
- 6) Shock front, retonation wave, and reaction zone interacted. (Fig. 2.8c)
- 7) *Steady wave*, ie the CJ detonation, established.

Devices designed to trip a DDT mechanism will be addressed in section 3.1.

#### **2.4.2 Modes of DDT**

To close our discussion on physical features, four different modes of DDT have been noted (Kuo 1996:273). Each mode is based on the location of the “explosion in an explosion”:

- 1) Between flame and shock front
- 2) At flame front
- 3) At shock front
- 4) At contact discontinuity



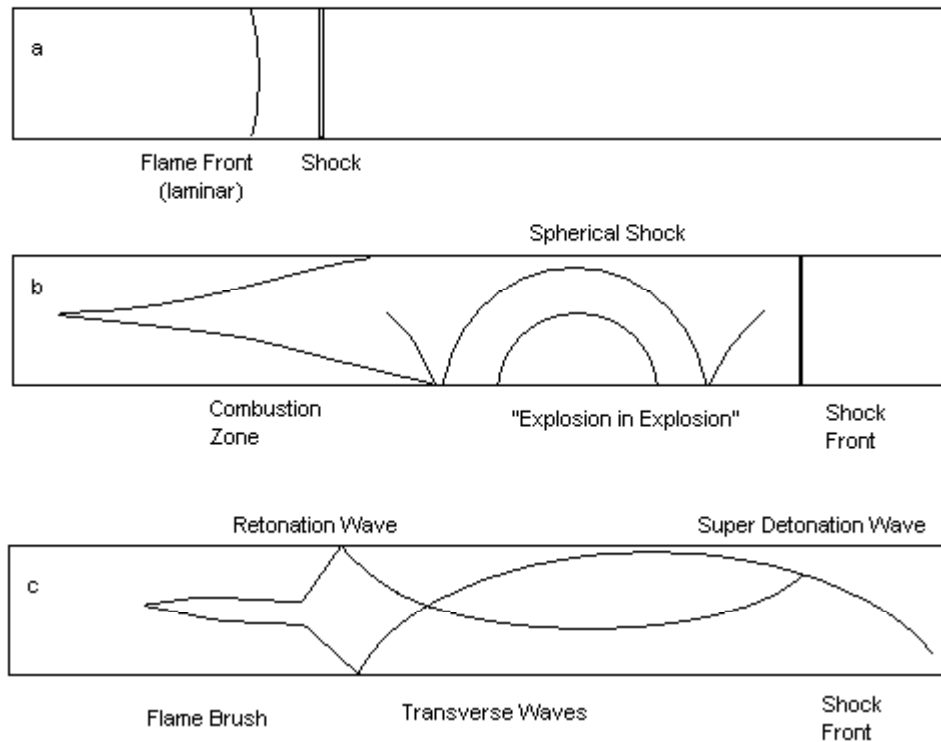


**Fig. 2.8 Deflagration to detonation transition (adapted from Kuo 1986 268:269)**

Using CFD for designing configurations before cutting metal for an experiment reduces research time and cost. Dr. Vish Katta had built an in-house program (UNICORN) that actually shows the propagation of the detonation triple points as seen in Fig. 2.7 (Katta, 1999). A time history of this motion matches the cell structure captured in smoke-foil experiments. Clearly with all of the detonation wave physical features, especially during transition, the CFD is limited. CFD, however, was currently the only way to make predictions on complicated geometries, especially with 3-D effects. Divergent cross-sections, 90-degree split sections, and split sections with a scoop have been modeled using CFD.

### **3 Materials and Method**

#### ***3.1 Detonation initiation***

In order for a pulse detonation engine (PDE) to function properly, the previously described deflagration to detonation transition (DDT) must occur. Additionally, it should occur in the least amount of time and space possible. The V-1 buzz bomb has shown that application is not a simple matter. Despite this, AFRL's research has paid off (Shelkin 1940; Schauer 2001; Katta 1999). Several DDT tripping geometries induced detonations. A pipe of sufficient length that can accommodate at least one cell width is necessary. A Shelkin spiral generates acoustic reflections that interact and form hot spots. These hot spots are the ideal setting for detonation transition. A spiral is the device of choice to ensure consistent detonations in the shortest distance, about 5 pipe diameters axially down a 2-inch diameter pipe.

#### ***3.2 Engine cycle***

Given a means to produce detonations, how could one produce thrust? Actually this is fairly simple. Fig. 3.1 shows a PDE cycle. First a fuel air mixture is injected into the thrust tube. Then the mixture is ignited and quickly transitioned to a propagating detonation wave. Finally, a charge of compressed air is used to force out remaining products and separate hot products from fresh reactants. This cycle repeats at a desired frequency, number of cycles per second. In fact, over a published range of frequencies, from 10-40 Hz, the thrust varies linearly with frequency (Schauer 2000). This means the engine can be throttled by controlling frequency rather than fuel or airflow rate, the conventional situation. Perhaps the most attractive feature of this cycle is that current

automotive engine valving can be used. This is the case in the AFRL setup described in section 3.4.

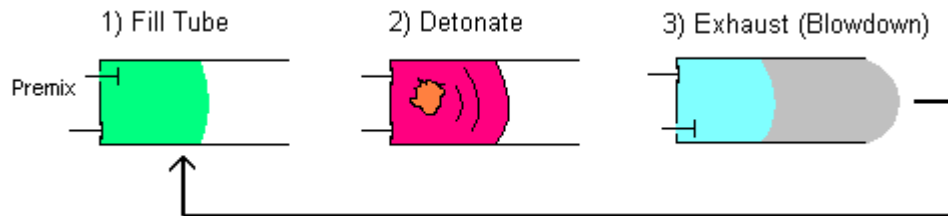


**Fig. 3.1 PDE engine cycle**

### ***3.3 Integrated propulsion system***

The engine cycle described above is for a single thrust tube. However, valving for numerous tubes can be employed. Though one tube may suffice, as with deliverable munitions, acoustical concerns and the desire for steady thrust make a multi-tube arrangement the probable design for vehicles.

### ***3.4 Research facility***

The Air Force Research Laboratory Combustion Sciences Branch (AFRL/PRTS) has built the primary research engine. The main components are illustrated in Fig. 3.2. All points of operation are monitored and controlled virtually using National Instruments LabVIEW™. Metered compressed air and fuel enter the engine. The reservoir pressure is monitored and an upstream critical orifice is used to ensure a choke point. The mass flow rate can then be maintained. For smaller volume configurations, smaller orifices can be used to ensure choking. A General Motors Quad 4, Dual Overhead Cam (DOHC) cylinder head, commonly used in the Pontiac Grand Am, provides the necessary valving.

The engine is mounted to a damped thrust stand that measures axial thrust. The engine can run up to four thrust tubes simultaneously (Schauer 2000). The entire system is controlled and monitored remotely including: lubrication, valve drive speed, fuel flow, main combustion air flow, purge air flow, timing, ignition delay (time of spark within detonation phase of PDE cycle), low and high frequency data collection, and automatic shutdown in the event of a critical system failure. Aside from physical experimental changes, certain key parameters were varied to optimize for configuration: tube fill fraction (amount of total volume filled during fill and purge phases), equivalence ratio ( $\phi$ ), frequency, and ignition delay. A complete description of the test facility is in “AFRL/PRSC Pulse Detonation Engine Program” (Schauer 2000).

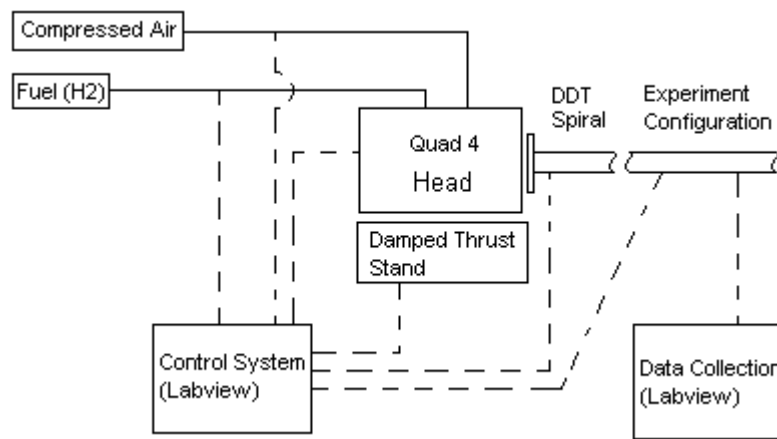


**Fig. 3.2 Schematic of research facility**

### **3.5 Data acquisition**

The data acquisition software written by Mr. Jeff Stutrud allows a preview of wave speeds, thrust, and pressures, and shows each transducer pressure trace (Stutrud 2001). This gives immediate feedback on the health of the acquisition system while

offering a first look at experimental results. The program uses a bottom constant threshold method for determining wave speeds. The bottom method uses the first crossing of a pressure trace over a threshold to signal detonation passage. The threshold is held constant, ignoring thermal drift. This method provides quick feedback for on the fly adjustments, but was not used for post-processing. The actual post-processing method will be discussed in section 4.1.

The data acquisition system acquired data at 4 million data points per second. The pressure transducers used were PCB Piezotronics Inc. model 102M232's series 111A general purpose miniature sensors (PFS 2000). These transducers have pressure ranges from vacuum to 3000 psi. The sensor useable frequency range is between 20 kHz and 30 kHz with a resonant frequency of 130kHz.

### ***3.6 Experimental configurations***

In order to make informed design decisions, a better understanding of geometric effect on detonation physics was required. The use of commercially available parts minimized time from design to build. Since the existing engine hardware mates to 2-inch pipe, this was one of the diameters of choice used for thrust tubes. In order to limit scope, only one other diameter was used to model the split tube. The second diameter was minimized to burn the least amount of fuel and air, since it was not meant to produce thrust. However, the diameter has to carry at least one detonation cell width, which for H<sub>2</sub> and air was 15 mm. A ¾ inch diameter tube fit the above criteria. Chapter 5 contains recommendations for considering other diameter pipes based on CFD findings.

### 3.6.1 Single tube configurations

Before examining configurations that split detonations, a complete baseline of single tube effects was conducted. The goal was to determine the most successful geometry to encourage a detonation wave to propagate through a split. A systematic investigation included converging, diverging and 90-degree turn geometries. Additionally, downstream geometric effects were examined via a 2-inch to 1 ½ inch reducer acting as a convergent nozzle. Although intuitively a gradual transition from 2 inch to ¾ inch tubing seemed the most promising to maintain a detonation, the effect of reflected shocks and encouragement of hot spots caused by the step boundary of a 2-inch to ¾ inch bushing could not be ruled out. Rather than rely solely on theory and CFD results, some straightforward testing provided valuable and unexpected information.

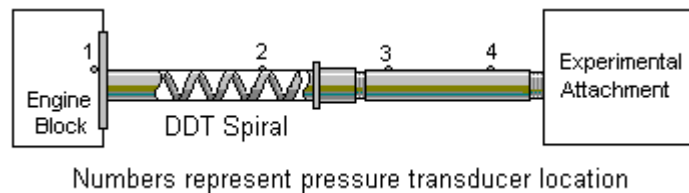


**Fig. 3.3 Baseline test configuration**

Fig. 3.3 shows the baseline test configuration. The engine block held pressure transducer 1 in the head of cylinder 1. A cutaway view reveals the 12-inch DDT spiral. This was the device to initiate DDT. The detonation wave propagated from left to right. Pressure transducers 3 and 4 were used to monitor the wave speed to ensure the wave speed entering the experimental attachment was at upper Chapman Jouget. The experimental attachments are divided into separate tests. Fig. 3.4 shows the first test matrix. Here baseline configurations, a and e, determined effects of downstream

geometries, b and f; step convergences, c and g; and gradual transition convergences, d and h.

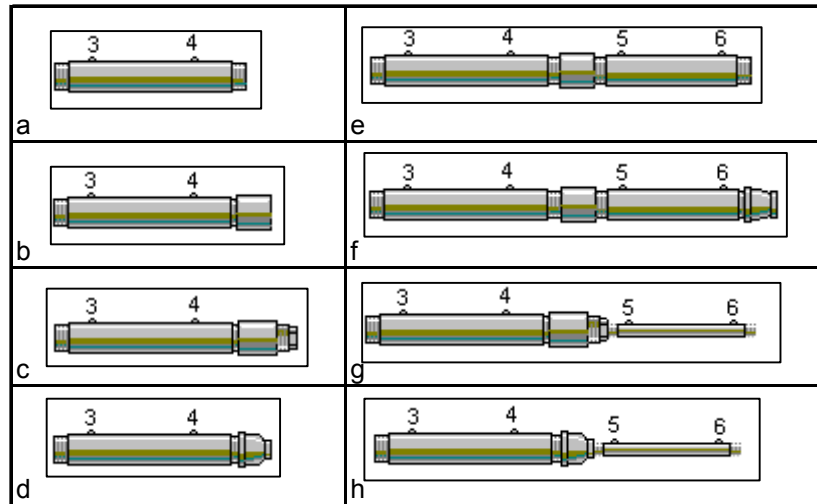


**Fig. 3.4 Test matrix 1A: axially converging geometries**

Test matrix 1B modeled potential geometries to use for split tube to thrust tube divergence. Here the baseline was a straight  $\frac{3}{4}$  inch tube shown in Fig. 3.5 a. Of interest were questions of expanding detonations through gradual transitions, b and c, vs. step expansions, d and e. Additionally, downstream geometric effects were investigated using a 2-inch to 1  $\frac{1}{2}$  inch reducer as a converging nozzle, c and e.

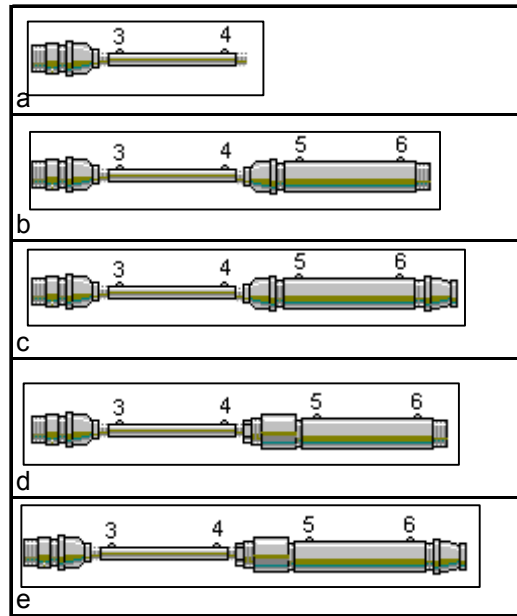


**Fig. 3.5 Test matrix 1B: axial diverging**

The final test matrix, 1C, for the first objective examined 90 degree turns. In this case, a 2-inch 90 and a 3/4-inch 90 provided the commercially available turn mechanism. Fig. 3.6 shows the geometries tested. Other configurations were considered, but cancelled after examining the results from Test Matrix 1A. The examples in a and e examined directly turning a detonation. Convergence immediately following a turn was tested by c and d, while e and f looked at expanding turns. The configuration shown in b looked at the effect of downstream geometry. CFD predicted that this expansion would dissipate a detonation (Katta, 2002). This would seemingly nullify the need to test the configuration in Fig. 3.6 e and f. However, due to previous experimental success with turning, configurations e and f were tested.



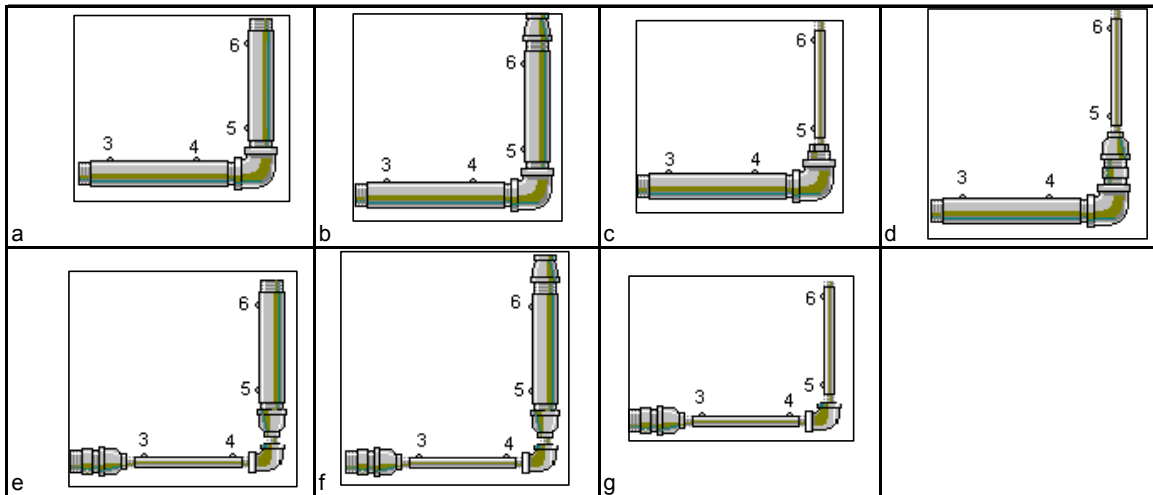
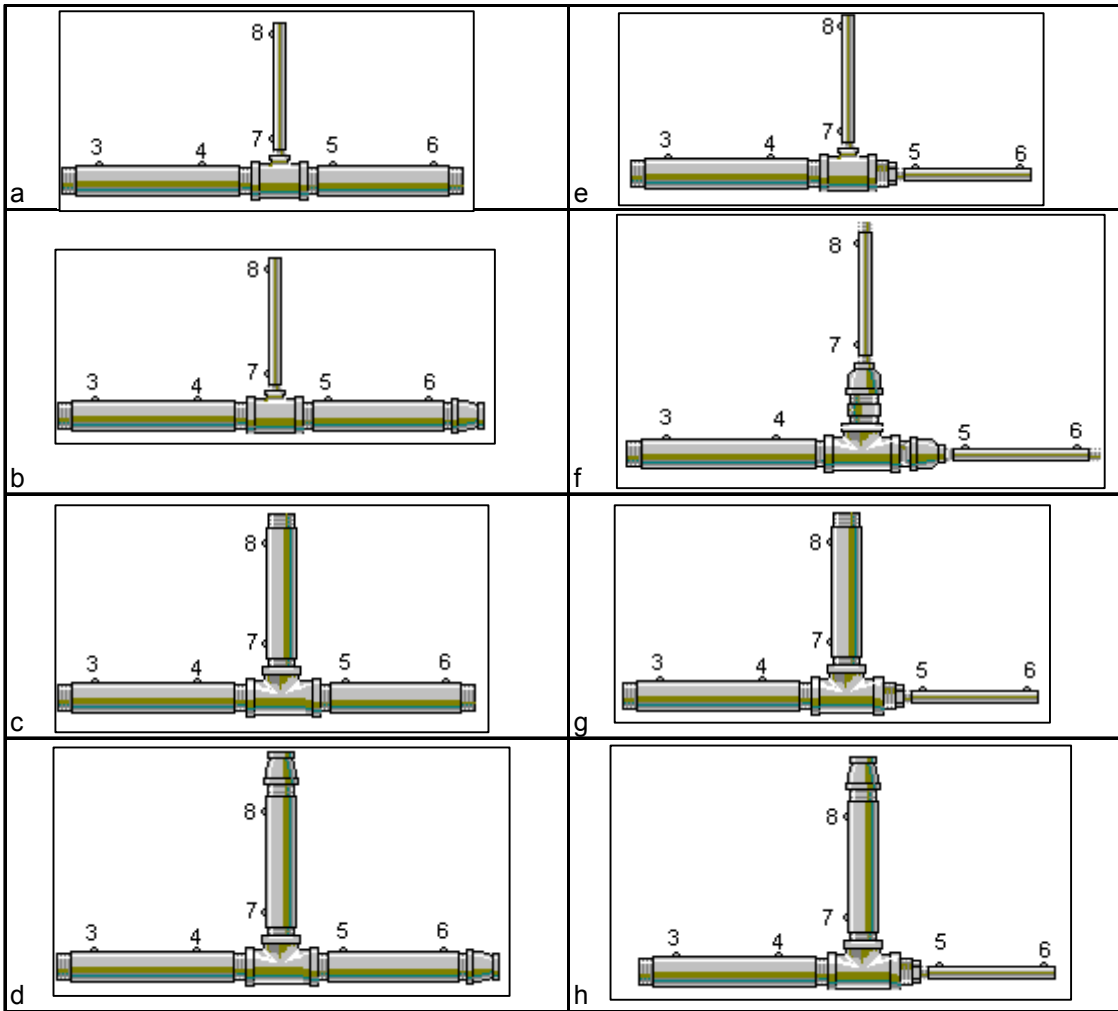


Fig. 3.6 Test matrix 1C: 90-degree turns

### 3.6.2 Split tube configurations

Once the configurations of objective 1 were tested, more complex splitting configurations were examined. A second systematic investigation was conducted to attempt a detonation split. The same principles applied, so that only commercially available parts were used. This limited the design to 90-degree splits via tees, and 45-degree splits via wyes. The findings from objective 1 were critical in determining the cause of physical phenomena that occurred in the splits.

Fig. 3.7, test matrix 2A, examines splits using tees. Although this right angle split geometry seems difficult for a detonation wave to negotiate and maintain strength, it provides the least complication to implement in a large-scale design.



**Fig. 3.7 Test matrix 2A: tee geometries**

Configurations a and d most closely modeled the Fig. 1.2 concept art. The four geometries on the right attempted to encourage the detonation into the split, *i.e.* tubes denoted by transducers 7 and 8. The effect of converging downstream conditions was examined by b, d, and h. The gradual transition in f was compared to the step transition in e.

Similar configurations employed in Fig. 3.8 replace tee connections with wye connections. Had the tee configurations failed to split a detonation, the wye could have proved easier for a detonation wave to negotiate. A comparison between tee and wye effects aided in the design process. Along with the geometric testing regime, an examination of fill fraction effects was conducted using Test Matrix 2A a and b, and Test Matrix 2B a and b, at fill fractions of 1.0 and 1.25. In addition to wave speed and pressure sensitivity to fill fraction, a comparison of effectiveness of fill fraction versus nozzle effects was made.

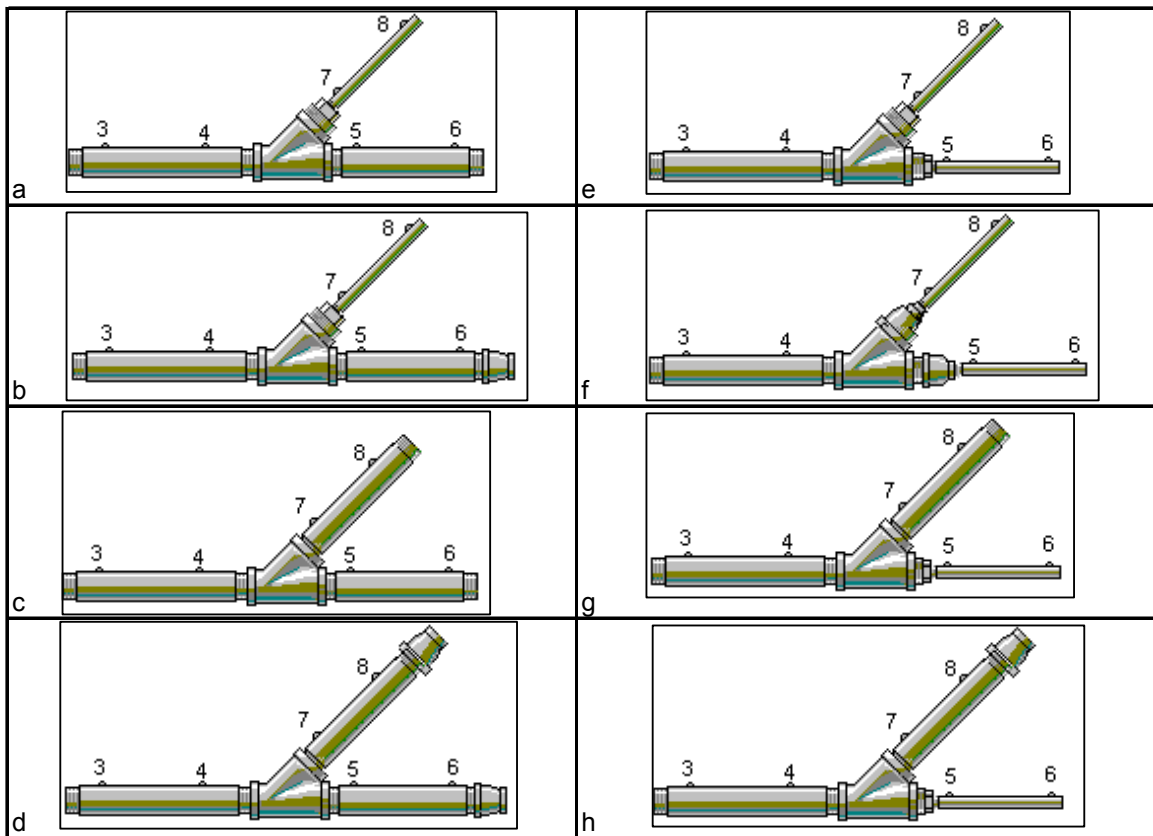
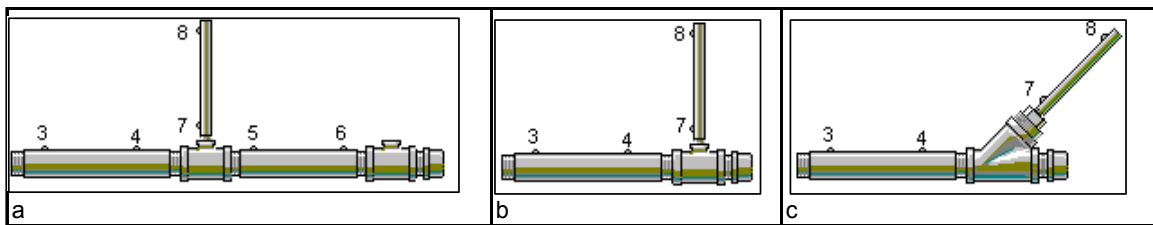


Fig. 3.8 Test matrix 2B: wye geometries

Along with a variety of configurations designed for splits, several geometries were tested using a 2-inch cap. These are shown in Fig. 3.9. The common inlet configuration in Fig. 3.3 applied. Here, the potential effect of high downstream pressure conditions was modeled. The tee in configuration Fig. 3.9 a acted as a pressure-release. The geometry in c tested a detonation's ability to negotiate a 45-degree turn. Since the 90-degree turns tested above are slightly different, the configuration in b acted as a baseline for comparison.



**Fig. 3.9 Test matrix 2C: capped geometries**

### **3.6.3 Dual thrust tube - single ignition source**

Objective 3 was the proof of concept. Here a double thrust tube configuration shown in Fig. 3.10 connected to the engine block. This configuration resulted directly from testing outcomes observed in objects 1 and 2. The two thrust tubes modeled one section of a multiple thrust tube array. Additional contingency designs were considered, but were not needed. Obviously, the full array would require extensive design for the required manifold and valving. Achieving detonation in the two-tube configuration with only one ignition source was a critical step toward total system design.

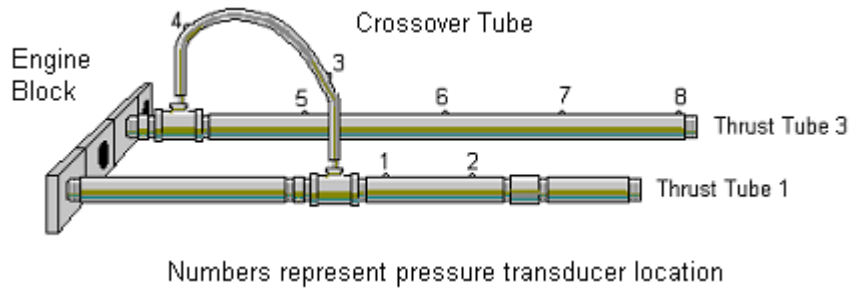


**Fig. 3.10 Dual thrust tube design**

An important challenge in testing this configuration was ignition timing. Due to the fixed valve phasing, the window of opportunity to fire either spark was limited. Fig. 3.11 shows the offset of cycles between the first and the third tube positions. The thrust tubes were numbered according to engine block location. These positions were chosen on the engine block because the valve position is only 90-degrees out of phase. (Typical engine spark plug firing order was 1-3-2-4 in 90 degree increments.) To fire spark 1, the cycle had to be within the burn cycle of tube 1. Additionally, tube 3 had to complete the fill cycle before the flame front completed traversing the crossover tube. Depending on the amount of time for the detonation to travel through the crossover to tube 3, this was just milliseconds after spark plug 1 fired.

In order to be conservative, the firing window was initially limited to the beginning of the tube 3 burn cycle. During actual testing, slightly more aggressive earlier firings were attempted, while being wary of backfiring. Table 3.1 provides ignition delay times based on run frequency. The delay times were measured from the beginning of the corresponding cylinder burn phase. Here, the effect of ignition delay on performance was systematically tested by varying ignition delay and measuring resulting thrust and wave speeds.

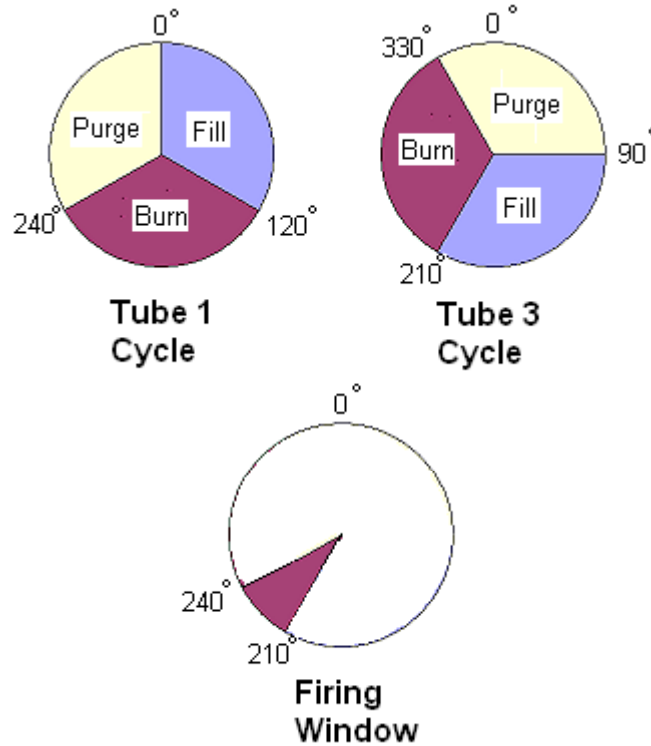


Fig. 3.11 Cycle diagrams and firing window

Table 3.1 Ignition delay time vs. frequency

	Frequency (Hz)	10.00	20.00	30.00	40.00
	Cycle Time (ms)	100.00	50.00	33.33	25.00
Spark Plug 1	minimum delay (ms)	25.00	12.50	8.33	6.30
	maximum delay (ms)	33.33	16.70	11.11	8.33
Spark Plug 3	minimum delay (ms)	0.00	0.00	0.00	0.00
	maximum delay (ms)	8.33	4.20	2.80	2.10

A narrow window is available for the firing sequence to be successful. For example, while running at 30 Hz, the firing window for spark plug 1 is only 2.80 ms. Though the configuration is intended to work while firing only spark 1, a thorough matrix was investigated consisting of firing spark 1 only, spark 3 only, and both sparks.

#### **3.6.4 DDT trip device**

This objective represents a potential avenue of research for optimizing the ignition system design. An alternate tripping device from the DDT spiral was examined. Although the DDT spiral clearly accelerated detonation transition, the dual thrust tube design offered an opportunity to greatly reduce transition length. A reflector was placed in the path of the detonation flow through the crossover at the entrance to thrust tube 3. The goal is to initiate a series of reflected shocks that would strengthen the detonation at the entrance of tube 3. It is hoped this strengthening of the detonation would in turn avoid potential quenching due to the large volumetric expansion.

## 4 Results and Analysis

### 4.1 *Data post processing*

In-house developed software is used for post processing (Parker 2001). It allows the user to choose between a top, middle, and bottom method for determining wave speed. Each method establishes the time of detonation passage. The bottom method looks for the first time a pressure trace crosses a chosen threshold. The top method looks for the peak pressure, and the middle method uses an algorithm that looks at these points and slopes. A sensitivity analysis of method vs. threshold has been conducted. For user selected thresholds of 50, 100, 150, and 200 psi, the top and middle method independently maintained results within 3%. The bottom method was greatly dependant on chosen threshold varying by more than 10% in some cases. Additionally, middle method results are typically published. Therefore, the middle method with a threshold of 100 psi was used for post-processing all data. Additionally, a linear regression method was employed to account for thermal drift.

The pressure across a detonation cell can range from 16.25 atm. to 116.5 atm (Katta, 1999). Since a single cell is slightly shorter than one inch, there are very large pressure gradients. Unfortunately, the pressure transducer diameter is 3/8 inch, therefore, these large pressure gradients will be averaged over a surface area on the same order as the cell size. This makes a typical discussion on uncertainty difficult. Even though the sensor may be accurate within 10 psi, the physics of the detonation cell can inherently produce much larger error.



A compilation of data is provided in Appendix C. Table 4.1 shows an example of results from Test Matrix 1B Fig. 3.5 a. Each configuration was run at least twice for repeatability. Each run was post-processed separately. The data was compared. If there was a discrepancy between runs, the average of each individual detonation wave speed was used. Data was usually acquired over a 0.5 s time period. Since the majority of tests were run at 20 Hz, 10 detonation peaks were normally acquired. However, for any run that measured something other than 10 detonations, the value was listed.

The first column lists the 2 ports used to calculate wave speed. The next two columns give average wave speed and standard deviation. The ‘% used’ column keeps track of the percentage of wave speeds used in determining average speed. Since the algorithm discarded wave speeds below 50 m/s and above 3000 m/s, several data points were ignored as outliers. In this column, values closer to 100% had fewer outliers.

**Table 4.1 Example data table: results test matrix 1B configuration a**

<b>Test Matrix 1B Configuration a Run 1</b>						
	<b>WAVE SPEEDS</b>					<b>PEAK PRESSURE</b>
Pressure ports	Average	Stdev	%used	% CJ	Transducer	(psig)
	(m/s)	(m/s)	of 10 total			
1 to 2	N/A	N/A	N/A	N/A	1	130.517151
2 to 3	2073.35	73.923	100%	5%	2	1116.443481
3 to 4	2829.77	121.86	100%	44%	3	459.733215
					4	527.817749
<b>THRUST</b>	7.42 lb					





The ‘% CJ’ column used the formula in Eqn. 6 to normalize the wave speeds. Wavespeed was the average wave speed in m/s. This column described the error of average wave speed from expected CJ speeds.

$$\frac{\text{wavespeed} - 1968\text{m/s}}{1968\text{m/s}} \cdot 100\% \quad [6]$$

Once the value was calculated, an engineering decision was made to determine the quality of the wave speed. In this case the values in Table 4.2 were used.

Rather than trying to decipher the information in each of the tables in Appendix C, a more convenient method was employed. The symbols in Table 4.2 were placed directly on the test configuration schematic. In this way, rapid comparison between geometry and effect to wave speed was possible. Additionally, for any average pressure that drops below the expected state 2 ZND value of 229 psig, the pressure transducer was circled. Therefore, if a wave speed showed ‘bad’ and there was a circle around either one or both corresponding transducer numbers, the system was not detonating.

**Table 4.2 Classification by %CJ**

Wave speed (m/s)		% CJ		Qualification	Symbol	Mnemonic
low	high	low	high			
2086.1	3000.0	6%	52%	over-driven		Multiple interactions
1869.6	2066.4	-5%	5%	excellent		Cell diamonds
1672.8	1869.6	-15%	-5%	good		Triple point
50.0	1672.8	-97%	-15%	bad		1-D shock

#### 4.2 Single tube results

The results for the first single tube test are illustrated in Fig. 4.1. The high wave speed and pressures shown in configurations a and b signify a transition phenomenon. Little effect on wave speed occurred when applying the step transition configuration c, versus the gradual transition in d. This was also the case when the 3/4-inch section was

attached, g vs. h. The reducer on configuration f also failed to affect the wave speeds seen in e. It should be noted that though the wave speed had decelerated slightly in e, this does not discount that detonations were occurring. Rather, this only signals a degradation in average wave speed that is not desirable in system design. From this test matrix, it seemed that converging configurations do not provide a tangible benefit for increasing wave speed.

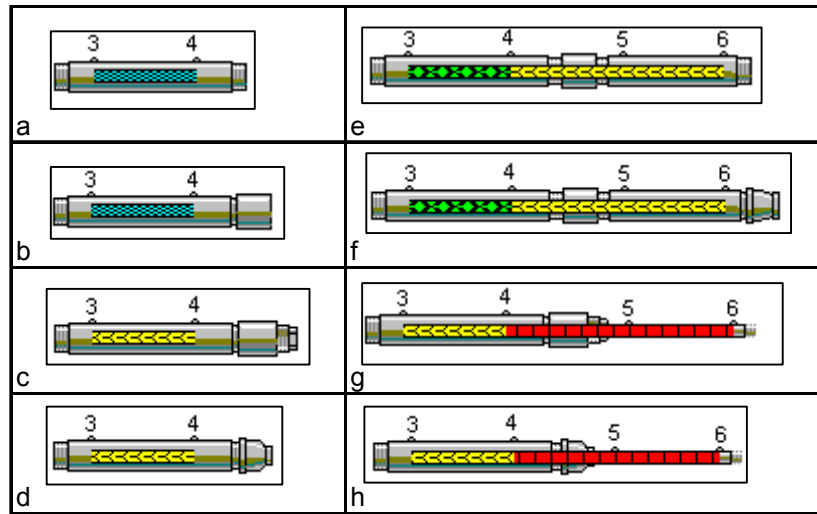


**Fig. 4.1 Results: test matrix 1A: axial converging**

The investigation turned toward diverging configurations. Due to the nature of the test configuration, only a converging-diverging section was possible. This is because the port to the engine block is 2-inch in diameter, and the DDT spiral used fit a 2-inch tube. CFD results predicted that the size of the expansion was too large for the detonation to negotiate (Katta, 2002). Results in Fig. 4.2 b,c,d and e confirmed this.

As with Test matrix 1A, the baseline configuration a could have had strong detonations. The results shed light onto desired geometries. Although a  $\frac{3}{4}$  inch to 2-inch expansion was too large, the gradual transition via the reducer maintained a relatively

high pressure. The pressure was at least 3 times larger in the expanded sections of b and c than in the same sections of d and e. A tripping device in the 2-inch diameter sections of configurations b or c would cause quicker transition than in d or e.

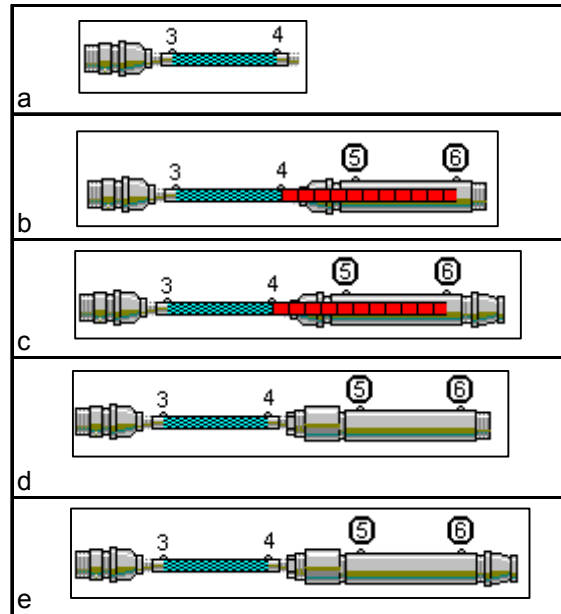


Fig. 4.2 Results: test matrix 1B: axial diverging

Fig. 4.3 shows the effect of turning detonations through 90-degrees. Unfortunately the commercially available stainless 90's had limited turning radii. (Other pipe materials like PVC have street 90's with larger turning radii.) The wave speed symbols between transducers 4 and 5 were omitted. This was due to the slightly larger inherent error when measuring around the bend.

The wave speeds and pressures throughout configurations a and b were consistent with CJ detonations. The converging bends of c and d reduced pressure and wave speed. The expanding bends of e and f also reduced pressure and wave speed. Since the horizontal segment in g did not achieve detonation wave speeds, it was not possible to

qualify the effect of a 3/4 inch 90-degree turn on a detonating structure. The effect of downstream geometry was apparent comparing the excellent wave speed in the horizontal sections of e and f to the bad wave speed in the same section of g. Both e and f were able to achieve CJ wave speeds between 3 and 4, while g was 40% lower.

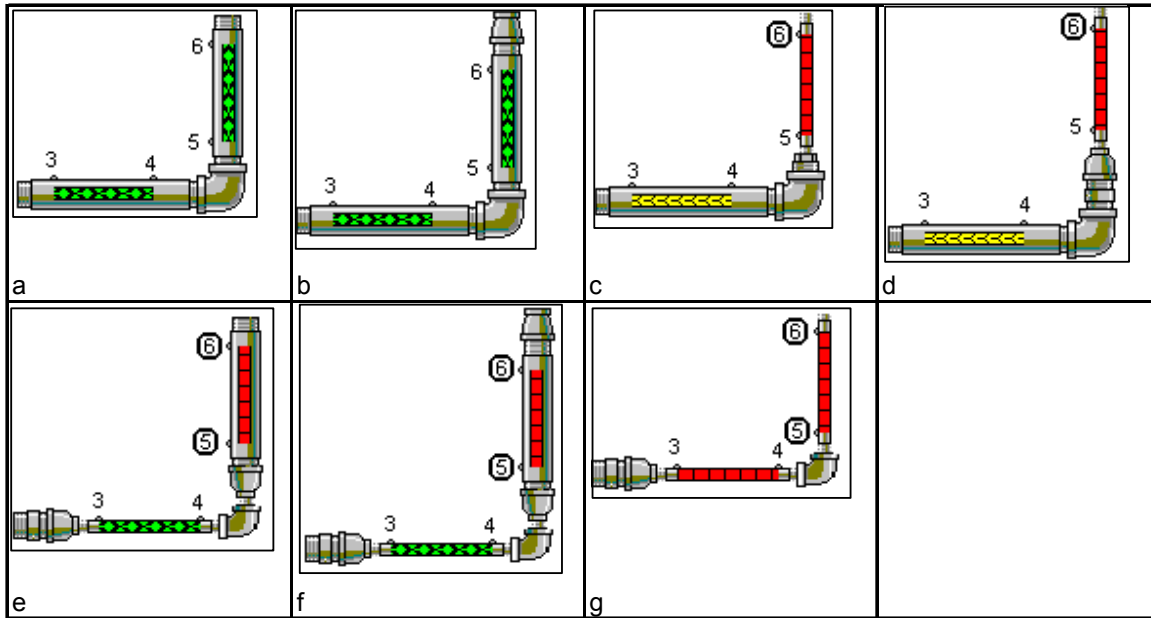


Fig. 4.3 Results test matrix 1C: 90-degree turns

Certain trends were noted by comparing configurations throughout the results of single tube configurations. The wave speeds in Fig. 4.3 a and b fall within 5% of expected CJ speeds as opposed Fig. 4.1 e and f. This may have indicated some detonation strengthening around a bend. Perhaps shock reflections were having some influence.

#### Summary of single tube results

- Converging configurations decreased wave speed
- 3/4 inch to 2 inch divergence was too large and decreased wave speed
- Gradual divergence maintained higher pressure than step divergence
- CJ detonations through like sized bends maintained strength
- Downstream geometries affected upstream wave speeds

### 4.3 Split tube results

Fig. 4.4 shows the results of tee configurations on wave speed and pressure. Configuration e in Fig. 4.4 achieved detonations in two separate tubes. Configuration b also had high enough wave speeds and pressures in the splits to be considered detonating. These wave speeds were lower than desired. The wave speed in the opposing tube increased with a nozzle as shown when comparing a to b or g to h. This could have been

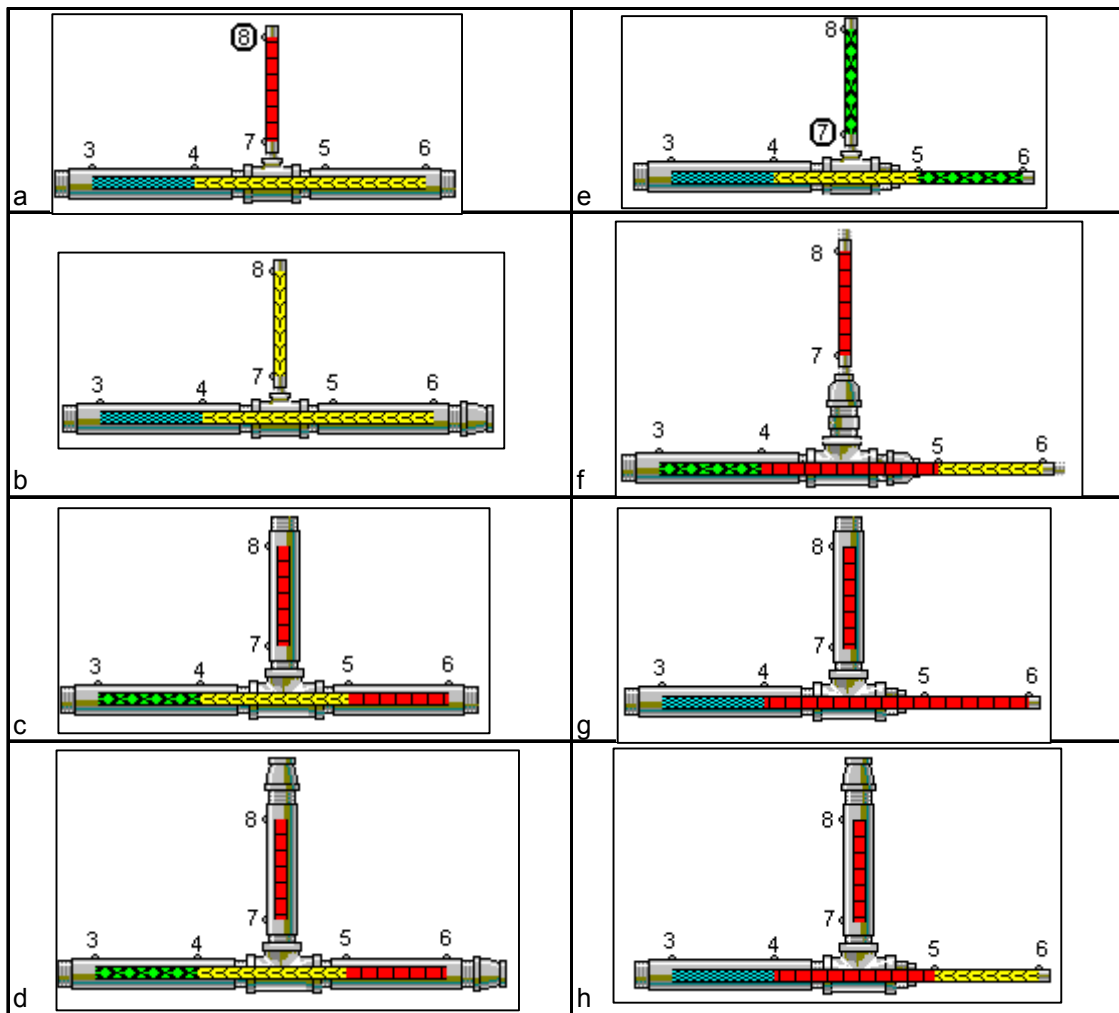


Fig. 4.4 Results test matrix 2A: tees

due to forcing mass flow, hence more fuel and air, into the other tube during the fill cycle. The step convergences of e performed much better than the gradual transitions of f. Perhaps this was due to larger shock interaction due to reflections off of the interior bushing wall. In this case, the physics could not be determined without more sophisticated instrumentation.

Fig. 4.5 shows the results of detonating through configurations with wyes. The step convergent configuration e met the desired objective to split a detonation. As with

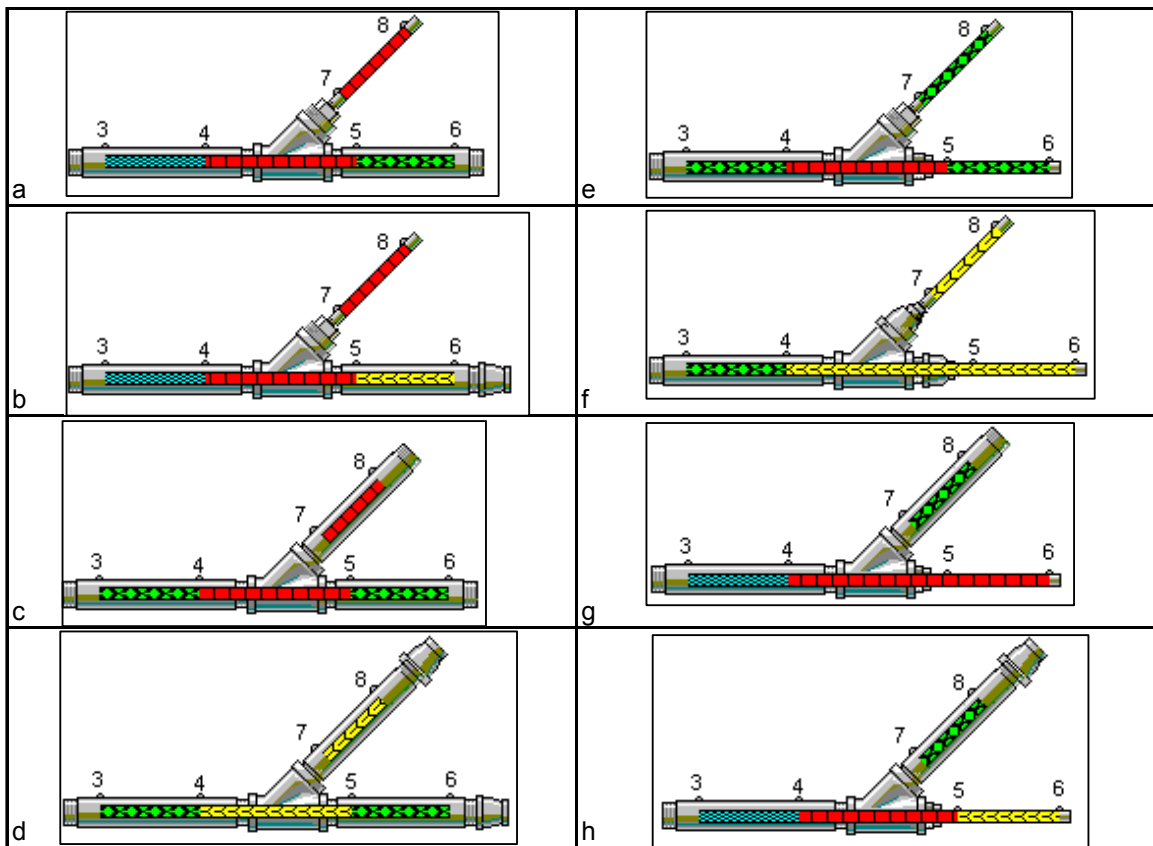


Fig. 4.5 Results test matrix 2B: wyes

the successful tee configuration, this step transition also had higher wave speeds in the splits than the gradual transition configuration f. This pointed to some interesting physics that was not predicted by the single tube step configuration results. Recall that in Fig. 4.1

configurations g and h both retarded the wave speeds regardless of step or gradual transition. Clearly, the downstream geometry had changed enough to encourage the higher speeds in the step configurations.

Fig. 4.6 shows the results of cap geometries. Configuration c shows that high wave speeds were not encouraged by the 45-degree turn. By comparing b and c, the upstream wave speed was increased with a 45-degree turn versus an abrupt 90-degree. This confirmed the earlier finding that downstream geometries do affect upstream wave speeds. Configuration a only showed a degradation of wave speeds achieved in Fig. 4.4 a. A more interesting result may have occurred had a shock or detonation reflected.

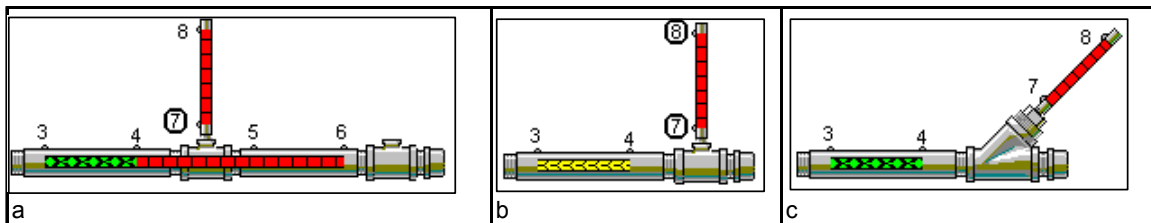


Fig. 4.6 Results test matrix 2C: caps

Along with the previous consideration of geometric effects, a test considering fill fraction was conducted. This testing used a different fill volume from the one used in Test Matrices 2A a and b and 2B a and b. Here a fill volume of  $169.2 \text{ in}^3$  was used for all cases.

Fig. 4.7 shows the effect of varying fill fraction. Here the higher fill fraction and or addition of the reducer increased wave speeds in critical areas of the configuration. A closer look shows that the addition of a reducer was the design change of choice. Although there was an increase in weight with the reducer, the fill fraction would increase fuel consumption by 25%. Additionally, the reducer provided better wave speed improvement. Comparing the reducer effect from a to b, where wave speeds reached CJ



speed in the 5 to 6 segment versus a lesser increase by using more fuel in e. The same results applied while comparing c,g, and d.

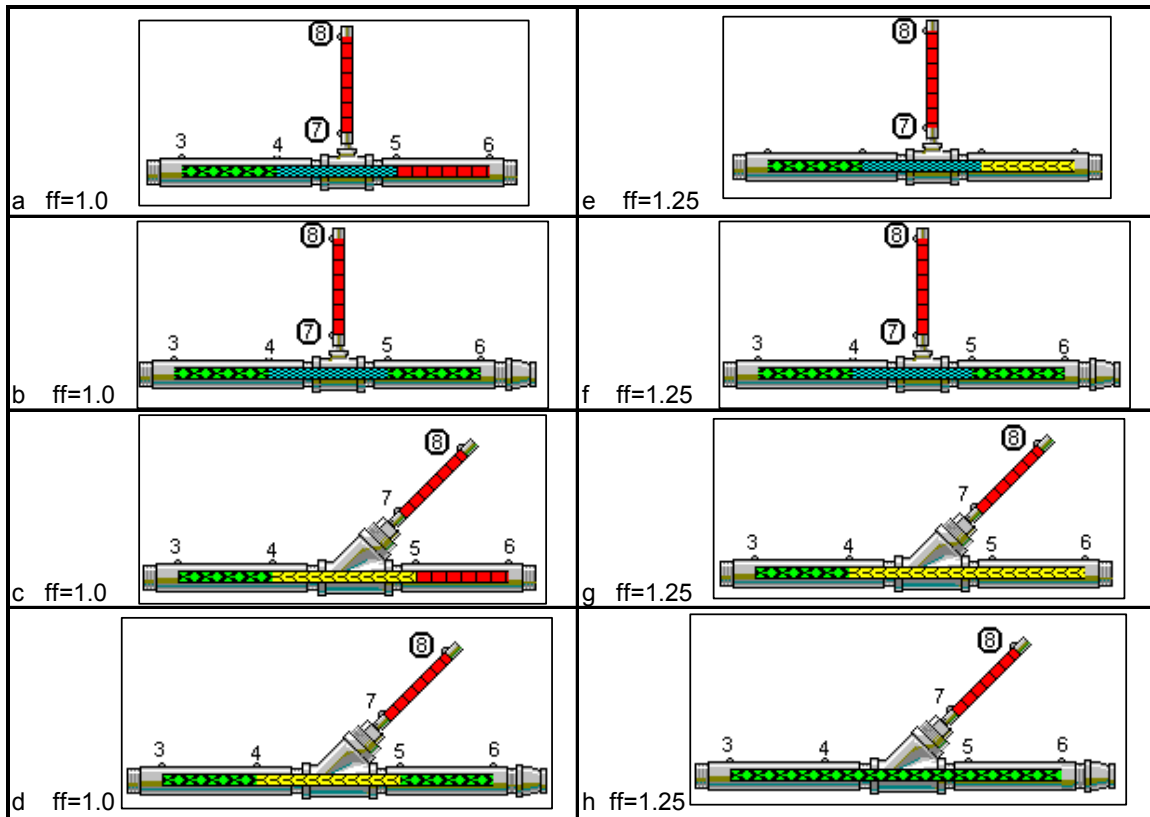


Fig. 4.7 Fill fraction effects

#### Summary of Objective 2 Results

- The double convergent tee and wye configurations split detonations
- Step transitions performed better than gradual in split configurations
- Fig. 4.4 b showed promise, but with lower wave speeds in the splits
- Nozzles on splits increased wave speeds in opposing tubes
- Downstream geometry affected upstream wave speeds.
- Increased fill fraction increased wave speeds
- A convergent reducer increased upstream wave speeds
- Reducer benefits outperform 125% fill fraction gains

#### 4.4 Dual thrust tube – single ignition source results

The configuration shown in Fig. 4.8 met objective 3 by having detonations in two thrust tubes using only one ignition source. The thrust tubes are numbered 1 and 3

corresponding to their cylinder position on the engine block. The  $\frac{3}{4}$  inch diameter stainless crossover tube is mated to each 2-inch diameter thrust tube via a standard 2-inch to  $\frac{3}{4}$  inch tee.

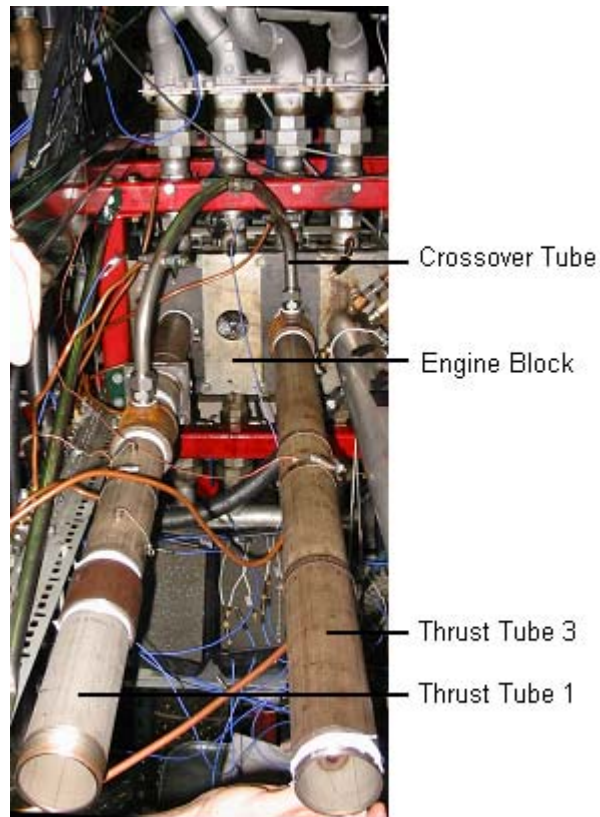


**Fig. 4.8 Single spark – dual detonation configuration**

The spark plug in tube 1 was the only ignition source. After ignition, a 12-inch spiral accelerated DDT before reaching the tee. At the tee, part of the detonation wave continued down tube 1. The exact physical state of combustion, *i.e.* whether detonation or deflagration, at the crossover entrance could not be determined without more complicated instrumentation. However, the wave speeds through the crossover accelerated to more than 10% above the Chapman Jouget detonation speed. This fact

combined with the high pressure reading near the crossover entrance, transducer 3 Fig. 4.9, implied a continuation of detonation, or at least a second rapid DDT event.

The geometric divergence into tube 3 quenched any detonation formed in the crossover tube by dissipating the shocks. The lower pressure at the first transducer in tube 3, transducer 5 Fig. 4.9, evidenced this phenomenon. However, the premixed reactants in tube 3 coupled with these weaker shocks readily recombined into a full detonation when confronted with a 16-inch DDT spiral. Thus another, arguably the third, deflagration to detonation transition mechanism occurred. Results show that downstream of the second spiral, the reaction in tube 3 was a detonation.

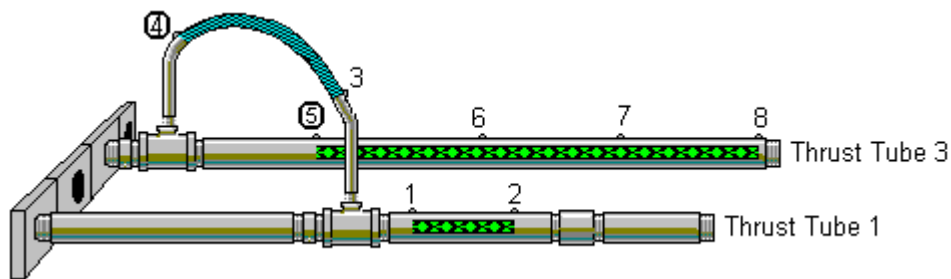


**Fig. 4.9 Dual detonation configuration results**

Despite the previous decision regarding Fig. 4.3 to hide wave speeds through turns, the high speed through the crossover necessitates discussion. These high wave speeds represent 1) a strong detonation or 2) a point along the transition path such as the von Neumann spike. The first consideration is the position along the Rankine Hugoniot curve. Because the pressure has dropped considerable by transducer 4, this can not represent a strong detonation. Therefore this high wave speed occurs as a result of the transition process.

One explanation is that Kuo's "explosion in the explosion" occurred downstream of pressure transducer 3. Then transducer 3 would have read the detonation wave and transducer 4 would have read the superdetonation wave. This would have definitely lowered the time and increased wave speed. Since transducer 4 was not reading ZND state 2 pressures, however, another event was probably happening here. Clearly the combustion process is still coupled with shocks since the pressure was over 10 times atmospheric at transducer 4 and tube 3 ignited. The crossover tube captured a transition mechanism, but without more complicated instrumentation, it was not possible to determine that mechanism's point along the transition path.

The average wave speeds, thrust produced, and peak pressures for the first successful double detonation run are presented in Table 4.3. This data corresponds to the following test conditions: fill fraction = 1.0, equivalence ratio,  $\phi = 1.0$ , frequency = 30 Hz, and ignition delay = 9.0 ms for spark plug 1. The data collected covers a 0.5 s interval, corresponding to 15 detonation waves.

Table 4.3 shows high average wave speeds. The pressures measured at downstream locations on the thrust tubes were at or above those predicted from ZND analysis. A variety of test conditions were applied. The results for these are located in Appendix C.

As a verification tool and comparison of the first test results, Table 4.4 presents a second data set for the exact same conditions. Here the detonation speeds were within 5 % of CJ speeds across the board. In both cases, the wave speeds between transducers 3 and 4 were above CJ wavespeed. The achievement these higher wave speeds above was

desirable from a thrust perspective as discussed in section 2.2, unfortunately not in the crossover tube.

**Table 4.3 Successful double detonation - run 1 data**

**Dual Tube - 30 Hz - Run 28**

CONDITIONS		WAVE SPEEDS						PRESSURE
fill vol	315 in <sup>3</sup>	Ports	Average	Stdev	%used	% CJ		(psig)
ff	1		(m/s)	(m/s)	of 15 total			
freq	30 Hz	1 to 2	1904.67	30.74	100%	-3%	2	724.53
Spark 1		3 to 4	2177.32	19.71	80%	11%	3	684.25
ign del (s)	0.009	5 to 6	1794.88	225.72	73%	-9%	4	158.02
		6 to 7	1962.63	13.07	100%	0%	5	151.18
		7 to 8	1887.99	33.00	100%	-4%	6	652.35
							7	693.57
		Thrust (lb)	29.65				8	616.50

**Table 4.4 Successful double detonation – run 2 data**

**Dual Tube - 30 Hz - Run 29**

CONDITIONS		WAVE SPEEDS						PRESSURE
fill vol	315 in <sup>3</sup>	Ports	Average	Stdev	%used	% CJ		(psig)
ff	1		(m/s)	(m/s)	of 15 total			
freq	30 Hz	1 to 2	1907.87	26.97	100%	-3%	2	600.17
Spark 1		3 to 4	2178.06	22.21	93%	11%	3	784.31
ign del (s)	0.009	5 to 6	1876.84	205.75	87%	-5%	4	582.73
		6 to 7	1959.61	16.89	100%	0%	5	172.94
		7 to 8	1877.70	25.95	100%	-5%	6	173.64
							7	684.11
		Thrust (lb)	29.65				8	721.50
								605.94

Regardless of the actual physical mechanism occurring in the crossover tube, two things stood out. On the up side, this configuration achieved the desired goal. On the down side, exact detonation mitosis did not occur. The offspring detonation in the crossover tube did not carry the same physical characteristics of the parent wave. There was room to improve the process and maintain full and steady detonation propagation throughout the entire process.

An examination of pressure traces for the first run provided valuable information. From this examination the traces at transducers 1, 2, 6, 7, and 8 indicate propagating detonation waves. The traces for the crossover tube transducers and the first transducer in tube 3 are provided. Fig. 4.10 shows that detonations occurred inside the crossover tube at transducer 3. Fig. 4.11 shows that the detonations did not propagate through the entire crossover tube.

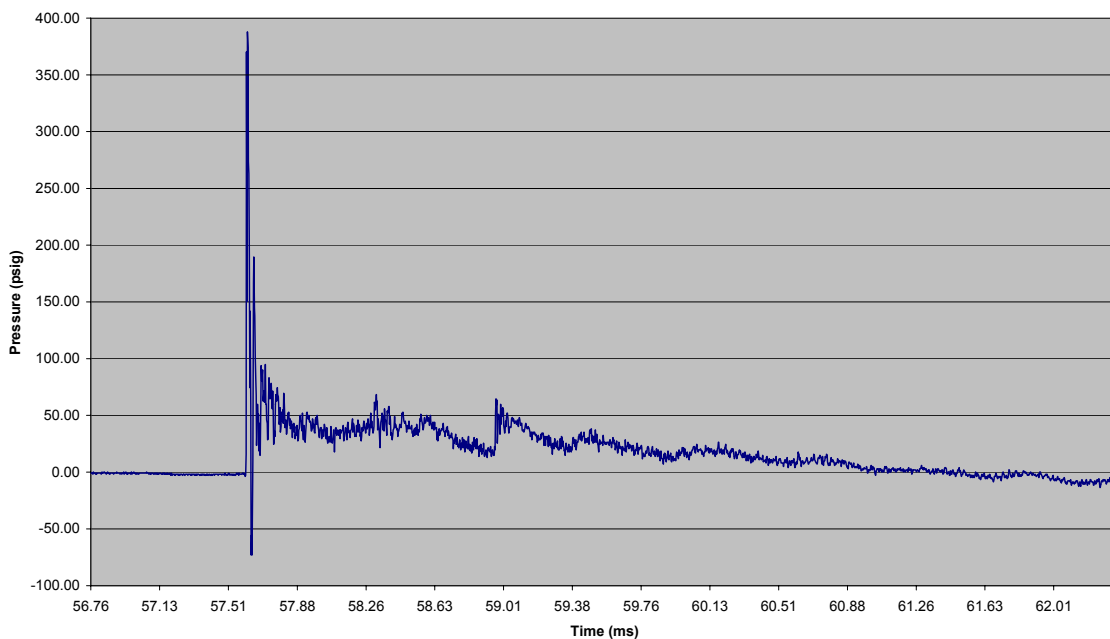


**Fig. 4.10 Dual tube transducer 3 pressure trace**

Although the pressure trace in Fig. 4.11 shows that von Neumann pressures did not occur, there was a sharp pressure rise. This pressure rise at transducer 4 suggests a shock wave followed by a combustion front, the first step in the DDT mechanism. Though this is not detonation, it shows shock interaction that is clearly not present at transducer 5. Figure 4.12 shows the gradual pressure rise that occurred near the entrance of tube 3 prior to DDT. This represents deflagration.

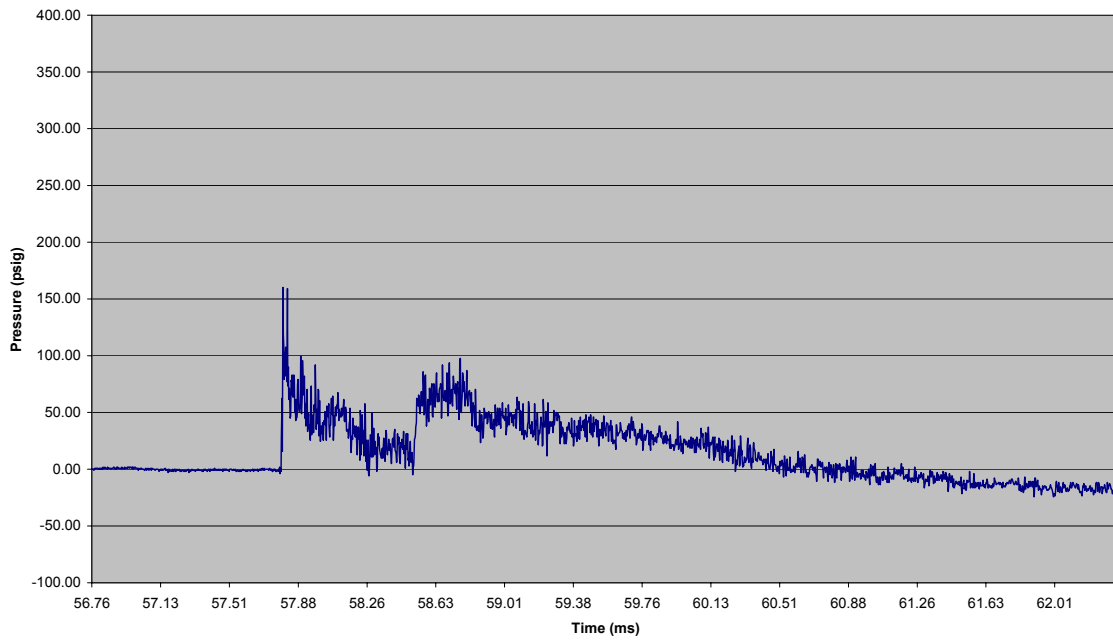


**Fig. 4.11 Dual tube transducer 4 pressure trace**

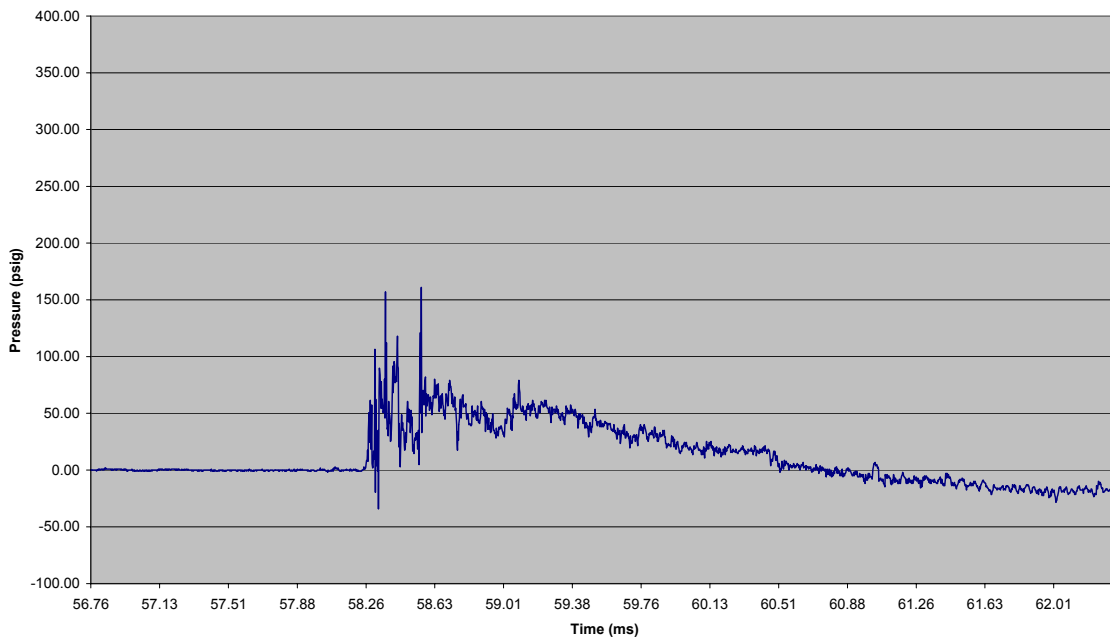


**Figure 4.12 Dual tube transducer 5 pressure trace**

Because timing is so critical to success of this technology, an examination of timing follows. In order to gain a full sense of the timing, a time line for a single cycle was developed. Figure 4.13 shows the key events in milliseconds (ms) for the successful dual thrust tube configuration. Only pressure transducers 1 and 8 are represented. This is because the total elapsed time between an event at the first transducer and the last is 1.11 ms.

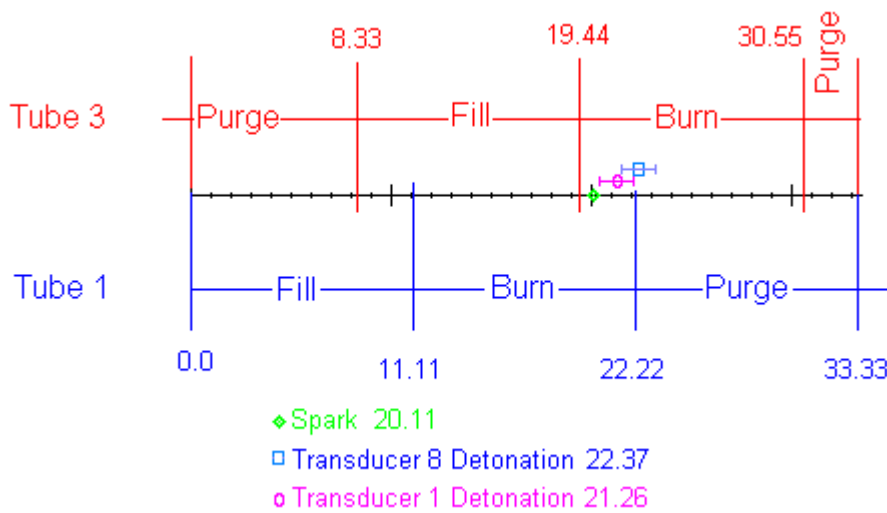


**Figure 4.13 Dual thrust tube time line (ms)**

#### Summary of Objective 3 Results

- A single spark initiated detonations in tubes 1 and 3 at 30 Hz
- Timing, frequency and ignition delay, is critical for success
- Timing is hardware dependant especially on crossover length
- Crossover physics may require more sophisticated instrumentation

#### **4.5 DDT trip device results**

The reflector shown in Fig. 4.14 was placed just downstream of the crossover tube. The 3 support legs allowed for distance variation. Tests were conducted with the reflector disk located 0.25-inch, 0.5-inch, and 0.625-inch downstream of the crossover



entrance into tube 3. The reflector disk was always perpendicular to the flow exiting the crossover tube. The results on wave speed and pressure are shown Fig. 4.15.

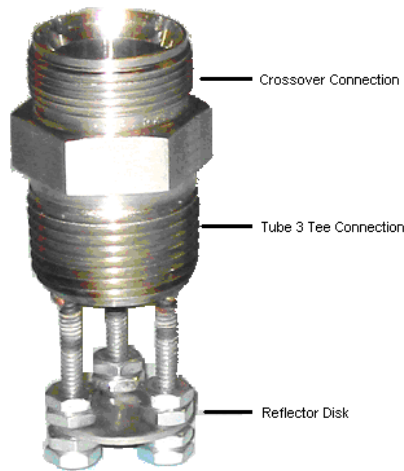


**Fig. 4.14 Reflector**

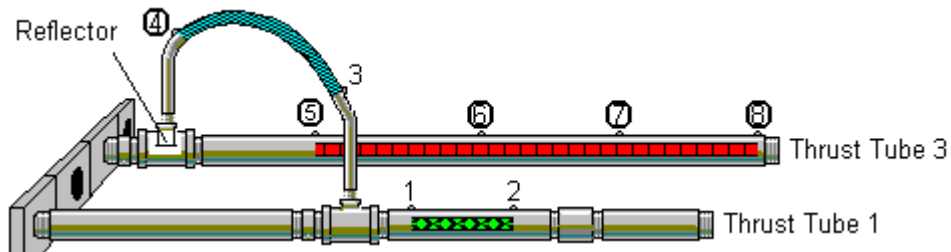


**Fig. 4.15 Reflector results**

The full data tables for all tests run are located in Appendix C. In addition to the simple configuration shown in Fig. 4.14, a second wider reflector was connected to the existing apparatus to extend to 1 inch into tube 3. This configuration was referred to as *layered*. Unfortunately under all conditions tested, tube 3 could not achieve detonation without the DDT spiral. The concept extrapolated from work by Zhdan, may still prove useful, but only through further design considerations and testing (Zhdan 1994).

#### Summary of Objective 4 Results

- Reflector and layer configurations did not induce tube 3 detonations



## 5 Conclusions and Recommendations

### 5.1 Conclusions

The testing successfully proved the ability to use a single ignition source to produce thrust in a dual detonation configuration. The initial phases of testing showed that varying geometry affected wave speed and peak pressure. Whether this happened due to the initial conditions of the reactants just after the fill phase, or as a result of detonation physics requires further investigation.

Some additional observations were made. The nozzles either provided an increase in wave speed or no detrimental effect on the wave speed was noted. A higher fill fraction had a positive impact on wave speed, but would probably be cost prohibitive, and less efficient. The diameter ratio of all expansion configurations was too large. Timing was critical in the success of the dual detonation configuration. This was largely due to the length of the crossover tube. And finally, more extensive instrumentation and testing are required to understand certain aspects of the physics, especially to make a successful reflector *trip* device.

### 5.2 Recommendations

The process revealed interesting responses of detonation waves to different geometries, frequencies, ignition delays and fill fractions. Several potential areas of study surfaced.

#### 1) Application of machined parts

The first recommendation is to optimize geometries beyond commercially available parts. As this work was conducted as proof of concept, the desire existed to

implement more sophisticated geometries for detonation encouragement. This aspiration was held in check in order to meet the overall objective quickly and cheaply. Several potential configurations follow that could increase or maintain detonation strength through complicated geometries.

Fig. 5.1 shows a variety of test configurations that might enhance detonation physics. Configuration b considers whether a higher incident Mach number requires a larger turn radius to maintain stable detonations. Configuration c introduces a scoop to influence mass flow into the cross pipe, and encourage shock reflections for increased detonation strength. Configuration d is an evolution of c in which the mass flow is split between the two pipes for better fill, and still maintains a degree of reflection. Configuration e uses a bump as a detonation trip, combined with the scoop. Configuration f combines all of these mechanisms: the bump to initiate detonation, the mass flow split for better fill, and the scoop for reflection.

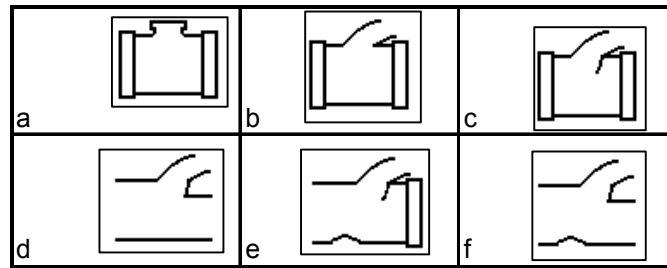


**Fig. 5.1 Recommended machined testing configurations**

2) Testing of different diameters other than 2-inch and  $\frac{3}{4}$ -inch

This recommendation is a direct response to the dissipation due to the  $\frac{3}{4}$  inch to 2-inch expansion. By considering a less extreme variation, such as a 1  $\frac{1}{2}$  inch to 2-inch expansion, it could be possible to maintain the detonation. A gradual transition via a commercial reducer showed more promise than a step transition based on this

experiment's results. Further, a machined transition mechanism using the method of characteristics, for example, could prove even more encouraging.

3) Schlieren photography of critical phenomena

Although slightly more exotic, a test of peculiar geometries observed with streak schlieren photography would help demonstrate physical mechanisms. Of particular interest are the crossover tube physics observed in the dual tube configuration. A test of this type could show how the detonation reacts to the split immediately followed by a turn.

4) Design more efficient valve timing system

The cycle shown for the successful dual tube configuration has room for improvement. The total cycle was 33.3 ms of which, only 3.5 ms was required for combustion. Rather than dividing the cycle into equal parts, a cycle that has a larger proportion of fill time with less time for purge and even less time for combustion better matches requirements. This improved timing could lower the total time required or be used to require less power for aspiration during the fill cycle.

5) Further development of reflector tripping mechanism

The fifth recommendation takes a much more exhaustive look at the potential for a reflection trip. Although the configuration used did not produce a strong detonation transition, this could be due to the rapid expansion. Other problems include reflection distance and direction. For example the reflector could be aimed upstream in tube 3 to encourage reflections of the tube's closed end. Additionally slightly larger diameter reflectors could be tried.

6) Full scale construction of single spark ignition system

The sixth recommendation is the culmination of the work presented here. This would involve a multi tube sustained detonation mechanism with only one spark. First the number of thrust tubes will determine a window of run frequencies. Then, the crossover tubes will have to be designed to meet those frequencies. Finally, a complete manifold, valving, and support system will have to be designed to accommodate this single ignition source PDE.

# Appendix A Rayleigh and Rankine-Hugoniot Development

## APPENDIX A. RALEIGH AND RANKINE-HUGONIOT RELATIONS DEVELOPMENT

### CONSERVATION LAWS

#### Continuity

$$\dot{m} = \rho_1 \cdot u_1 = \rho_2 \cdot u_2 \quad [1]$$

#### x-Momentum

(no shear or body force: only force is pressure)

$$P_1 + \rho_1 \cdot u_1^2 = P_2 + \rho_2 \cdot u_2^2 \quad [2]$$

#### Energy

$$c_p \cdot T_1 + \frac{u_1^2}{2} + q = c_p \cdot T_2 + \frac{u_2^2}{2} \quad [3]$$

### *Rayleigh Relation Development*

Rearrange Momentum

$$\rho_1 \cdot u_1^2 - \rho_2 \cdot u_2^2 = P_2 - P_1 \quad \text{factor out } \dot{m}^2 \quad \text{Consider Continuity}$$

$$\dot{m}^2 \cdot \left( \frac{1}{\rho_1} - \frac{1}{\rho_2} \right) = P_2 - P_1 \quad \text{factor out a (-)}$$

$$-\dot{m}^2 = \frac{P_2 - P_1}{\frac{1}{\rho_2} - \frac{1}{\rho_1}} \quad \text{Rayleigh Line Relation}$$

For a fixed flow rate and fixing  $P_1$  and  $1/\rho_1$  yields the following relationship in the form of the equation of a line:  $y=mx+b$ .

$$P_2 = \left( -\dot{m}^2 \right) \cdot \left( \frac{1}{\rho_2} \right) + \left( \dot{m}^2 \cdot \frac{1}{\rho_1} + P_1 \right)$$

### Rankine-Hugoniot Relation Development

Starting with COE equation 3:

$$c_p \cdot T_1 + \frac{u_1^2}{2} + q = c_p \cdot T_2 + \frac{u_2^2}{2} \quad \text{Substitute Ideal Gas} \quad P = \rho \cdot R \cdot T$$

$$\frac{c_p}{R} \cdot \frac{P_1}{\rho_1} + \frac{u_1^2}{2} + q = \frac{c_p}{R} \cdot \frac{P_2}{\rho_2} + \frac{u_2^2}{2} \quad \text{Since} \quad \frac{c_p}{R} = \frac{\gamma}{\gamma - 1}$$

$$\frac{\gamma}{\gamma - 1} \cdot \left( \frac{P_1}{\rho_1} - \frac{P_2}{\rho_2} \right) + \frac{1}{2} \cdot (u_1^2 - u_2^2) + q = 0 \quad [3a]$$

Examine Momentum and solve for  $u_1^2$  and  $-u_2^2$

$$\begin{aligned} \rho_1 \cdot u_1^2 - \rho_2 \cdot u_2^2 &= P_2 - P_1 \\ u_1^2 &= \frac{P_2 - P_1 + \rho_2 \cdot u_2^2}{\rho_1} \\ -(u_2^2) &= \frac{P_2 - P_1 - \rho_1 \cdot u_1^2}{\rho_2} \end{aligned}$$

Substitute into equation 3a:

$$\frac{\gamma}{\gamma - 1} \cdot \left( \frac{P_1}{\rho_1} - \frac{P_2}{\rho_2} \right) + \frac{1}{2} \cdot \left[ \left( \frac{P_2 - P_1}{\rho_1} + \frac{\rho_2 \cdot u_2^2}{\rho_1} \right) + \left( \frac{P_2 - P_1}{\rho_2} - \frac{\rho_1 \cdot u_1^2}{\rho_2} \right) \right] + q = 0$$

Rearrange Continuity equation 1 and combining yields:

$$\frac{\gamma}{\gamma - 1} \cdot \left( \frac{P_1}{\rho_1} - \frac{P_2}{\rho_2} \right) + \frac{1}{2} \cdot (P_2 - P_1) \cdot \left( \frac{1}{\rho_1} + \frac{1}{\rho_2} \right) + q = 0 \quad \text{Additionally, this can be recast:}$$

$$(h_2 - h_1) = \frac{\gamma}{\gamma - 1} \cdot \left( \frac{P_2}{\rho_2} - \frac{P_1}{\rho_1} \right) - q$$



### Rayleigh Lines Plotted

Given standard sea level conditions:

$$P_1 := 1 \cdot \text{atm}$$

$$\rho_1 := .855 \frac{\text{kg}}{\text{m}^3}$$

Let's examine the effect of varying mass flow rate:

$$m_{\dot{0}} := 0 \cdot \frac{\text{kg}}{\text{s} \cdot \text{m}^2}$$

$$m_{\dot{1}} := 1.5 \cdot 10^3 \cdot \frac{\text{kg}}{\text{s} \cdot \text{m}^2}$$

$$m_{\dot{2}} := 1.72 \cdot 10^3 \cdot \frac{\text{kg}}{\text{s} \cdot \text{m}^2}$$

$$m_{\dot{3}} := 1.9 \cdot 10^3 \cdot \frac{\text{kg}}{\text{s} \cdot \text{m}^2}$$

$$m_{\dot{4}} := 10 \cdot 10^{10} \cdot \frac{\text{kg}}{\text{s} \cdot \text{m}^2}$$

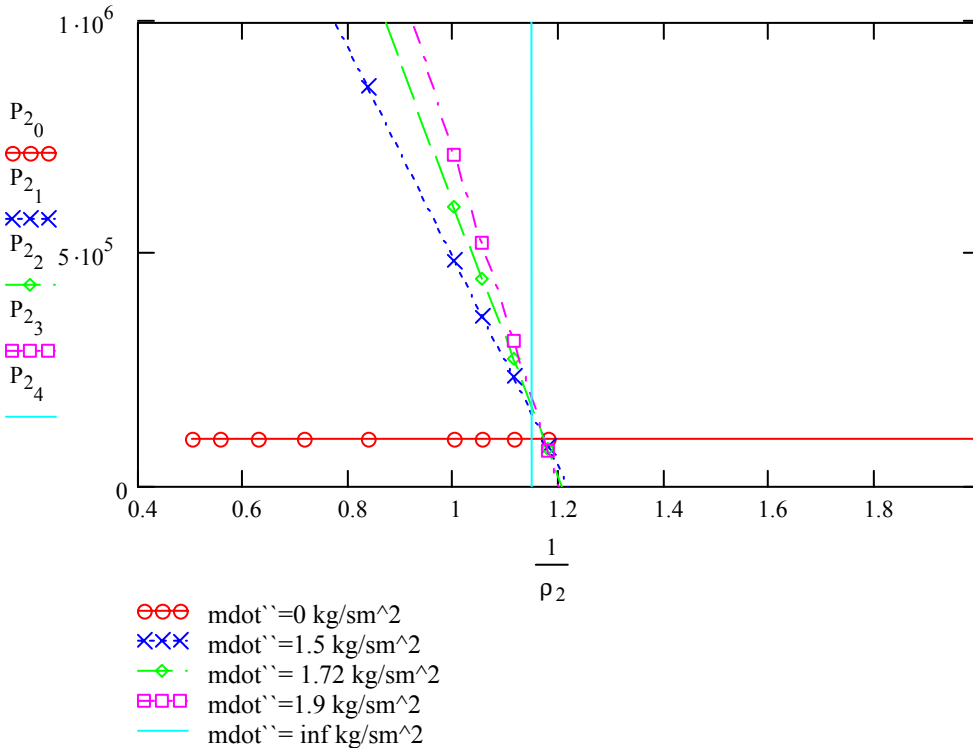
$i := 0, 1..4$

$$\rho_2 := \begin{pmatrix} .5 \\ .85 \\ .9 \\ .95 \\ 1 \\ 1.2 \\ 1.4 \\ 1.6 \\ 1.8 \\ 2 \end{pmatrix} \cdot \frac{\text{kg}}{\text{m}^3}$$

$$P_{2_i} := \left[ \frac{-\left(m_{\dot{i}}\right)^2 \cdot \rho_1 + \left(m_{\dot{i}}\right)^2 \cdot \rho_2 + P_1 \cdot \rho_2 \cdot \rho_1}{\left(\rho_2 \cdot \rho_1\right)} \right]$$

The Raleigh Equation solved for  $P_2$  given  $P_1$ ,  $m_{\dot{0}}$ ,  $\rho_2$ , and  $\rho_1$ .

### RALIEGH LINES



**Rankine-Hugoniot Curve Plotted**

$$\frac{\gamma}{\gamma - 1} \cdot \left( \frac{P_2}{\rho_2} - \frac{P_1}{\rho_1} \right) - \frac{1}{2} \cdot (P_2 - P_1) \cdot \left[ \left( \frac{1}{\rho_1} \right) + \left( \frac{1}{\rho_2} \right) \right] - q = 0$$

$$\begin{aligned} \gamma &:= 1.4 & T_1 &:= 298 \text{ K} & q &:= 3.421 \cdot 10^6 \cdot \frac{\text{J}}{\text{kg}} \\ P_1 &:= 1 \cdot \text{atm} & \rho_1 &:= 0.885 \frac{\text{kg}}{\text{m}^3} \end{aligned}$$

$$P_2 := \left[ \frac{-(\gamma \cdot P_1 \cdot \rho_2 + P_1 \cdot \rho_2 - P_1 \cdot \rho_1 \cdot \gamma + P_1 \cdot \rho_1 + 2 \cdot q \cdot \rho_1 \cdot \rho_2 \cdot \gamma - 2 \cdot q \cdot \rho_1 \cdot \rho_2)}{(-\rho_1 \cdot \gamma + \rho_2 \cdot \gamma - \rho_2 - \rho_1)} \right]$$

$$P_{1v} := \left( \frac{\rho_2}{\rho_2} \cdot P_1 \right) \quad \rho_{1v} := \left( \frac{\rho_2}{\rho_2} \cdot \rho_1 \right)$$

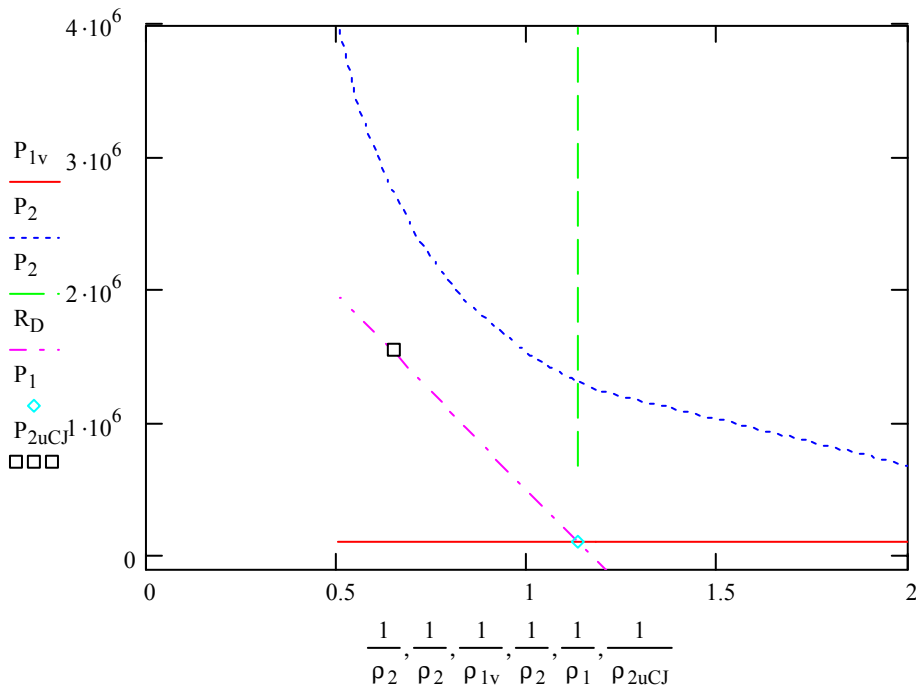
$$m_{\text{dot}} := 1.72 \cdot 10^3 \cdot \frac{\text{kg}}{\text{s}}$$

$$P_{2u\text{CJ}} := 1.548 \cdot 10^6 \cdot \text{Pa}$$

$$\rho_{2u\text{CJ}} := 1.546 \cdot \frac{\text{kg}}{\text{m}^3}$$

$$R_D := \left( \frac{-m_{\text{dot}}^2}{\rho_2 \cdot \text{m}^4} + P_1 + \frac{m_{\text{dot}}^2}{\rho_1 \cdot \text{m}^4} \right)$$

**RANKINE HUGONIOT RELATIONS**



## Appendix B ZND Detonation Analysis H<sub>2</sub> and Air

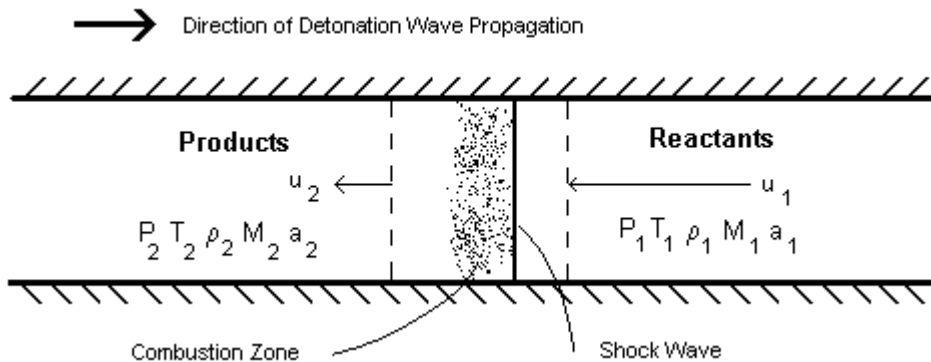
### PROBLEM STATEMENT

Determine the properties upstream and downstream of a detonation wave for pre-mixed H<sub>2</sub> and air.

**GIVEN:**  
 $P_1 := 1 \cdot \text{atm}$   
 $T_1 := 298.15 \text{K}$   
 $\phi := 1$

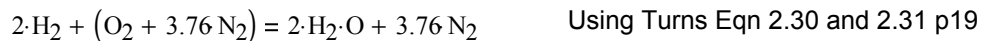
### ASSUME:

Sea level standard air	Calorically perfect gas
1-D	Negligible body forces
Steady flow	Adiabatic conditions (no heat loss to surroundings)
Constant area	Neglect dissociation of products



### THERMOCHEMISTRY

Reaction Mechanism:



Using Turns Appendix A for determining cp values (Guess T<sub>2</sub>=3000 K):

Reactants (State 1)	MWi	Ni	$\chi^i = \text{Ni}/\text{N}_{\text{tot}}$	$Y_i = \chi^i \text{MW}_i / \text{M}_{\text{wmix}}$	$c_{pi} (\text{kJ}/\text{kmolK})$
H2	2.0159	2.0000	0.2959	0.0285	28.8710
O2	31.9988	1.0000	0.1479	0.2264	29.3150
N2	28.0134	3.7600	0.5562	0.7451	29.0710
$\text{MW}_1 = \sum \text{MW}_i \cdot \chi^i$	20.9114			$c_{p1} = (\sum \chi^i \cdot c_{pi}) / \text{MW}_1$	1.3891
Products (State 2)	MWi	Ni	$\chi^i = \text{Ni}/\text{N}_{\text{tot}}$	$Y_i = \chi^i \text{MW}_i / \text{M}_{\text{wmix}}$	$c_{pi} (\text{kJ}/\text{kmolK})$
H2O	18.0153	2.0000	0.3472	0.2549	55.7790
N2	28.0134	3.7600	0.6528	0.7451	37.0280
$\text{MW}_2 = \sum \text{MW}_i \cdot \chi^i$	24.5418			$c_{p2} = (\sum \chi^i \cdot c_{pi}) / \text{MW}_2$	1.7741

$$\text{MW}_1 := 20.9114 \frac{\text{kg}}{\text{kmol}}$$

$$\text{MW}_2 := 24.5418 \frac{\text{kg}}{\text{kmol}}$$

Using the information above and Turns Appendix A we calculate  $c_{p1}$  (Use  $T_1 = 298\text{K}$ ):

$$c_{p1} = \frac{\sum \chi^i c_{pi}}{\text{MW}_1}$$

$$c_{p1} := \frac{\begin{matrix} \text{H}_2 & & \text{O}_2 & & \text{N}_2 \\ 0.2959 \left( 28.871 \frac{\text{kJ}}{\text{kmolK}} \right) + 0.1479 \left( 29.315 \frac{\text{kJ}}{\text{kmolK}} \right) + 0.5562 \left( 29.071 \frac{\text{kJ}}{\text{kmolK}} \right) \end{matrix}}{\text{MW}_1}$$

$$c_{p1} = 1.389 \frac{\text{kJ}}{\text{kg} \cdot \text{K}}$$

In order to determine  $c_{p2}$ , we have to guess  $T_2$  and iterate:

Guess:  $T_{2g} := 3000\text{K}$

$$c_{p2} = \frac{\sum \chi^i c_{pi}}{\text{MW}_2}$$

$$c_{p2} := \frac{\begin{matrix} \text{H}_2\text{O} & & \text{N}_2 \\ 0.3472 \left( 55.779 \frac{\text{kJ}}{\text{kmolK}} \right) + 0.6528 \left( 37.028 \frac{\text{kJ}}{\text{kmolK}} \right) \end{matrix}}{\text{MW}_2}$$

$$c_{p2} = 1.774 \frac{\text{kJ}}{\text{kg} \cdot \text{K}}$$

Now determine  $R_2$  and  $\gamma_2$ :

$$R_u := 8313.4 \frac{\text{J}}{\text{kmol}\cdot\text{K}}$$

$$R_2 := \frac{R_u}{MW_2} \quad \boxed{R_2 = 0.339 \frac{\text{kJ}}{\text{kg}\cdot\text{K}}}$$

$$\gamma_2 := 1 + \frac{R_2}{c_{p2} - R_2} \quad \boxed{\gamma_2 = 1.236}$$

Estimate  $q$  from Eqn 16.7 and Turns Appendix A

$$q = \sum_{\text{state1}} Y_i \cdot h_{fi} - \sum_{\text{state2}} Y_i \cdot h_{fi}$$

$$q = Y_{\text{H}_2} \cdot (0) + Y_{\text{O}_2\text{R}} \cdot (0) + Y_{\text{N}_2\text{R}} \cdot (0) - [Y_{\text{H}_2\text{O}} \cdot h_{\text{foH}_2\text{O}} + Y_{\text{O}_2\text{Pr}} \cdot (0) + Y_{\text{N}_2\text{Pr}} \cdot (0)]$$

$$q = -Y_{\text{H}_2\text{O}} \cdot h_{\text{foH}_2\text{O}} = -\chi_{\text{H}_2\text{O}} \cdot \frac{MW_{\text{H}_2\text{O}}}{MW_{\text{Pr}}} \cdot \frac{h_{\text{foH}_2\text{O}}}{MW_{\text{H}_2\text{O}}}$$

$$h_{\text{foH}_2\text{O}} := (-241845) \cdot \frac{\text{kJ}}{\text{kmol}} \quad \chi_{\text{H}_2\text{O}} := 0.3472$$

$$q := -\chi_{\text{H}_2\text{O}} \cdot \frac{h_{\text{foH}_2\text{O}}}{MW_2} \quad \boxed{q = 3.421 \times 10^6 \frac{\text{J}}{\text{kg}}}$$

$$u_D := \sqrt{2 \cdot (\gamma_2 + 1) \cdot \gamma_2 \cdot R_2 \cdot \left( \frac{c_{p1}}{c_{p2}} \cdot T_1 + \frac{q}{c_{p2}} \right)}$$

$$\boxed{u_D = 2.012 \times 10^3 \frac{\text{m}}{\text{s}}}$$

If we included dissociation, our estimate of  $u_D$  would be smaller, as  $q$  would be smaller

Check T2 using Eqn 16.26

$$T_2 := \frac{2 \cdot \gamma_2^2}{\gamma_2 + 1} \cdot \left( \frac{c_{p1}}{c_{p2}} \cdot T_1 + \frac{q}{c_{p2}} \right)$$

$$T_2 = 2.954 \times 10^3 \text{ K}$$

$$\frac{T_2 - T_{2g}}{T_2} = -1.544\%$$

Verify P2 >> P1 Assumption

$$\left[ \frac{\rho_2}{\rho_1} \right] := \frac{\gamma_2 + 1}{\gamma_2} \quad \left[ \frac{\rho_2}{\rho_1} \right] = 1.809$$

$$\frac{T_2}{T_1} = 9.909$$

$$\left[ \frac{P_2}{P_1} \right] := \left[ \frac{\rho_2}{\rho_1} \right] \cdot \frac{T_2}{T_1} \cdot \frac{MW_1}{MW_2} \quad \left[ \frac{P_2}{P_1} \right] = 15.274$$

Assuming a ZND structure, determine the key state properties for the detonation wave described above ie calculate  $\rho$ , P, T, and M at states 1, 2', and 2.

$$R_1 := \frac{R_u}{MW_1} \quad R_1 = 397.553 \frac{\text{J}}{\text{kg} \cdot \text{K}}$$

$$c_{v1} := c_{p1} - R_1 \quad c_{v1} = 991.541 \frac{\text{J}}{\text{kg} \cdot \text{K}}$$

$$\gamma_1 := \frac{c_{p1}}{c_{v1}} \quad \gamma_1 = 1.401$$

$$u_1 := u_D \quad u_1 = 2.012 \times 10^3 \frac{\text{m}}{\text{s}}$$

$$\rho_1 := \frac{P_1}{R_1 \cdot T_1} \quad \rho_1 = 0.855 \frac{\text{kg}}{\text{m}^3}$$

$$M_1 := \frac{u_1}{\sqrt{\gamma_1 \cdot R_1 \cdot T_1}} \quad M_1 = 4.938$$

Now utilizing normal shock relations:

$$\left[ \frac{P_{2'}}{P_1} \right] := \frac{1}{\gamma_1 + 1} \cdot [2 \cdot \gamma_1 \cdot M_1^2 - (\gamma_1 - 1)] \quad \left[ \frac{P_{2'}}{P_1} \right] = 28.283$$

$$\left[ \frac{T_{2'}}{T_1} \right] := \left[ 2 + (\gamma_1 - 1) \cdot M_1^2 \right] \cdot \frac{2 \cdot \gamma_1 \cdot M_1^2 - (\gamma_1 - 1)}{(\gamma_1 + 1)^2 \cdot M_1^2} \quad \left[ \frac{T_{2'}}{T_1} \right] = 5.69$$

$$\left[ \frac{\rho_{2'}}{\rho_1} \right] := \frac{(\gamma_1 + 1) \cdot M_1^2}{(\gamma_1 - 1) \cdot M_1^2 + 2} \quad \left[ \frac{\rho_{2'}}{\rho_1} \right] = 4.971$$

Looking at the state 2' properties:

$$P_{2'} := P_1 \cdot \left[ \frac{P_{2'}}{P_1} \right] \quad \boxed{P_{2'} = 2.866 \times 10^6 \text{ Pa}}$$

$$T_{2'} := T_1 \cdot \left[ \frac{T_{2'}}{T_1} \right] \quad \boxed{T_{2'} = 1.696 \times 10^3 \text{ K}}$$

$$\rho_{2'} := \rho_1 \cdot \left[ \frac{\rho_{2'}}{\rho_1} \right] \quad \boxed{\rho_{2'} = 4.249 \frac{\text{kg}}{\text{m}^3}}$$

Applying Continuity:

$$\dot{m}_{\text{dot}''} := \rho_1 \cdot u_1 \quad \boxed{\dot{m}_{\text{dot}''} = 1.72 \times 10^3 \frac{\text{kg}}{\text{m}^2 \text{ s}}}$$

$$u_{2'} := \frac{\dot{m}_{\text{dot}''}}{\rho_{2'}} \quad \boxed{u_{2'} = 404.746 \frac{\text{m}}{\text{s}}}$$

ASSUME:  $\gamma_{2'} := \gamma_1$        $R_{2'} := R_1$

$$M_{2'} := \frac{u_{2'}}{\sqrt{\gamma_{2'} \cdot R_{2'} \cdot T_{2'}}} \quad \boxed{M_{2'} = 0.416}$$

Looking at state 2 properties:

$$P_2 := P_1 \cdot \left[ \frac{P_2}{P_1} \right] \quad \boxed{P_2 = 1.548 \times 10^6 \text{ Pa}}$$

$$\boxed{T_2 = 2.954 \times 10^3 \text{ K}}$$

$$\rho_2 := \rho_1 \cdot \left[ \frac{\rho_2}{\rho_1} \right] \quad \boxed{\rho_2 = 1.546 \frac{\text{kg}}{\text{m}^3}}$$

Returning to Continuity:

$$u_2 := \frac{\dot{m}}{\rho_2} \quad \boxed{u_2 = 1.112 \times 10^3 \frac{\text{m}}{\text{s}}}$$

$$M_2 := \frac{u_2}{\sqrt{\gamma_2 \cdot R_2 \cdot T_2}} \quad \boxed{M_2 = 1}$$

First Order ZND Approximations:

Property	State1	State 2'	State 2
$\rho/\rho_1$	1	5	1.8
$P/P_1$	1	28.3	15.3
$T/T_1$	1	5.7	9.9
M	4.9	0.42	1
u (m/s)	2012	405	1112



## Appendix C Tables of Test Results

**Test Matrix 1A Configuration a Run 1**

WAVE SPEEDS							PRESSURE
Ports	Average	Stdev	%used	% CJ			(psig)
	(m/s)	(m/s)	of 10 total			1	
1 to 2	N/A	N/A	N/A	N/A		2	99.39
2 to 3	N/A	N/A	N/A	N/A		3	978.92
3 to 4	2451.61	43.29	100%	25%		4	564.34
							500.77
<b>THRUST</b>	8.31 lb						

**Test Matrix 1A Configuration a Run 2**

WAVE SPEEDS							PRESSURE
Ports	Average	Stdev	%used	% CJ			(psig)
	(m/s)	(m/s)	of 10 total			1	
1 to 2	N/A	N/A	N/A	N/A		2	102.64
2 to 3	N/A	N/A	N/A	N/A		3	1142.80
3 to 4	2405.53	73.03	100%	22%		4	552.94
							514.10
<b>THRUST</b>	8.31 lb						

**Test Matrix 1A Configuration b Run 1**

WAVE SPEEDS							PRESSURE
Ports	Average	Stdev	%used	% CJ			(psig)
	(m/s)	(m/s)	of 10 total			1	
1 to 2	N/A	N/A	N/A	N/A		2	97.11
2 to 3	N/A	N/A	N/A	N/A		3	1175.64
3 to 4	2472.20	45.77	1	26%		4	558.00
							537.23
<b>THRUST</b>	8.34 lb						

**Test Matrix 1A Configuration b Run 2**

WAVE SPEEDS							PRESSURE
Ports	Average	Stdev	%used	% CJ			(psig)
	(m/s)	(m/s)	of 10 total			1	
1 to 2	N/A	N/A	N/A	N/A		2	93.91
2 to 3	N/A	N/A	N/A	N/A		3	1097.87
3 to 4	2471.19	72.21	1	26%		4	592.60
							509.38
<b>THRUST</b>	8.33 lb						

**Test Matrix 1A Configuration c Run 1**

WAVE SPEEDS							PRESSURE
Ports	Average	Stdev	%used	% CJ			(psig)
	(m/s)	(m/s)	of 10 total			1	
1 to 2	N/A	N/A	N/A	N/A		2	136.60
2 to 3	2116.50	108.48	100%	8%		3	1048.79
3 to 4	1864.98	37.51	100%	-5%		4	473.72
							520.23
<b>THRUST</b>	8.33 lb						

**Test Matrix 1A Configuration c Run 2**

WAVE SPEEDS							PRESSURE
Ports	Average	Stdev	%used	% CJ			(psig)
	(m/s)	(m/s)	of 10 total			1	
1 to 2	N/A	N/A	N/A	N/A		2	126.69
2 to 3	2177.29	136.48	100%	11%		3	943.31
3 to 4	1848.66	22.04	100%	-6%		4	490.90
							466.70
<b>THRUST</b>	8.35 lb						

**Test Matrix 1A Configuration d Run 1**

WAVE SPEEDS							PRESSURE
Ports	Average	Stdev	%used	% CJ			(psig)
	(m/s)	(m/s)	of 10 total			1	
1 to 2	N/A	N/A	N/A	N/A		2	140.89
2 to 3	1970.34	143.68	100%	0%		3	978.12
3 to 4	1738.15	65.14	100%	-12%		4	753.28
							538.42
<b>THRUST</b>	8.84 lb						

**Test Matrix 1A Configuration d Run 2**

WAVE SPEEDS							PRESSURE
Ports	Average	Stdev	%used	% CJ			(psig)
	(m/s)	(m/s)	of 10 total			1	
1 to 2	N/A	N/A	N/A	N/A		2	142.84
2 to 3	1971.99	112.65	100%	0%		3	1158.62
3 to 4	1735.34	55.06	100%	-12%		4	696.18
							459.98
<b>THRUST</b>	8.81 lb						

**Test Matrix 1A Configuration e Run 1**

WAVE SPEEDS							PRESSURE
Ports	Average	Stdev	%used	% CJ			(psig)
	(m/s)	(m/s)	of 10 total			1	74.87
1 to 2	N/A	N/A	N/A	N/A		2	305.33
2 to 3	1799.76	218.20	100%	-9%		3	541.59
3 to 4	1987.87	41.86	100%	1%		4	468.84
4 to 5	1784.06	48.85	100%	-9%		5	394.36
5 to 6	1698.53	99.38	100%	-14%		6	477.06
<b>THRUST</b>	9.12 lb						

**Test Matrix 1A Configuration e Run 2**

WAVE SPEEDS							PRESSURE
Ports	Average	Stdev	%used	% CJ			(psig)
	(m/s)	(m/s)	of 11 total			1	72.89
1 to 2	N/A	N/A	N/A	N/A		2	237.51
2 to 3	1864.05	326.02	100%	-5%		3	474.50
3 to 4	1990.87	45.88	100%	1%		4	454.84
4 to 5	1763.62	74.13	100%	-10%		5	380.77
5 to 6	1751.34	82.86	100%	-11%		6	584.94
<b>THRUST</b>	9.13 lb						

**Test Matrix 1A Configuration f Run 1**

WAVE SPEEDS							PRESSURE
Ports	Average	Stdev	%used	% CJ			(psig)
	(m/s)	(m/s)	of 10 total			1	74.85
1 to 2	N/A	N/A	N/A	N/A		2	394.71
2 to 3	1916.01	219.50	100%	-3%		3	489.88
3 to 4	1999.23	32.79	100%	2%		4	453.58
4 to 5	1777.22	51.20	100%	-10%		5	364.41
5 to 6	1741.54	68.49	100%	-12%		6	601.81
<b>THRUST</b>	9.12 lb						

**Test Matrix 1A Configuration f Run 2**

WAVE SPEEDS							PRESSURE
Ports	Average	Stdev	%used	% CJ			(psig)
	(m/s)	(m/s)	of 10 total			1	78.62
1 to 2	N/A	N/A	N/A	N/A		2	429.71
2 to 3	2009.04	142.78	100%	2%		3	442.35
3 to 4	1970.93	36.30	100%	0%		4	456.57
4 to 5	1756.53	50.05	100%	-11%		5	358.58
5 to 6	1741.34	67.77	100%	-12%		6	546.97
<b>THRUST</b>	9.13 lb						

**Test Matrix 1A Configuration g Run 1**

WAVE SPEEDS							PRESSURE
Ports	Average	Stdev	%used	% CJ			(psig)
	(m/s)	(m/s)	of 10 total			1	
1 to 2	N/A	N/A	N/A	N/A		2	1059.33
2 to 3	1986.72	101.63	100%	1%		3	721.09
3 to 4	1693.36	100.62	100%	-14%		4	490.60
4 to 5	1295.22	48.15	100%	-34%		5	767.78
5 to 6	1593.38	73.58	100%	-19%		6	242.89
<b>THRUST</b>	9.09 lb						

**Test Matrix 1A Configuration g Run 2**

WAVE SPEEDS							PRESSURE
Ports	Average	Stdev	%used	% CJ			(psig)
	(m/s)	(m/s)	of 10 total			1	
1 to 2	N/A	N/A	N/A	N/A		2	1072.12
2 to 3	1937.23	156.36	100%	-2%		3	733.56
3 to 4	1688.43	87.62	100%	-14%		4	538.68
4 to 5	1351.67	61.24	100%	-31%		5	698.89
5 to 6	1601.11	86.65	100%	-19%		6	264.60
<b>THRUST</b>	8.77 lb						

**Test Matrix 1A Configuration g Run 3**

WAVE SPEEDS							PRESSURE
Ports	Average	Stdev	%used	% CJ			(psig)
	(m/s)	(m/s)	of 10 total			1	
1 to 2	N/A	N/A	N/A	N/A		2	1158.32
2 to 3	2144.65	132.87	100%	9%		3	616.77
3 to 4	1763.71	57.51	100%	-10%		4	534.42
4 to 5	1333.37	36.83	100%	-32%		5	493.97
5 to 6	1595.55	47.56	100%	-19%		6	356.03
<b>THRUST</b>	8.40 lb						

**Test Matrix 1A Configuration g Run 4**

WAVE SPEEDS							PRESSURE
Ports	Average	Stdev	%used	% CJ			(psig)
	(m/s)	(m/s)	of 10 total			1	
1 to 2	N/A	N/A	N/A	N/A		2	901.33
2 to 3	2035.07	101.42	100%	3%		3	580.96
3 to 4	1775.70	30.16	100%	-10%		4	525.69
4 to 5	1312.09	39.37	100%	-33%		5	533.18
5 to 6	1563.01	33.88	100%	-21%		6	314.94
<b>THRUST</b>	8.38 lb						

**Test Matrix 1A Configuration h Run 1**

WAVE SPEEDS							PRESSURE
Ports	Average	Stdev	%used	% CJ			(psig)
	(m/s)	(m/s)	of 10 total			1	
1 to 2	N/A	N/A	N/A	N/A		2	150.00
2 to 3	2004.57	143.18	100%	2%		3	843.51
3 to 4	1723.49	55.83	100%	-12%		4	760.09
4 to 5	1422.75	47.14	100%	-28%		5	449.73
5 to 6	1563.79	33.15	100%	-21%		6	662.70
							223.47
<b>THRUST</b>	9.18 lb						

**Test Matrix 1A Configuration h Run 2**

WAVE SPEEDS							PRESSURE
Ports	Average	Stdev	%used	% CJ			(psig)
	(m/s)	(m/s)	of 10 total			1	
1 to 2	N/A	N/A	N/A	N/A		2	153.48
2 to 3	1975.43	90.40	100%	0%		3	1190.47
3 to 4	1699.62	29.10	100%	-14%		4	712.70
4 to 5	1450.34	55.64	100%	-26%		5	489.05
5 to 6	1568.46	47.37	100%	-20%		6	684.29
							240.56
<b>THRUST</b>	9.17 lb						

**Test Matrix 1B Configuration a Run 1**

WAVE SPEEDS							PRESSURE
Ports	Average	Stdev	%used	% CJ			(psig)
	(m/s)	(m/s)	of 10 total			1	
1 to 2	N/A	N/A	N/A	N/A		2	130.517151
2 to 3	2073.35	73.923	1	5%		3	1116.44348
3 to 4	2829.77	121.86	1	44%		4	459.733215
							527.817749
<b>THRUST</b>	7.42 lb						

**Test Matrix 1B Configuration a Run 2**

WAVE SPEEDS							PRESSURE
Ports	Average	Stdev	%used	% CJ			(psig)
	(m/s)	(m/s)	of 10 total			1	
1 to 2	N/A	N/A	N/A	N/A		2	135.849777
2 to 3	2107.51	76.755	1	7%		3	1115.84436
3 to 4	2875.99	66.904	0.8	46%		4	539.918518
							440.209412
<b>THRUST</b>	7.45 lb						



**Test Matrix 1B Configuration c Run 1**

WAVE SPEEDS							PRESSURE
Ports	Average	Stdev	%used	% CJ			(psig)
	(m/s)	(m/s)	of 10 total			1	
1 to 2	N/A	N/A	N/A	N/A		2	175.21
2 to 3	1939.79	101.04	100%	-1%		3	1335.34
3 to 4	2200.95	88.95	100%	12%		4	686.65
4 to 5	1333.40	14.46	60%	-32%		5	637.88
5 to 6	524.71	390.71	90%	-73%		6	80.97
							135.84
<b>THRUST</b>	7.24 lb						

**Test Matrix 1B Configuration c Run 2**

WAVE SPEEDS							PRESSURE
Ports	Average	Stdev	%used	% CJ			(psig)
	(m/s)	(m/s)	of 10 total			1	
1 to 2	N/A	N/A	N/A	N/A		2	172.76
2 to 3	1934.55	101.76	100%	-2%		3	1282.02
3 to 4	2199.48	89.55	100%	12%		4	598.46
4 to 5	1314.92	26.81	90%	-33%		5	610.75
5 to 6	787.17	232.65	100%	-60%		6	74.47
							100.20
<b>THRUST</b>	7.24 lb						

**Test Matrix 1B Configuration d Run 1**

WAVE SPEEDS							PRESSURE
Ports	Average	Stdev	%used	% CJ			(psig)
	(m/s)	(m/s)	of 10 total			1	
1 to 2	N/A	N/A	N/A	N/A		2	169.94
2 to 3	1946.56	151.29	100%	-1%		3	1185.39
3 to 4	2260.52	100.67	100%	15%		4	638.50
4 to 5	N/A	N/A	N/A	N/A		5	598.74
5 to 6	N/A	N/A	N/A	N/A		6	23.88
							17.18
<b>THRUST</b>	7.24 lb						

**Test Matrix 1B Configuration d Run 2**

WAVE SPEEDS							PRESSURE
Ports	Average	Stdev	%used	% CJ			(psig)
	(m/s)	(m/s)	of 10 total			1	
1 to 2	N/A	N/A	N/A	N/A		2	177.67
2 to 3	1907.12	108.92	100%	-3%		3	957.16
3 to 4	2211.27	98.22	100%	12%		4	1092.06
4 to 5	N/A	N/A	N/A	N/A		5	611.48
5 to 6	N/A	N/A	N/A	N/A		6	25.90
							10.26
<b>THRUST</b>	7.24 lb						

**Test Matrix 1B Configuration e Run 1**

WAVE SPEEDS							PRESSURE
Ports	Average	Stdev	%used	% CJ			(psig)
	(m/s)	(m/s)	of 10 total			1	
1 to 2	N/A	N/A	N/A	N/A		2	1246.06
2 to 3	1932.37	114.51	100%	-2%		3	729.78
3 to 4	2197.09	78.39	100%	12%		4	634.47
4 to 5	N/A	N/A	N/A	N/A		5	22.35
5 to 6	N/A	N/A	N/A	N/A		6	12.32
<b>THRUST</b>							
	7.24 lb						

**Test Matrix 1B Configuration e Run 2**

WAVE SPEEDS							PRESSURE
Ports	Average	Stdev	%used	% CJ			(psig)
	(m/s)	(m/s)	of 10 total			1	
1 to 2	N/A	N/A	N/A	N/A		2	1164.58
2 to 3	1935.13	139.70	100%	-2%		3	801.75
3 to 4	2239.23	82.98	100%	14%		4	636.33
4 to 5	N/A	N/A	N/A	N/A		5	18.67
5 to 6	N/A	N/A	N/A	N/A		6	8.46
<b>THRUST</b>							
	7.24 lb						

**Test Matrix 1C Configuration a Run 1**

WAVE SPEEDS							PRESSURE
Ports	Average	Stdev	%used	% CJ			(psig)
	(m/s)	(m/s)	of 10 total			1	
1 to 2	N/A	N/A	N/A	N/A		2	519.35
2 to 3	1954.78	110.55	100%	-1%		3	437.81
3 to 4	1897.23	36.33	100%	-4%		4	485.76
4 to 5	1785.79	38.95	100%	-9%		5	605.40
5 to 6	1953.57	43.57	100%	-1%		6	423.18
<b>THRUST</b>							
	N/A						

**Test Matrix 1C Configuration a Run 2**

WAVE SPEEDS							PRESSURE
Ports	Average	Stdev	%used	% CJ			(psig)
	(m/s)	(m/s)	of 10 total			1	
1 to 2	N/A	N/A	N/A	N/A		2	533.93
2 to 3	1962.16	184.74	100%	0%		3	445.57
3 to 4	1915.57	78.51	100%	-3%		4	528.65
4 to 5	1796.72	40.43	100%	-9%		5	602.12
5 to 6	1956.70	55.95	100%	-1%		6	397.11
<b>THRUST</b>							
	N/A						



**Test Matrix 1C Configuration b Run 1**

WAVE SPEEDS						PRESSURE
Ports	Average	Stdev	%used	% CJ		(psig)
	(m/s)	(m/s)	of 11 total			
					1	91.93
1 to 2	N/A	N/A	N/A	N/A	2	759.08
2 to 3	2000.43	134.60	100%	2%	3	440.29
3 to 4	1905.01	67.37	100%	-3%	4	454.90
4 to 5	1789.21	60.59	100%	-9%	5	617.53
5 to 6	1962.47	58.11	100%	0%	6	423.22
<b>THRUST</b>	N/A					

**Test Matrix 1C Configuration b Run 2**

WAVE SPEEDS						PRESSURE
Ports	Average	Stdev	%used	% CJ		(psig)
	(m/s)	(m/s)	of 10 total			
					1	90.19
1 to 2	N/A	N/A	N/A	N/A	2	753.13
2 to 3	2028.23	185.94	100%	3%	3	468.73
3 to 4	1888.61	74.48	100%	-4%	4	513.02
4 to 5	1795.37	45.35	100%	-9%	5	577.68
5 to 6	1969.91	65.24	100%	0%	6	393.87
<b>THRUST</b>	N/A					

**Test Matrix 1C Configuration c Run 1**

WAVE SPEEDS						PRESSURE
Ports	Average	Stdev	%used	% CJ		(psig)
	(m/s)	(m/s)	of 10 total			
					1	148.62
1 to 2	N/A	N/A	N/A	N/A	2	1043.13
2 to 3	1947.26	107.54	100%	-1%	3	689.86
3 to 4	1724.96	47.63	100%	-12%	4	540.01
4 to 5	1238.22	34.29	100%	-37%	5	438.38
5 to 6	1409.71	27.94	100%	-28%	6	178.52
<b>THRUST</b>	N/A					

**Test Matrix 1C Configuration c Run 2**

WAVE SPEEDS						PRESSURE
Ports	Average	Stdev	%used	% CJ		(psig)
	(m/s)	(m/s)	of 10 total			
					1	152.64
1 to 2	N/A	N/A	N/A	N/A	2	996.54
2 to 3	1964.05	161.93	100%	0%	3	692.36
3 to 4	1712.88	95.47	100%	-13%	4	607.43
4 to 5	1247.03	66.23	100%	-37%	5	441.39
5 to 6	1420.32	69.79	100%	-28%	6	179.76
<b>THRUST</b>	N/A					

**Test Matrix 1C Configuration d Run 1**

WAVE SPEEDS						PRESSURE
Ports	Average	Stdev	%used	% CJ		(psig)
	(m/s)	(m/s)	of 10 total			
					1	147.12
1 to 2	N/A	N/A	N/A	N/A	2	1137.05
2 to 3	2017.93	101.67	100%	3%	3	722.98
3 to 4	1819.47	99.42	100%	-8%	4	570.72
4 to 5	1278.69	54.14	100%	-35%	5	303.70
5 to 6	1363.41	33.95	100%	-31%	6	175.14
<b>THRUST</b>	N/A					

**Test Matrix 1C Configuration d Run 2**

WAVE SPEEDS						PRESSURE
Ports	Average	Stdev	%used	% CJ		(psig)
	(m/s)	(m/s)	of 10 total			
					1	147.65
1 to 2	N/A	N/A	N/A	N/A	2	1005.49
2 to 3	2030.29	110.32	100%	3%	3	701.83
3 to 4	1807.41	50.35	100%	-8%	4	579.22
4 to 5	1262.70	37.48	100%	-36%	5	329.91
5 to 6	1344.85	21.43	100%	-32%	6	159.90
<b>THRUST</b>	N/A					

**Test Matrix 1C Configuration e Run 1**

WAVE SPEEDS						PRESSURE
Ports	Average	Stdev	%used	% CJ		(psig)
	(m/s)	(m/s)	of 10 total			
					1	179.11
1 to 2	N/A	N/A	N/A	N/A	2	1087.66
2 to 3	1811.64	47.76	100%	-8%	3	939.89
3 to 4	1954.05	73.08	100%	-1%	4	689.36
4 to 5	1267.99	27.44	70%	-36%	5	57.09
5 to 6	633.42	291.82	100%	-68%	6	51.13
<b>THRUST</b>	N/A					

**Test Matrix 1C Configuration e Run 2**

WAVE SPEEDS						PRESSURE
Ports	Average	Stdev	%used	% CJ		(psig)
	(m/s)	(m/s)	of 10 total			
					1	198.26
1 to 2	N/A	N/A	N/A	N/A	2	1357.14
2 to 3	1825.55	57.01	100%	-7%	3	755.52
3 to 4	1930.14	92.39	100%	-2%	4	680.17
4 to 5	1092.82	338.40	90%	-44%	5	93.21
5 to 6	815.80	420.45	90%	-59%	6	56.16
<b>THRUST</b>	N/A					

**Test Matrix 1C Configuration f Run 1**

WAVE SPEEDS							PRESSURE
Ports	Average	Stdev	%used	% CJ			(psig)
	(m/s)	(m/s)	of 10 total			1	
1 to 2	N/A	N/A	N/A	N/A		2	1146.16
2 to 3	1849.00	116.30	100%	-6%		3	1060.07
3 to 4	1970.91	44.34	100%	0%		4	675.93
4 to 5	1228.78	86.42	91%	-38%		5	51.67
5 to 6	822.43	95.14	64%	-58%		6	56.73
<b>THRUST</b>	N/A						

**Test Matrix 1C Configuration f Run 2**

WAVE SPEEDS							PRESSURE
Ports	Average	Stdev	%used	% CJ			(psig)
	(m/s)	(m/s)	of 10 total			1	
1 to 2	N/A	N/A	N/A	N/A		2	1160.26
2 to 3	1810.66	113.18	100%	-8%		3	1030.60
3 to 4	1988.73	60.48	100%	1%		4	706.09
4 to 5	1149.13	278.07	80%	-42%		5	123.73
5 to 6	707.68	238.86	80%	-64%		6	53.46
<b>THRUST</b>	N/A						

**Test Matrix 1C Configuration g Run 1**

WAVE SPEEDS							PRESSURE
Ports	Average	Stdev	%used	% CJ			(psig)
	(m/s)	(m/s)	of 11 total			1	
1 to 2	N/A	N/A	N/A	N/A		2	1270.79
2 to 3	1677.46	92.15	100%	-15%		3	983.79
3 to 4	1578.99	66.39	100%	-20%		4	336.92
4 to 5	1191.54	65.50	100%	-39%		5	165.83
5 to 6	1117.38	57.60	100%	-43%		6	110.67
<b>THRUST</b>	N/A						

**Test Matrix 1C Configuration g Run 2**

WAVE SPEEDS							PRESSURE
Ports	Average	Stdev	%used	% CJ			(psig)
	(m/s)	(m/s)	of 10 total			1	
1 to 2	N/A	N/A	N/A	N/A		2	1272.81
2 to 3	1679.33	76.66	100%	-15%		3	738.42
3 to 4	1613.53	52.29	100%	-18%		4	336.43
4 to 5	1200.42	15.42	100%	-39%		5	170.39
5 to 6	1238.97	115.83	100%	-37%		6	113.95
<b>THRUST</b>	N/A						

**Test Matrix 2A Configuration a Run 1**

<b>WAVE SPEEDS</b>						<b>PRESSURE</b>
Ports	Average	Stdev	%used	% CJ		(psig)
	(m/s)	(m/s)	of 10 total			
					1	71.52
1 to 2	N/A	N/A	N/A	N/A	2	354.13
2 to 3	1874.57	180.32	100%	-5%	3	679.18
3 to 4	2087.91	22.05	100%	6%	4	518.73
4 to 5	1782.86	54.86	100%	-9%	5	528.47
5 to 6	1782.58	45.35	100%	-9%	6	207.15
7 to 8	1143.69	121.63	100%	-42%	7	247.65
					8	153.63
<b>THRUST</b>	8.43 lb					

**Test Matrix 2A Configuration a Run 2**

<b>WAVE SPEEDS</b>						<b>PRESSURE</b>
Ports	Average	Stdev	%used	% CJ		(psig)
	(m/s)	(m/s)	of 10 total			
					1	71.05
1 to 2	N/A	N/A	N/A	N/A	2	378.61
2 to 3	1904.08	224.78	100%	-3%	3	686.87
3 to 4	2095.32	31.63	100%	6%	4	509.16
4 to 5	1772.09	58.99	100%	-10%	5	550.95
5 to 6	1765.63	67.89	90%	-10%	6	313.17
7 to 8	1094.30	73.23	100%	-44%	7	235.40
					8	147.49
<b>THRUST</b>	8.45 lb					

**Test Matrix 2A Configuration b Run 1**

<b>WAVE SPEEDS</b>						<b>PRESSURE</b>
Ports	Average	Stdev	%used	% CJ		(psig)
	(m/s)	(m/s)	of 10 total			
					1	72.16
1 to 2	N/A	N/A	N/A	N/A	2	351.77
2 to 3	2055.16	174.18	100%	4%	3	450.51
3 to 4	2098.09	27.35	100%	7%	4	538.97
4 to 5	1803.56	52.58	100%	-8%	5	657.60
5 to 6	1762.74	39.66	100%	-10%	6	369.55
7 to 8	1844.70	187.33	100%	-6%	7	514.91
					8	419.55
<b>THRUST</b>	8.38 lb					

**Test Matrix 2A Configuration b Run 2**

<b>WAVE SPEEDS</b>						<b>PRESSURE</b>
Ports	Average	Stdev	%used	% CJ		(psig)
	(m/s)	(m/s)	of 10 total			
					1	76.07
1 to 2	N/A	N/A	N/A	N/A	2	467.46
2 to 3	1978.01	242.59	80%	1%	3	679.67
3 to 4	2103.95	30.02	100%	7%	4	497.18
4 to 5	1802.90	39.67	100%	-8%	5	548.18
5 to 6	1759.86	42.94	100%	-11%	6	233.21
7 to 8	1776.64	131.83	100%	-10%	7	443.98
					8	424.91
<b>THRUST</b>	8.38 lb					

**Test Matrix 2A Configuration c Run 1**

<b>WAVE SPEEDS</b>						<b>PRESSURE</b>
Ports	Average	Stdev	%used	% CJ		(psig)
	(m/s)	(m/s)	of 10 total			
					1	71.72
1 to 2	N/A	N/A	N/A	N/A	2	427.43
2 to 3	1909.00	188.55	100%	-3%	3	460.24
3 to 4	1964.49	35.37	100%	0%	4	502.58
4 to 5	1702.83	75.44	100%	-13%	5	466.41
5 to 6	1539.44	65.71	100%	-22%	6	362.59
7 to 8	1246.77	196.24	100%	-37%	7	426.60
					8	589.59
<b>THRUST</b>	9.06 lb					

**Test Matrix 2A Configuration c Run 2**

<b>WAVE SPEEDS</b>						<b>PRESSURE</b>
Ports	Average	Stdev	%used	% CJ		(psig)
	(m/s)	(m/s)	of 10 total			
					1	71.45
1 to 2	N/A	N/A	N/A	N/A	2	432.88
2 to 3	1904.21	112.75	100%	-3%	3	464.87
3 to 4	1978.59	29.13	100%	1%	4	444.85
4 to 5	1710.04	54.44	100%	-13%	5	462.85
5 to 6	1520.08	53.03	100%	-23%	6	403.73
7 to 8	1166.83	100.61	100%	-41%	7	376.18
					8	415.56
<b>THRUST</b>	9.11 lb					

**Test Matrix 2A Configuration d Run 1**

<b>WAVE SPEEDS</b>						<b>PRESSURE</b>
Ports	Average	Stdev	%used	% CJ		(psig)
	(m/s)	(m/s)	of 10 total			
					1	79.54
1 to 2	N/A	N/A	N/A	N/A	2	421.93
2 to 3	1893.50	167.91	90%	-4%	3	475.92
3 to 4	2037.87	25.84	100%	4%	4	479.52
4 to 5	1814.44	29.04	100%	-8%	5	448.97
5 to 6	1532.76	34.56	100%	-22%	6	340.85
7 to 8	1654.82	318.03	100%	-16%	7	549.13
					8	770.81
<b>THRUST</b>	8.47 lb					

**Test Matrix 2A Configuration d Run 2**

<b>WAVE SPEEDS</b>						<b>PRESSURE</b>
Ports	Average	Stdev	%used	% CJ		(psig)
	(m/s)	(m/s)	of 10 total			
					1	77.21
1 to 2	N/A	N/A	N/A	N/A	2	446.08
2 to 3	1901.70	285.06	100%	-3%	3	520.89
3 to 4	2030.99	82.80	100%	3%	4	560.61
4 to 5	1788.04	87.45	100%	-9%	5	463.81
5 to 6	1517.68	67.74	100%	-23%	6	343.95
7 to 8	1538.70	226.71	100%	-22%	7	540.75
					8	619.33
<b>THRUST</b>	8.45 lb					

**Test Matrix 2A Configuration e Run 1**

<b>WAVE SPEEDS</b>						<b>PRESSURE</b>
Ports	Average	Stdev	%used	% CJ		(psig)
	(m/s)	(m/s)	of 33 total			
					1	111.38
1 to 2	N/A	N/A	N/A	N/A	2	3.30
2 to 3	N/A	N/A	N/A	N/A	3	557.98
3 to 4	2015.50	75.08	85%	2%	4	328.45
4 to 5	1718.94	58.45	73%	-13%	5	450.01
5 to 6	1925.92	148.07	79%	-2%	6	404.27
7 to 8	2010.03	168.34	82%	2%	7	182.73
					8	585.73
<b>THRUST</b>	~0 lb					

**Test Matrix 2A Configuration e Run 2**

WAVE SPEEDS						PRESSURE
Ports	Average	Stdev	%used	% CJ		(psig)
	(m/s)	(m/s)	of 33 total			1 112.48
1 to 2	N/A	N/A	N/A	N/A		2 3.23
2 to 3	N/A	N/A	N/A	N/A		3 532.70
3 to 4	2141.78	219.44	94%	9%		4 466.31
4 to 5	1624.35	317.93	73%	-17%		5 461.65
5 to 6	1894.92	165.05	76%	-4%		6 382.08
7 to 8	1947.31	147.49	94%	-1%		7 214.10
						8 539.20
<b>THRUST</b>	~0 lb					

**Test Matrix 2A Configuration f Run 1**

WAVE SPEEDS						PRESSURE
Ports	Average	Stdev	%used	% CJ		(psig)
	(m/s)	(m/s)	of 10 total			1 120.01
1 to 2	N/A	N/A	N/A	N/A		2 811.59
2 to 3	2164.28	275.00	100%	10%		3 572.49
3 to 4	2039.04	14.38	100%	4%		4 628.28
4 to 5	1619.06	81.04	100%	-18%		5 375.23
5 to 6	1686.15	362.14	100%	-14%		6 288.85
7 to 8	1475.91	84.87	100%	-25%		7 255.27
						8 271.02
<b>THRUST</b>	7.85 lb					

**Test Matrix 2A Configuration f Run 2**

WAVE SPEEDS						PRESSURE
Ports	Average	Stdev	%used	% CJ		(psig)
	(m/s)	(m/s)	of 10 total			1 117.17
1 to 2	N/A	N/A	N/A	N/A		2 967.26
2 to 3	2183.08	287.87	100%	11%		3 584.04
3 to 4	2046.09	18.78	100%	4%		4 616.34
4 to 5	1600.84	28.60	100%	-19%		5 417.45
5 to 6	1688.16	155.84	100%	-14%		6 269.93
7 to 8	1441.24	84.75	100%	-27%		7 367.72
						8 230.57
<b>THRUST</b>	7.88 lb					

**Test Matrix 2A Configuration g Run 1**

WAVE SPEEDS						PRESSURE
Ports	Average	Stdev	%used	% CJ		(psig)
	(m/s)	(m/s)	of 33 total			1 76.02
1 to 2	N/A	N/A	N/A	N/A		2 2.56
2 to 3	N/A	N/A	N/A	N/A		3 467.21
3 to 4	2136.60	93.29	88%	9%		4 450.93
4 to 5	1465.68	68.24	73%	-26%		5 520.48
5 to 6	1399.61	732.81	100%	-29%		6 440.22
7 to 8	1462.18	210.97	76%	-26%		7 480.50
						8 545.63
<b>THRUST</b>	~0					

**Test Matrix 2A Configuration g Run 2**

WAVE SPEEDS						PRESSURE
Ports	Average	Stdev	%used	% CJ		(psig)
	(m/s)	(m/s)	of 33 total			1 76.31
1 to 2	N/A	N/A	N/A	N/A		2 2.95
2 to 3	N/A	N/A	N/A	N/A		3 497.68
3 to 4	2175.13	179.53	73%	11%		4 485.61
4 to 5	1458.89	74.63	88%	-26%		5 463.93
5 to 6	1686.52	332.03	97%	-14%		6 457.95
7 to 8	1442.41	185.48	70%	-27%		7 448.85
						8 547.04
<b>THRUST</b>	~0					

**Test Matrix 2A Configuration h Run 1**

WAVE SPEEDS						PRESSURE
Ports	Average	Stdev	%used	% CJ		(psig)
	(m/s)	(m/s)	of 33 total			1 82.23
1 to 2	N/A	N/A	N/A	N/A		2 2.92
2 to 3	N/A	N/A	N/A	N/A		3 495.85
3 to 4	2149.55	100.72	94%	9%		4 478.00
4 to 5	1506.35	69.89	94%	-23%		5 436.50
5 to 6	1722.71	308.57	97%	-12%		6 477.72
7 to 8	1532.06	196.31	91%	-22%		7 474.85
						8 558.84
<b>THRUST</b>	~0					



**Test Matrix 2A Configuration h Run 2**

WAVE SPEEDS						PRESSURE
Ports	Average	Stdev	%used	% CJ		(psig)
	(m/s)	(m/s)	of 33 total			
					1	81.02
1 to 2	N/A	N/A	N/A	N/A	2	2.90
2 to 3	N/A	N/A	N/A	N/A	3	482.22
3 to 4	2181.16	200.41	82%	11%	4	488.67
4 to 5	1494.43	67.41	85%	-24%	5	410.58
5 to 6	1782.98	92.28	88%	-9%	6	403.63
7 to 8	1581.04	227.67	88%	-20%	7	493.54
					8	461.21
<b>THRUST</b>	~0					

**Test Matrix 2B Configuration a Run 1**

WAVE SPEEDS						PRESSURE
Ports	Average	Stdev	%used	% CJ		(psig)
	(m/s)	(m/s)	of 33 total			
					1	79.01
1 to 2	N/A	N/A	N/A	N/A	2	3.06
2 to 3	N/A	N/A	N/A	N/A	3	463.37
3 to 4	2114.24	65.42	70%	7%	4	290.47
4 to 5	1377.71	46.12	67%	-30%	5	536.89
5 to 6	1860.66	123.89	85%	-5%	6	379.58
7 to 8	1158.78	523.74	100%	-41%	7	569.36
					8	296.72
<b>THRUST</b>	9.29 lb					

**Test Matrix 2B Configuration a Run 2**

WAVE SPEEDS						PRESSURE
Ports	Average	Stdev	%used	% CJ		(psig)
	(m/s)	(m/s)	of 33 total			
					1	78.09
1 to 2	N/A	N/A	N/A	N/A	2	3.45
2 to 3	N/A	N/A	N/A	N/A	3	490.94
3 to 4	2172.13	131.11	67%	10%	4	438.71
4 to 5	1371.67	81.97	94%	-30%	5	504.38
5 to 6	1861.56	118.06	94%	-5%	6	347.73
7 to 8	1069.04	545.68	97%	-46%	7	604.14
					8	301.63
<b>THRUST</b>	9.32 lb					

**Test Matrix 2B Configuration b Run 1**

WAVE SPEEDS						PRESSURE
Ports	Average	Stdev	%used	% CJ		(psig)
	(m/s)	(m/s)	of 33 total			1
						83.45
1 to 2	N/A	N/A	N/A	N/A		2
						3.31
2 to 3	N/A	N/A	N/A	N/A		3
						517.86
3 to 4	2172.83	107.21	70%	10%		4
						496.68
4 to 5	1386.81	250.57	88%	-30%		5
						435.45
5 to 6	1833.51	160.70	88%	-7%		6
						348.27
7 to 8	1555.82	539.84	97%	-21%		7
						568.42
						8
						452.61
<b>THRUST</b>	9.34 lb					

**Test Matrix 2B Configuration b Run 2**

WAVE SPEEDS						PRESSURE
Ports	Average	Stdev	%used	% CJ		(psig)
	(m/s)	(m/s)	of 33 total			1
						84.64
1 to 2	N/A	N/A	N/A	N/A		2
						3.32
2 to 3	N/A	N/A	N/A	N/A		3
						550.63
3 to 4	2176.53	149.38	85%	11%		4
						418.77
4 to 5	1461.20	70.41	85%	-26%		5
						459.34
5 to 6	1855.03	225.74	85%	-6%		6
						400.80
7 to 8	1699.87	393.80	94%	-14%		7
						563.96
						8
						446.14
<b>THRUST</b>	9.39 lb					

**Test Matrix 2B Configuration c Run 1**

WAVE SPEEDS						PRESSURE
Ports	Average	Stdev	%used	% CJ		(psig)
	(m/s)	(m/s)	of 11 total			1
						67.92
1 to 2	N/A	N/A	N/A	N/A		2
						327.20
2 to 3	1835.66	149.34	100%	-7%		3
						506.54
3 to 4	1985.44	14.12	100%	1%		4
						589.04
4 to 5	1617.23	56.13	100%	-18%		5
						770.39
5 to 6	1951.30	78.03	100%	-1%		6
						385.89
7 to 8	1529.30	109.28	100%	-22%		7
						574.21
						8
						532.92
<b>THRUST</b>	10.8 lb					

**Test Matrix 2B Configuration c Run 2**

<b>WAVE SPEEDS</b>						<b>PRESSURE</b>
Ports	Average	Stdev	%used	% CJ		(psig)
	(m/s)	(m/s)	of 10 total			
					1	71.01
1 to 2	N/A	N/A	N/A	N/A	2	290.57
2 to 3	1775.78	168.16	100%	-10%	3	419.84
3 to 4	1921.44	189.85	100%	-2%	4	559.19
4 to 5	1678.20	144.11	100%	-15%	5	581.40
5 to 6	1879.32	107.68	100%	-5%	6	342.75
7 to 8	1501.29	211.03	100%	-24%	7	506.91
					8	578.91
<b>THRUST</b>	10.79 lb					

**Test Matrix 2B Configuration d Run 1**

<b>WAVE SPEEDS</b>						<b>PRESSURE</b>
Ports	Average	Stdev	%used	% CJ		(psig)
	(m/s)	(m/s)	of 10 total			
					1	77.79
1 to 2	N/A	N/A	N/A	N/A	2	525.31
2 to 3	1965.37	195.27	100%	0%	3	489.33
3 to 4	2036.36	20.46	100%	3%	4	502.37
4 to 5	1748.54	52.63	100%	-11%	5	509.28
5 to 6	1867.68	92.61	100%	-5%	6	355.96
7 to 8	1720.21	83.00	100%	-13%	7	616.40
					8	531.40
<b>THRUST</b>	10.77 lb					

**Test Matrix 2B Configuration d Run 2**

<b>WAVE SPEEDS</b>						<b>PRESSURE</b>
Ports	Average	Stdev	%used	% CJ		(psig)
	(m/s)	(m/s)	of 10 total			
					1	79.36
1 to 2	N/A	N/A	N/A	N/A	2	308.75
2 to 3	1835.12	119.33	100%	-7%	3	494.31
3 to 4	2043.77	36.50	100%	4%	4	531.06
4 to 5	1712.54	90.68	100%	-13%	5	764.65
5 to 6	1888.28	126.72	100%	-4%	6	360.99
7 to 8	1699.21	80.44	100%	-14%	7	637.59
					8	633.76
<b>THRUST</b>	10.74 lb					

**Test Matrix 2B Configuration e Run 1**

WAVE SPEEDS						PRESSURE
Ports	Average	Stdev	%used	% CJ		(psig)
	(m/s)	(m/s)	of 11 total			
1 to 2	N/A	N/A	N/A	N/A		122.13
2 to 3	2201.23	311.52	100%	12%		967.57
3 to 4	2046.09	18.90	100%	4%		587.20
4 to 5	1627.30	66.07	100%	-17%		614.31
5 to 6	1781.25	52.79	100%	-9%		739.03
7 to 8	1740.39	148.72	100%	-12%		473.88
						700.80
						377.69
<b>THRUST</b>	8.33 lb					

**Test Matrix 2B Configuration e Run 2**

WAVE SPEEDS						PRESSURE
Ports	Average	Stdev	%used	% CJ		(psig)
	(m/s)	(m/s)	of 10 total			
1 to 2	N/A	N/A	N/A	N/A		124.44
2 to 3	2223.74	187.73	100%	13%		1290.06
3 to 4	2034.99	21.41	100%	3%		575.58
4 to 5	1603.79	41.95	100%	-19%		615.95
5 to 6	1764.25	48.93	100%	-10%		873.89
7 to 8	1652.87	53.36	100%	-16%		581.52
						683.74
						413.58
<b>THRUST</b>	9.53 lb					

**Test Matrix 2B Configuration e Run 3**

WAVE SPEEDS						PRESSURE
Ports	Average	Stdev	%used	% CJ		(psig)
	(m/s)	(m/s)	of 33 total			
1 to 2	N/A	N/A	N/A	N/A		124.60
2 to 3	N/A	N/A	N/A	N/A		2.72
3 to 4	1945.58	93.58	97%	-1%		583.44
4 to 5	1310.50	249.75	73%	-33%		465.67
5 to 6	2033.00	268.70	73%	3%		569.21
7 to 8	1961.35	187.04	85%	0%		415.88
						631.51
						525.59
<b>THRUST</b>	8.38 lb					

**Test Matrix 2B Configuration e Run 4**

<b>WAVE SPEEDS</b>						<b>PRESSURE</b>
Ports	Average	Stdev	%used	% CJ		(psig)
	(m/s)	(m/s)	of 33 total			
					1	124.58
1 to 2	N/A	N/A	N/A	N/A	2	779.37
2 to 3	N/A	N/A	N/A	N/A	3	603.61
3 to 4	1936.54	98.84	88%	-2%	4	611.59
4 to 5	1375.76	73.93	61%	-30%	5	398.10
5 to 6	1844.88	431.78	64%	-6%	6	340.87
7 to 8	2010.66	143.34	76%	2%	7	725.12
					8	386.42
<b>THRUST</b>	8.41 lb					

**Test Matrix 2B Configuration f Run 1**

<b>WAVE SPEEDS</b>						<b>PRESSURE</b>
Ports	Average	Stdev	%used	% CJ		(psig)
	(m/s)	(m/s)	of 10 total			
					1	124.58
1 to 2	N/A	N/A	N/A	N/A	2	779.37
2 to 3	1936.09	300.80	90%	-2%	3	603.61
3 to 4	2020.19	33.52	100%	3%	4	611.59
4 to 5	1696.53	49.21	100%	-14%	5	398.10
5 to 6	1778.48	46.45	100%	-10%	6	340.87
7 to 8	1728.87	81.10	100%	-12%	7	725.12
					8	386.42
<b>THRUST</b>	10.77 lb					

**Test Matrix 2B Configuration f Run 2**

<b>WAVE SPEEDS</b>						<b>PRESSURE</b>
Ports	Average	Stdev	%used	% CJ		(psig)
	(m/s)	(m/s)	of 10 total			
					1	125.34
1 to 2	N/A	N/A	N/A	N/A	2	756.46
2 to 3	1907.90	310.31	100%	-3%	3	586.59
3 to 4	2007.65	21.52	100%	2%	4	661.23
4 to 5	1670.33	58.47	100%	-15%	5	516.05
5 to 6	1808.05	137.03	100%	-8%	6	351.49
7 to 8	1758.54	90.48	100%	-11%	7	603.61
					8	341.78
<b>THRUST</b>	10.75 lb					

**Test Matrix 2B Configuration g Run 1**

<b>WAVE SPEEDS</b>						<b>PRESSURE</b>
Ports	Average	Stdev	%used	% CJ		(psig)
	(m/s)	(m/s)	of 33 total			
					1	79.79
1 to 2	N/A	N/A	N/A	N/A	2	2.80
2 to 3	N/A	N/A	N/A	N/A	3	502.35
3 to 4	2113.61	90.97	73%	7%	4	494.93
4 to 5	1454.65	262.97	82%	-26%	5	452.09
5 to 6	1446.14	484.17	100%	-27%	6	413.58
7 to 8	1766.63	198.10	91%	-10%	7	419.05
					8	407.08
<b>THRUST</b>	8.24 lb					

**Test Matrix 2B Configuration g Run 2**

<b>WAVE SPEEDS</b>						<b>PRESSURE</b>
Ports	Average	Stdev	%used	% CJ		(psig)
	(m/s)	(m/s)	of 33 total			
					1	79.32
1 to 2	N/A	N/A	N/A	N/A	2	2.80
2 to 3	N/A	N/A	N/A	N/A	3	502.08
3 to 4	2138.66	88.46	82%	9%	4	479.87
4 to 5	1378.81	41.18	79%	-30%	5	447.12
5 to 6	1453.41	471.02	97%	-26%	6	387.46
7 to 8	1872.47	187.08	79%	-5%	7	404.39
					8	440.68
<b>THRUST</b>	8.28 lb					

**Test Matrix 2B Configuration h Run 1**

<b>WAVE SPEEDS</b>						<b>PRESSURE</b>
Ports	Average	Stdev	%used	% CJ		(psig)
	(m/s)	(m/s)	of 33 total			
					1	87.13
1 to 2	N/A	N/A	N/A	N/A	2	3.62
2 to 3	N/A	N/A	N/A	N/A	3	572.66
3 to 4	2148.56	181.72	76%	9%	4	443.72
4 to 5	1388.55	63.18	67%	-29%	5	208.05
5 to 6	1897.86	265.55	70%	-4%	6	459.25
7 to 8	1889.54	250.76	88%	-4%	7	391.16
					8	452.46
<b>THRUST</b>	8.36 lb					

**Test Matrix 2B Configuration h Run 1**

WAVE SPEEDS						PRESSURE
Ports	Average	Stdev	%used	% CJ		(psig)
	(m/s)	(m/s)	of 33 total			1 87.90
1 to 2	N/A	N/A	N/A	N/A		2 3.03
2 to 3	N/A	N/A	N/A	N/A		3 505.41
3 to 4	2150.28	96.87	79%	9%		4 490.15
4 to 5	1388.89	55.12	85%	-29%		5 406.53
5 to 6	1651.11	520.08	91%	-16%		6 481.45
7 to 8	1843.33	213.63	88%	-6%		7 416.08
						8 379.50
<b>THRUST</b>	8.37 lb					

**Test Matrix 2C Configuration a Run 1**

WAVE SPEEDS						PRESSURE
Ports	Average	Stdev	%used	% CJ		(psig)
	(m/s)	(m/s)	of 34 total			1 111.66
1 to 2	N/A	N/A	N/A	N/A		2 4.04
2 to 3	N/A	N/A	N/A	N/A		3 664.03
3 to 4	1909.20	106.05	94%	-3%		4 460.21
4 to 5	1606.31	69.68	91%	-18%		5 519.80
5 to 6	1495.66	278.73	100%	-24%		6 373.20
7 to 8	1424.98	306.42	100%	-28%		7 211.78
						8 387.30
<b>THRUST</b>	~0 lb					

**Test Matrix 2C Configuration a Run 2**

WAVE SPEEDS						PRESSURE
Ports	Average	Stdev	%used	% CJ		(psig)
	(m/s)	(m/s)	of 34 total			1 105.45
1 to 2	N/A	N/A	N/A	N/A		2 3.05
2 to 3	N/A	N/A	N/A	N/A		3 586.82
3 to 4	1968.16	91.23	88%	0%		4 481.85
4 to 5	1580.52	264.93	94%	-20%		5 444.89
5 to 6	1509.54	90.95	97%	-23%		6 325.18
7 to 8	1377.29	453.29	94%	-30%		7 202.23
						8 378.03
<b>THRUST</b>	~0 lb					

**Test Matrix 2C Configuration b Run 1**

WAVE SPEEDS							PRESSURE
Ports	Average	Stdev	%used	% CJ			(psig)
	(m/s)	(m/s)	of 33 total			1	
1 to 2	N/A	N/A	N/A	N/A		2	3.23
2 to 3	N/A	N/A	N/A	N/A		3	741.63
3 to 4	1924.30	159.34	85%	-2%		4	564.79
4 to 5	1377.29	453.29	94%	-30%		7	156.61
						8	140.05
<b>THRUST</b>	~0 lb						

**Test Matrix 2C Configuration b Run 2**

WAVE SPEEDS							PRESSURE
Ports	Average	Stdev	%used	% CJ			(psig)
	(m/s)	(m/s)	of 33 total			1	
1 to 2	N/A	N/A	N/A	N/A		2	3.91
2 to 3	N/A	N/A	N/A	N/A		3	741.92
3 to 4	1728.16	550.89	91%	-12%		4	560.05
4 to 5	1142.54	204.47	91%	-42%		7	179.19
						8	161.52
<b>THRUST</b>	~0 lb						

**Test Matrix 2C Configuration c Run 1**

WAVE SPEEDS							PRESSURE
Ports	Average	Stdev	%used	% CJ			(psig)
	(m/s)	(m/s)	of 33 total			1	
1 to 2	N/A	N/A	N/A	N/A		2	3.49
2 to 3	N/A	N/A	N/A	N/A		3	710.36
3 to 4	1989.59	190.65	91%	1%		4	451.79
4 to 5	1623.86	297.76	88%	-17%		7	391.45
						8	408.75
<b>THRUST</b>	8.44 lb						



**Test Matrix 2C Configuration c Run 2**

WAVE SPEEDS							PRESSURE
Ports	Average	Stdev	%used	% CJ			(psig)
	(m/s)	(m/s)	of 33 total				
						1	140.77
1 to 2	N/A	N/A	N/A	N/A		2	4.35
2 to 3	N/A	N/A	N/A	N/A		3	736.12
3 to 4	2067.44	155.48	82%	5%		4	546.73
4 to 5	1504.21	273.48	94%	-24%		7	475.72
						8	304.54
<b>THRUST</b>	8.44 lb						

**Fill Fraction Effect Configuration a Run 1**

WAVE SPEEDS							PRESSURE
Ports	Average	Stdev	%used	% CJ			(psig)
	(m/s)	(m/s)	of 10 total				
						2	110.25
1 to 2	N/A	N/A	N/A	N/A		3	605.31
2 to 3	N/A	N/A	N/A	N/A		4	551.72
3 to 4	1970.06	39.55	90%	0%		5	535.80
4 to 5	2249.54	31.71	100%	14%		6	448.40
5 to 6	1644.09	32.43	100%	-16%		7	204.00
7 to 8	903.95	5.94	100%	-54%		8	143.39
<b>THRUST</b>	9.18 lb						

**Fill Fraction Effect Configuration b Run 1**

WAVE SPEEDS							PRESSURE
Ports	Average	Stdev	%used	% CJ			(psig)
	(m/s)	(m/s)	of 10 total				
						2	95.01
1 to 2	N/A	N/A	N/A	N/A		3	591.35
2 to 3	N/A	N/A	N/A	N/A		4	525.53
3 to 4	2014.66	15.71	100%	2%		5	533.07
4 to 5	2275.46	26.65	100%	16%		6	401.22
5 to 6	1772.82	31.37	100%	-10%		7	174.97
7 to 8	917.57	7.02	100%	-53%		8	142.52
<b>THRUST</b>	10.51 lb						

**Fill Fraction Effect Configuration c Run 1**

WAVE SPEEDS							PRESSURE
Ports	Average	Stdev	%used	% CJ			(psig)
	(m/s)	(m/s)	of 10 total			2	94.88
1 to 2	N/A	N/A	N/A	N/A		3	669.84
2 to 3	N/A	N/A	N/A	N/A		4	670.19
3 to 4	2043.23	26.12	100%	4%		5	608.42
4 to 5	2332.39	33.06	100%	19%		6	651.09
5 to 6	1886.22	40.44	100%	-4%		7	178.83
7 to 8	957.44	11.99	100%	-51%		8	161.75
<b>THRUST</b>	9.39 lb						

**Fill Fraction Effect Configuration d Run 1**

WAVE SPEEDS							PRESSURE
Ports	Average	Stdev	%used	% CJ			(psig)
	(m/s)	(m/s)	of 10 total			2	92.63
1 to 2	N/A	N/A	N/A	N/A		3	632.07
2 to 3	N/A	N/A	N/A	N/A		4	551.18
3 to 4	2041.90	27.53	100%	4%		5	628.50
4 to 5	2331.30	33.08	100%	18%		6	588.20
5 to 6	1955.10	34.44	100%	-1%		7	180.28
7 to 8	944.32	8.63	100%	-52%		8	164.36
<b>THRUST</b>	10.68 lb						

**Fill Fraction Effect Configuration e Run 1**

WAVE SPEEDS							PRESSURE
Ports	Average	Stdev	%used	% CJ			(psig)
	(m/s)	(m/s)	of 10 total			2	97.17
1 to 2	N/A	N/A	N/A	N/A		3	665.06
2 to 3	N/A	N/A	N/A	N/A		4	521.93
3 to 4	1965.55	26.87	100%	0%		5	572.09
4 to 5	1762.21	50.05	100%	-10%		6	310.84
5 to 6	1609.53	49.13	100%	-18%		7	328.98
7 to 8	1184.75	13.09	100%	-40%		8	214.03
<b>THRUST</b>	10.49 lb						

**Fill Fraction Effect Configuration f Run 1**

<b>WAVE SPEEDS</b>						<b>PRESSURE</b>
Ports	Average	Stdev	%used	% CJ		(psig)
	(m/s)	(m/s)	of 10 total			2 95.95
1 to 2	N/A	N/A	N/A	N/A		3 572.88
2 to 3	N/A	N/A	N/A	N/A		4 489.35
3 to 4	1966.66	20.43	100%	0%		5 594.94
4 to 5	1835.83	35.45	100%	-7%		6 301.13
5 to 6	1751.68	47.17	100%	-11%		7 309.26
7 to 8	1139.57	24.98	100%	-42%		8 207.49
<b>THRUST</b>	11.57 lb					

**Fill Fraction Effect Configuration g Run 1**

<b>WAVE SPEEDS</b>						<b>PRESSURE</b>
Ports	Average	Stdev	%used	% CJ		(psig)
	(m/s)	(m/s)	of 10 total			2 101.17
1 to 2	N/A	N/A	N/A	N/A		3 673.02
2 to 3	N/A	N/A	N/A	N/A		4 580.80
3 to 4	2010.92	27.23	100%	2%		5 753.92
4 to 5	1834.67	41.02	100%	-7%		6 571.29
5 to 6	1862.16	24.90	100%	-5%		7 342.33
7 to 8	1182.94	14.26	100%	-40%		8 207.48
<b>THRUST</b>	10.27 lb					

**Fill Fraction Effect Configuration h Run 1**

<b>WAVE SPEEDS</b>						<b>PRESSURE</b>
Ports	Average	Stdev	%used	% CJ		(psig)
	(m/s)	(m/s)	of 10 total			2 104.48
1 to 2	N/A	N/A	N/A	N/A		3 690.05
2 to 3	N/A	N/A	N/A	N/A		4 554.97
3 to 4	2009.51	23.81	100%	2%		5 621.65
4 to 5	1889.26	21.54	100%	-4%		6 600.57
5 to 6	1953.54	25.48	100%	-1%		7 307.96
7 to 8	1154.48	20.81	100%	-41%		8 158.33
<b>THRUST</b>	11.62 lb					

**Reflector 0.25" gap**

WAVE SPEEDS							PRESSURE
Ports	Average	Stdev	%used	% CJ			(psig)
	(m/s)	(m/s)	of 15 total				
1 to 2	1848.16	19.38	100%	-6%		1	477.66
3 to 4	2205.85	40.82	33%	12%		2	647.22
5 to 6	615.45	289.04	53%	-69%		3	109.44
6 to 7	938.11	49.73	100%	-52%		4	290.21
7 to 8	808.42	23.44	100%	-59%		5	30.56
						6	110.97
						7	94.64
						8	116.89

**Reflector 0.5" gap**

WAVE SPEEDS							PRESSURE
Ports	Average	Stdev	%used	% CJ			(psig)
	(m/s)	(m/s)	of 15 total				
1 to 2	1851.94	22.46	100%	-6%		1	536.02
3 to 4	2201.95	40.15	100%	12%		2	679.45
5 to 6	720.61	292.87	73%	-63%		3	410.88
6 to 7	926.08	50.80	100%	-53%		4	181.58
7 to 8	793.32	14.51	100%	-60%		5	35.04
						6	112.44
						7	94.96
						8	111.01

**Reflector 0.625" gap**

WAVE SPEEDS							PRESSURE
Ports	Average	Stdev	%used	% CJ			(psig)
	(m/s)	(m/s)	of 15 total				
1 to 2	1865.30	56.61	100%	-5%		1	546.41
3 to 4	2178.61	94.92	93%	11%		2	737.96
5 to 6	596.80	394.03	93%	-70%		3	501.08
6 to 7	979.04	196.22	100%	-50%		4	148.25
7 to 8	785.36	9.94	100%	-60%		5	36.32
						6	116.25
						7	99.09
						8	110.81

**Reflector/Layer 1.0" gap**

WAVE SPEEDS							PRESSURE
Ports	Average	Stdev	%used	% CJ			(psig)
	(m/s)	(m/s)	of 15 total				
1 to 2	1879.49	34.52	100%	-4%		1	559.34
3 to 4	2225.57	41.19	100%	13%		2	736.91
5 to 6	1028.04	337.02	100%	-48%		3	582.05
6 to 7	898.86	56.78	100%	-54%		4	157.24
7 to 8	770.66	10.24	100%	-61%		5	45.44
						6	109.01
						7	88.99
						8	101.89

**Dual Tube - Transducer Configuration 1 - Run 1**

CONDITIONS		WAVE SPEEDS						PRESSURE
fill vol	315 in <sup>3</sup>	Ports	Average	Stdev	%used	% CJ		(psig)
ff	1		(m/s)	(m/s)	of 10 total			1 154.16
freq	20 Hz	1 to 2	1455.60	733.23	90%	-26%		2 358.11
Spark 1		2 to 3	1737.97	179.36	100%	-12%		3 643.50
ign delay	0.012 s	4 to 5	1855.16	30.60	100%	-6%		4 531.13
		5 to 6	1735.70	38.68	100%	-12%		5 163.46
		7 to 8	1630.80	227.50	100%	-17%		6 216.10
								7 654.31
		Thrust	18.07 lb					8 538.44

**Dual Tube - Transducer Configuration 1 - Run 2**

CONDITIONS		WAVE SPEEDS						PRESSURE
fill vol	315 in <sup>3</sup>	Ports	Average	Stdev	%used	% CJ		(psig)
ff	1		(m/s)	(m/s)	of 10 total			1 166.63
freq	20 Hz	1 to 2	1349.94	557.84	90%	-31%		2 525.78
Spark 1		2 to 3	2011.24	280.76	100%	2%		3 595.23
ign delay	0.012 s	4 to 5	1845.03	52.25	100%	-6%		4 424.13
		5 to 6	1770.22	103.78	100%	-10%		5 150.66
		7 to 8	1627.51	229.99	100%	-17%		6 240.67
								7 514.42
		Thrust	17.91 lb					8 630.90

**Dual Tube - Ignition Delay 0.012s - Run 4**

CONDITIONS		WAVE SPEEDS						PRESSURE
fill vol	315 in <sup>3</sup>	Ports	Average	Stdev	%used	% CJ		(psig)
ff	1		(m/s)	(m/s)	of 10 total			1 577.82
freq	20 Hz	1 to 2	1894.92	34.87	100%	-4%		2 702.98
Spark 1		3 to 4	1836.07	56.49	100%	-7%		3 446.76
ign delay(s)	0.012 s	5 to 6	1150.63	109.76	100%	-42%		4 217.94
		6 to 7	1624.85	217.51	100%	-17%		5 168.21
		7 to 8	1389.21	141.31	100%	-29%		6 539.16
								7 632.69
		Thrust (lb)	17.95 lb					8 344.03

**Dual Tube - Ignition Delay 0.013s - Run 10**

CONDITIONS		WAVE SPEEDS						PRESSURE
fill vol	315 in <sup>3</sup>	Ports	Average	Stdev	%used	% CJ		(psig)
ff	1		(m/s)	(m/s)	of 10 total			1 561.53
freq	20 Hz	1 to 2	1916.84	17.95	100%	-3%		2 746.95
Spark 1		3 to 4	1879.30	70.25	100%	-5%		3 562.22
ign delay(s)	0.012 s	5 to 6	1108.79	141.00	100%	-44%		4 300.15
		6 to 7	1468.55	229.72	100%	-25%		5 171.68
		7 to 8	1174.59	118.49	100%	-40%		6 436.84
								7 494.25
		Thrust (lb)	18.23					8 227.72

**Dual Tube - Ignition Delay 0.014s - Run 11**

CONDITIONS		WAVE SPEEDS						PRESSURE
fill vol	315 in <sup>3</sup>	Ports	Average	Stdev	%used	% CJ		(psig)
ff	1		(m/s)	(m/s)	of 10 total		1	677.34
freq	20 Hz	1 to 2	1940.99	15.62	100%	-1%	2	633.89
Spark 1		3 to 4	1941.66	28.24	100%	-1%	3	491.90
ign delay(s)	0.014 s	5 to 6	1381.26	258.93	90%	-30%	4	290.83
		6 to 7	1712.07	40.77	100%	-13%	5	226.03
		7 to 8	1197.49	38.27	100%	-39%	6	672.90
							7	524.69
		Thrust (lb)	18.42				8	232.18

**Dual Tube - Ignition Delay 0.015s - Run 12**

CONDITIONS		WAVE SPEEDS						PRESSURE
fill vol	315 in <sup>3</sup>	Ports	Average	Stdev	%used	% CJ		(psig)
ff	1		(m/s)	(m/s)	of 10 total		1	558.63
freq	20 Hz	1 to 2	1939.66	13.16	100%	-1%	2	705.40
Spark 1		3 to 4	1910.03	22.28	100%	-3%	3	502.01
ign delay(s)	0.015	5 to 6	1272.03	99.60	100%	-35%	4	247.66
		6 to 7	1665.59	42.31	100%	-15%	5	240.97
		7 to 8	1159.27	29.02	100%	-41%	6	574.96
<b>NOTE:</b>							7	449.61
Fires @ 10 Hz		Thrust (lb)	10.71				8	219.39

**Dual Tube - Spark 3 Ignition Delay 0.0 s - Backfired**

**Dual Tube - Spark 3 Ignition Delay 0.002s - Run 5**

CONDITIONS		WAVE SPEEDS						PRESSURE
fill vol	315 in <sup>3</sup>	Ports	Average	Stdev	%used	% CJ		(psig)
ff	1		(m/s)	(m/s)	of 10 total		1	126.56
freq	20 Hz	1 to 2	666.63	250.02	100%	-66%	2	121.43
Spark 3		3 to 4 (-)	1263.07	132.20	90%	-36%	3	122.11
ign delay(s)	0.002	5 to 6	1787.23	77.96	100%	-9%	4	86.30
		6 to 7	1746.00	38.35	100%	-11%	5	813.22
		7 to 8	1306.40	36.94	100%	-34%	6	575.58
							7	546.06
		Thrust (lb)	17.98				8	281.06

**Dual Tube - Spark 3 Ignition Delay 0.002s - Run 6**

CONDITIONS		WAVE SPEEDS						PRESSURE
fill vol	315 in <sup>3</sup>	Ports	Average	Stdev	%used	% CJ		(psig)
ff	1		(m/s)	(m/s)	of 10 total		1	107.79
freq	20 Hz	1 to 2	1000.28	629.52	100%	-49%	2	118.39
Spark 3		3 to 4 (-)	1246.37	121.40	90%	-37%	3	114.07
ign delay(s)	0.002	5 to 6	1764.59	73.88	100%	-10%	4	92.17
		6 to 7	1755.16	26.56	100%	-11%	5	899.93
		7 to 8	1301.46	26.60	100%	-34%	6	649.84
							7	536.07
		Thrust (lb)	17.91				8	284.32

**Dual Tube - Spark 3 Ignition Delay 0.0005s - Run 7**

CONDITIONS		WAVE SPEEDS						PRESSURE
fill vol	315 in <sup>3</sup>	Ports	Average	Stdev	%used	% CJ		(psig)
ff	1		(m/s)	(m/s)	of 10 total		1	104.85
freq	20 Hz	1 to 2	760.24	206.02	100%	-61%	2	86.21
Spark 3		3 to 4 (-)	1419.54	406.20	80%	-28%	3	128.76
ign delay(s)	0.0005	5 to 6	1803.99	67.04	100%	-8%	4	106.58
		6 to 7	1798.58	32.81	100%	-9%	5	1011.24
		7 to 8	1418.54	45.57	100%	-28%	6	627.93
							7	477.71
		Thrust (lb)	15.88				8	321.42

**Dual Tube - Spark 3 Ignition Delay 0.0005s - Run 8**

CONDITIONS		WAVE SPEEDS						PRESSURE
fill vol	315 in <sup>3</sup>	Ports	Average	Stdev	%used	% CJ		(psig)
ff	1		(m/s)	(m/s)	of 10 total		1	105.66
freq	20 Hz	1 to 2	798.49	106.58	100%	-59%	2	94.43
Spark 3		3 to 4 (-)	2103.43	583.50	80%	7%	3	105.31
ign delay(s)	0.001	5 to 6	1786.86	44.47	100%	-9%	4	90.08
		6 to 7	1777.68	28.02	100%	-10%	5	1122.47
		7 to 8	1408.57	36.25	100%	-28%	6	723.26
							7	604.75
		Thrust (lb)	15.92				8	354.91

**Dual Tube - Spark 3 Ignition Delay 0.003s- No Good - Firing @ 10 Hz**

**Dual Tube - Spark 3 Ignition Delay 0.0025s - Run 9**

CONDITIONS		WAVE SPEEDS						PRESSURE
fill vol	315 in <sup>3</sup>	Ports	Average	Stdev	%used	% CJ		(psig)
ff	1		(m/s)	(m/s)	of 10 total		1	133.21
freq	20 Hz	1 to 2	887.70	139.41	100%	-55%	2	100.73
Spark 3		3 to 4 (-)	1334.43	403.42	80%	-32%	3	107.75
ign delay(s)	0.0025	5 to 6	1767.30	69.71	100%	-10%	4	79.27
		6 to 7	1742.52	21.41	100%	-11%	5	779.13
		7 to 8	1269.66	23.23	100%	-35%	6	573.71
							7	633.00
		Thrust (lb)	18.03				8	261.11

**Dual Tube - Spark 1 & 3 - Run 13**

CONDITIONS		WAVE SPEEDS						PRESSURE
fill vol	315 in <sup>3</sup>	Ports	Average	Stdev	%used	% CJ		(psig)
ff	1		(m/s)	(m/s)	of 10 total		1	535.32
freq	20 Hz	1 to 2	1895.83	24.07	100%	-4%	2	825.96
Spark 1&3		3 to 4	1836.35	79.95	100%	-7%	3	455.67
ign 1 (cnt)	-943	5 to 6	1147.49	146.25	100%	-42%	4	220.15
ign 3 (cnt)	-1	6 to 7	1561.61	234.98	100%	-21%	5	184.60
		7 to 8	1356.29	183.89	90%	-31%	6	371.60
							7	482.63
		Thrust (lb)	17.89				8	320.84

Dual Tube - Spark 1 & 3 - Run 14

CONDITIONS		WAVE SPEEDS						PRESSURE
fill vol	315 in^3	Ports	Average	Stdev	%used	% CJ		(psig)
ff	1		(m/s)	(m/s)	of 10 total		1	538.12
freq	20 Hz	1 to 2	1886.05	24.47	100%	-4%	2	679.98
Spark 1&3		3 to 4	1851.88	27.28	100%	-6%	3	499.15
ign 1 (cnt)	-943	5 to 6	1117.71	163.63	100%	-43%	4	243.49
ign 3 (cnt)	-1	6 to 7	1654.85	219.29	100%	-16%	5	271.35
		7 to 8	1380.49	173.94	100%	-30%	6	620.66
							7	607.88
		Thrust (lb)	17.89				8	360.26

Dual Tube - Spark 1 & 3 - Run 15

CONDITIONS		WAVE SPEEDS						PRESSURE
fill vol	315 in^3	Ports	Average	Stdev	%used	% CJ		(psig)
ff	1		(m/s)	(m/s)	of 10 total		1	568.27
freq	20 Hz	1 to 2	1897.37	34.33	100%	-4%	2	766.62
Spark 1&3		3 to 4	1871.98	29.12	100%	-5%	3	453.61
ign 1 (cnt)	-943	5 to 6	1309.45	458.16	100%	-33%	4	285.21
ign 3 (cnt)	-991	6 to 7	1650.34	209.13	100%	-16%	5	249.09
		7 to 8	1265.28	104.72	100%	-36%	6	516.88
							7	544.24
		Thrust (lb)	18.03				8	250.94

Dual Tube - Spark 1 & 3 - Run 16

CONDITIONS		WAVE SPEEDS						PRESSURE
fill vol	315 in^3	Ports	Average	Stdev	%used	% CJ		(psig)
ff	1		(m/s)	(m/s)	of 10 total		1	483.28
freq	20 Hz	1 to 2	1878.69	21.00	100%	-5%	2	727.19
Spark 1&3		3 to 4	1881.64	16.94	100%	-4%	3	416.36
ign 1 (cnt)	-963	5 to 6	1726.04	119.65	100%	-12%	4	278.62
ign 3 (cnt)	-991	6 to 7	1745.02	39.32	100%	-11%	5	962.00
		7 to 8	1332.52	34.06	100%	-32%	6	823.54
							7	662.10
		Thrust (lb)	18				8	316.32

Dual Tube - Spark 1 & 3 - Run 17

CONDITIONS		WAVE SPEEDS						PRESSURE
fill vol	315 in^3	Ports	Average	Stdev	%used	% CJ		(psig)
ff	1		(m/s)	(m/s)	of 10 total		1	597.80
freq	20 Hz	1 to 2	1896.99	21.39	100%	-4%	2	791.81
Spark 1&3		3 to 4	1886.09	35.59	100%	-4%	3	492.95
ign 1 (cnt)	-963	5 to 6	1721.08	150.03	100%	-13%	4	218.18
ign 3 (cnt)	-991	6 to 7	1729.55	33.98	100%	-12%	5	832.96
		7 to 8	1270.88	25.51	100%	-35%	6	683.28
							7	595.54
		Thrust (lb)	18.25				8	264.00



Dual Tube - Spark 1 & 3 - Run 18

CONDITIONS		WAVE SPEEDS						PRESSURE
fill vol	315 in^3	Ports	Average	Stdev	%used	% CJ		(psig)
ff	1		(m/s)	(m/s)	of 10 total		1	605.80
freq	20 Hz	1 to 2	1923.08	14.36	100%	-2%	2	658.60
Spark 1&3		3 to 4	1618.87	76.88	100%	-18%	3	513.18
ign 1 (cnt)	-983	5 to 6	1675.76	120.27	100%	-15%	4	184.91
ign 3 (cnt)	-991	6 to 7	1727.60	16.15	100%	-12%	5	823.55
		7 to 8	1288.11	30.46	100%	-35%	6	558.82
							7	566.08
		Thrust (lb)	18.35				8	300.08

Dual Tube - Spark 1 & 3 - Run 19

CONDITIONS		WAVE SPEEDS						PRESSURE
fill vol	315 in^3	Ports	Average	Stdev	%used	% CJ		(psig)
ff	1		(m/s)	(m/s)	of 10 total		1	617.41
freq	20 Hz	1 to 2	1928.34	23.64	100%	-2%	2	667.67
Spark 1&3		3 to 4	1346.55	578.48	100%	-32%	3	468.31
ign 1 (cnt)	-983	5 to 6	1739.68	48.89	100%	-12%	4	209.52
ign 3 (cnt)	-991	6 to 7	1733.11	32.43	100%	-12%	5	938.74
		7 to 8	1263.25	39.30	100%	-36%	6	602.43
							7	556.55
		Thrust (lb)	18.04				8	265.64

Dual Tube - Spark 1 & 3 - Run 20

CONDITIONS		WAVE SPEEDS						PRESSURE
fill vol	315 in^3	Ports	Average	Stdev	%used	% CJ		(psig)
ff	1		(m/s)	(m/s)	of 10 total		1	503.63
freq	20 Hz	1 to 2	1791.55	219.60	100%	-9%	2	759.32
Spark 1&3		3 to 4	1814.29	#####	10%	-8%	3	168.70
ign 1 (cnt)	-971	5 to 6	1787.70	71.81	100%	-9%	4	110.71
ign 3 (cnt)	-971	6 to 7	1759.23	24.86	100%	-11%	5	863.80
		7 to 8	1393.48	33.14	100%	-29%	6	711.28
							7	660.58
		Thrust (lb)	18.05				8	338.88

Dual Tube - Nozzles - Run 21

CONDITIONS		WAVE SPEEDS						PRESSURE
fill vol	327 in^3	Ports	Average	Stdev	%used	% CJ		(psig)
ff	1		(m/s)	(m/s)	of 11 total		1	481.92
freq	20 Hz	1 to 2	1922.91	10.02	100%	-2%	2	648.89
Spark 1		3 to 4	1835.53	63.49	100%	-7%	3	468.82
ign del (s)	0.014	5 to 6	1228.18	190.02	82%	-38%	4	220.40
		6 to 7	1589.23	199.00	100%	-19%	5	219.09
		7 to 8	1307.67	116.41	100%	-34%	6	570.92
							7	677.11
		Thrust (lb)	18.16				8	280.50

Dual Tube - Nozzles - Run 22

CONDITIONS		WAVE SPEEDS						PRESSURE
fill vol	327 in^3	Ports	Average	Stdev	%used	% CJ		(psig)
ff	1.1		(m/s)	(m/s)	of 10 total			1 546.23
freq	20 Hz	1 to 2	1930.91	24.33	100%	-2%		2 773.75
Spark 1		3 to 4	1819.74	69.33	100%	-8%		3 515.94
ign del (s)	0.014	5 to 6	1298.99	412.63	90%	-34%		4 192.94
		6 to 7	1558.16	270.49	100%	-21%		5 218.46
		7 to 8	1332.18	227.94	100%	-32%		6 548.41
								7 564.15
		Thrust (lb)	18.92					8 345.79

Dual Tube - Open breather holes on crossover - Run 24

CONDITIONS		WAVE SPEEDS						PRESSURE
fill vol	315 in^3	Ports	Average	Stdev	%used	% CJ		(psig)
ff	1		(m/s)	(m/s)	of 10 total			1 540.45
freq	20 Hz	1 to 2	1934.56	15.25	100%	-2%		2 698.50
Spark 1		3 to 4	1059.41	60.11	90%	-46%		3 222.27
ign del (s)	0.014	5 to 6	1321.73	541.85	80%	-33%		4 117.75
		6 to 7	1502.36	274.80	100%	-24%		5 203.82
		7 to 8	1168.55	118.24	100%	-41%		6 678.88
								7 421.93
		Thrust (lb)	16.84					8 233.91

Dual Tube - Open breather holes on crossover - Run 25

CONDITIONS		WAVE SPEEDS						PRESSURE
fill vol	315 in^3	Ports	Average	Stdev	%used	% CJ		(psig)
ff	1		(m/s)	(m/s)	of 10 total			1 615.57
freq	20 Hz	1 to 2	1932.03	17.13	100%	-2%		2 741.66
Spark 1		3 to 4	1078.50	42.66	90%	-45%		3 191.74
ign del (s)	0.014	5 to 6	1532.41	843.32	70%	-22%		4 97.19
		6 to 7	1394.30	251.50	100%	-29%		5 170.44
		7 to 8	1138.72	89.55	100%	-42%		6 593.21
								7 385.24
		Thrust (lb)	17.54					8 223.38

Dual Tube - 10 Hz Overfill - Run 26

CONDITIONS		WAVE SPEEDS						PRESSURE
fill vol	315 in^3	Ports	Average	Stdev	%used	% CJ		(psig)
ff	1.5		(m/s)	(m/s)	of 5 total			1 13.26
freq	10 Hz	1 to 2	471.59	229.64	100%	-76%		2 15.18
Spark 1		3 to 4	761.89	1094.22	80%	-61%		3 28.60
ign del (s)	0.028	5 to 6	1424.41	#####	40%	-28%		4 23.23
		6 to 7	1293.23	60.20	100%	-34%		5 102.90
		7 to 8	1174.20	15.68	100%	-40%		6 188.50
								7 142.65
		Thrust (lb)	7.23					8 106.13

Dual Tube - 30 Hz - Run 28

CONDITIONS		WAVE SPEEDS						PRESSURE
fill vol	315 in <sup>3</sup>	Ports	Average	Stdev	%used	% CJ		(psig)
ff	1		(m/s)	(m/s)	of 15 total			1 724.53
freq	30 Hz	1 to 2	1904.67	30.74	100%	-3%		2 684.25
Spark 1		3 to 4	2177.32	19.71	80%	11%		3 504.97
ign del (s)	0.009	5 to 6	1794.88	225.72	73%	-9%		4 158.02
		6 to 7	1962.63	13.07	100%	0%		5 151.18
		7 to 8	1887.99	33.00	100%	-4%		6 652.35
								7 693.57
		Thrust (lb)	29.65					8 616.50

Dual Tube - 30 Hz - Run 29

CONDITIONS		WAVE SPEEDS						PRESSURE
fill vol	315 in <sup>3</sup>	Ports	Average	Stdev	%used	% CJ		(psig)
ff	1		(m/s)	(m/s)	of 15 total			1 600.17
freq	30 Hz	1 to 2	1907.87	26.97	100%	-3%		2 784.31
Spark 1		3 to 4	2178.06	22.21	93%	11%		3 582.73
ign del (s)	0.009	5 to 6	1876.84	205.75	87%	-5%		4 172.94
		6 to 7	1959.61	16.89	100%	0%		5 173.64
		7 to 8	1877.70	25.95	100%	-5%		6 684.11
								7 721.50
		Thrust (lb)	29.65					8 605.94

Dual Tube - 30 Hz - Run 30

CONDITIONS		WAVE SPEEDS						PRESSURE
fill vol	315 in <sup>3</sup>	Ports	Average	Stdev	%used	% CJ		(psig)
ff	1		(m/s)	(m/s)	of 15 total			1 327.46
freq	30 Hz	1 to 2	1273.73	526.27	100%	-35%		2 518.77
Spark 1 & 2		3 to 4	N/A	N/A	N/A	N/A		3 333.54
ign del (s)	0.009	5 to 6	2212.16	53.67	100%	12%		4 103.00
		6 to 7	2039.68	15.55	100%	4%		5 937.09
		7 to 8	2009.59	11.65	100%	2%		6 571.88
								7 602.66
		Thrust (lb)	29.29					8 588.70

Dual Tube - No Chin Spiral in Tube 3 - Run 31

CONDITIONS		WAVE SPEEDS						PRESSURE
fill vol	315 in <sup>3</sup>	Ports	Average	Stdev	%used	% CJ		(psig)
ff	1		(m/s)	(m/s)	of 15 total			1 574.74
freq	30 Hz	1 to 2	1887.60	53.70	100%	-4%		2 749.88
Spark 1		3 to 4	2209.91	51.48	100%	12%		3 494.29
ign del (s)	0.009	5 to 6	1275.53	539.63	80%	-35%		4 153.61
		6 to 7	922.98	8.18	100%	-53%		5 58.17
		7 to 8	813.64	15.15	100%	-59%		6 122.28
								7 110.76
		Thrust (lb)	29.16					8 138.99

## References

- Chapman, D.L. "On the Rate of Explosion of Gases," *Philosophical Magazine*, 45:90-103, (1899).
- Friedman, R. "Kinetics of the Combustion Wave," *American Rocket Society Journal*, 24:349-354, (November 1953).
- Glassman, Irvin. *Combustion*. San Diego: Academic Press, 1996.
- Katta, Vish R., L.P. Chin, and Fred R. Schauer, "Numerical Studies on Cellular Detonation Wave Subjected to Sudden Expansion," *Proceedings of the 17<sup>th</sup> International Colloquium on the Dynamics of Explosions and Reactive Systems*. Heidelberg, Germany, (1999).
- Katta, Vish. Air Force Research Laboratory/ Propulsion Research and Testing Section, Wright-Patterson AFB OH. Personal Interview. January 2002.
- Kuo, Kenneth K. *Principles of Combustion*. New York: John Wiley & Sons, 1986.
- Morrison, Richard Boyd. *A Shock-Tube Investigation of Detonative Combustion*. Ann Arbor: Engineering Research Institute, University of Michigan, 1955.
- Oppenheim, A.K., "Research and Development of Impulsive Ducts in Germany," *B.I.O.S. Final Report No. 1777, Item No. 266, England*, (1949).
- Parker, Jason T. and Fred R. Schauer, "Analysis and Compression Algorithms for Megabyte Range PDE Data Sets" Presentation to Dayton Cincinnati Aerospace Sciences Symposium. Dayton OH. 7 March 2002.
- Parker, Jason T. *Algorithm Summaries with Appended Source Code*. Unpublished report for Air Force Research Laboratory, Propulsion Research and Testing Section, Wright-Patterson AFB OH, Summer 2001.
- Rolling, August J., Paul I. King, John Hoke, and Fred R. Schauer, "Detonation propagation through a tube array." Presentation to Twenty-Sixth Annual Dayton-Cincinnati Aerospace Science Symposium. Dayton, OH. March 2001.
- Schauer, Fred R., Jeff Stutrud, Royce Bradley, and Vish Katta. "AFRL/PRSC Pulse Detonation Engine Program," invited paper at 12<sup>th</sup> PERC Symposium, Ohio Aerospace Institute, Cleveland, OH, (26-27 October 2000).

Schauer, Fred R., Royce Bradley, Vish Katta, and John Hoke, "Detonation Initiation and Performance in Complex Hydrocarbon Fueled Pulsed Detonation Engines," 50<sup>th</sup> JANNAF Propulsion Meeting, Salt Lake City UT, 11-13 July 2001.

Shelkin, K.I. *Soviet Journal of Technical Physics*, Vol. 10 page 823-827, 1940.

Soloukhin, R.I. *Shock Waves and Detonations in Gases*. Moscow: Mono Book Corp., 1966.

Stutrud, Jeff. *Tutorial on the Online Wave Speed Program VI*. Unpublished Report for Air Force Research Laboratory, Propulsion Research and Testing Section, Wright-Patterson AFB OH, 4 December 2001.

Turns, Stephen R. *An Introduction to Combustion*. New York: McGraw Hill, 2000.

Williams, F.A. *Combustion Theory*. Reading, Mass.: Addison-Wesley Publishing Co., 1965.

Zhdan, S.A., V.V. Mitrofanov, and A.I. Sychev, "Reactive impulse from the explosion of a gas mixture in a semi-infinite space," *Combustion, Explosion, and Shock Waves*, Vol. 30, No.5:657-660, 1994.

<b>REPORT DOCUMENTATION PAGE</b>			<i>Form Approved</i> <i>OMB No. 074-0188</i>		
<p>The public reporting burden for this collection of information is estimated to average 1 hour per response, including the time for reviewing instructions, searching existing data sources, gathering and maintaining the data needed, and completing and reviewing the collection of information. Send comments regarding this burden estimate or any other aspect of the collection of information, including suggestions for reducing this burden to Department of Defense, Washington Headquarters Services, Directorate for Information Operations and Reports (0704-0188), 1215 Jefferson Davis Highway, Suite 1204, Arlington, VA 22202-4302. Respondents should be aware that notwithstanding any other provision of law, no person shall be subject to a penalty for failing to comply with a collection of information if it does not display a currently valid OMB control number.</p> <p><b>PLEASE DO NOT RETURN YOUR FORM TO THE ABOVE ADDRESS.</b></p>					
<b>1. REPORT DATE (DD-MM-YYYY)</b> 26-03-2002		<b>2. REPORT TYPE</b> Master's Thesis		<b>3. DATES COVERED (From – To)</b>	
<b>4. TITLE AND SUBTITLE</b> ALTERNATIVE PULSE DETONATION ENGINE IGNITION SYSTEM INVESTIGATION THROUGH DETONATION SPLITTING			<b>5a. CONTRACT NUMBER</b>		
			<b>5b. GRANT NUMBER</b>		
			<b>5c. PROGRAM ELEMENT NUMBER</b>		
<b>6. AUTHOR(S)</b> Rolling, August J., Captain, USAF			<b>5d. PROJECT NUMBER</b>		
			<b>5e. TASK NUMBER</b>		
			<b>5f. WORK UNIT NUMBER</b>		
<b>7. PERFORMING ORGANIZATION NAMES(S) AND ADDRESS(S)</b> Air Force Institute of Technology Graduate School of Engineering and Management (AFIT/ENY) 2950 P Street, Building 640 WPAFB OH 45433-7765			<b>8. PERFORMING ORGANIZATION REPORT NUMBER</b>  AFIT/GAE/ENY/02-10		
<b>9. SPONSORING/MONITORING AGENCY NAME(S) AND ADDRESS(ES)</b> AFRL/PRTS Attn: Dr. Fred Schauer Wright-Patterson AFB, OH 45413 (937) 255-6462			<b>10. SPONSOR/MONITOR'S ACRONYM(S)</b>		
			<b>11. SPONSOR/MONITOR'S REPORT NUMBER(S)</b>		
<b>12. DISTRIBUTION/AVAILABILITY STATEMENT</b> Approved for public release; distribution unlimited					
<b>13. SUPPLEMENTARY NOTES</b> Advisor: Dr. Paul I. King, (937) 255-3636 ext. 4628 paul.king@afit.edu					
<b>14. ABSTRACT</b> A Pulse Detonation Engine (PDE) combusts fuel air mixtures through a form of combustion: detonation. Recent PDE research has focused on designing working subsystems. This investigation continued this trend by examining ignition system alternatives. Existing designs required spark plugs in each separate thrust tube to ignite premixed reactants. A single thrust tube could require the spark plug to fire hundreds of times per second for long durations. The goal was to minimize hardware and increase reliability by limiting the number of ignition sources. This research used a continuously propagating detonation wave as both a thrust mechanism and an ignition system and required only one initial ignition source. This investigation was a proof of concept for such an ignition system. First a systematic look at various geometric effects on detonations was made. These results were used to further examine configurations for splitting detonations, physically dividing one detonation wave into two separate detonation waves. With this knowledge a dual thrust tube system was built and tested proving that a single spark could be used to initiate detonation in separate thrust tubes. Finally, a new <i>tripping</i> device for better deflagration to detonation transition (DDT) was examined. Existing devices induced DDT axially. The new device attempted to reflect an incoming detonation to initiate direct DDT in a cross flow.					
<b>15. SUBJECT TERMS</b> Pulse Detonation Engine, Detonation Splitting, Single Spark Ignition					
<b>16. SECURITY CLASSIFICATION OF:</b>		<b>17. LIMITATION OF ABSTRACT</b>	<b>18. NUMBER OF PAGES</b>	<b>19a. NAME OF RESPONSIBLE PERSON</b>	
		UL	106	Paul I. King	
<b>a. REPORT</b> Unclassified	<b>b. ABSTRACT</b> Unclassified	<b>c. THIS PAGE</b> Unclassified	<b>19b. TELEPHONE NUMBER (Include area code)</b> (937) 255-3636 ext. 4628		

Standard Form 298 (Rev. 8-98)  
Prescribed by ANSI Std. Z39-18

*Form Approved*  
*OMB No. 074-0188*

